

PhD degree in Systems Medicine (curriculum in Molecular Oncology)  
European School of Molecular Medicine (SEMM),  
University of Milan and University of Naples "Federico II"  
Settore disciplinare: bio/10

## **RELEVANCE OF NUMB ISOFORMS IN BREAST CANCER**

*D'UVA VERONICA*

IEO, Milan

Matricola n. R11141

*Supervisor:* Prof. Di Fiore Pier Paolo  
IEO, Milan

*Added Supervisors:* Prof. Pece Salvatore - Colaluca Ivan  
IEO, Milan

Anno accademico 2017-2018

# TABLE OF CONTENTS

<b>FIGURES LEGEND .....</b>	<b>4</b>
<b>LIST OF ABBREVIATIONS .....</b>	<b>6</b>
<b>1 ABSTRACT .....</b>	<b>8</b>
<b>2 INTRODUCTION.....</b>	<b>10</b>
<b>2.1 NUMB FROM ITS DISCOVERY...THE LESSON FROM <i>DROSOPHILA</i> .....</b>	<b>10</b>
<b>2.2 NUMB STRUCTURE.....</b>	<b>14</b>
<b>2.3 THE MULTIPLE NUMB FUNCTIONS.....</b>	<b>16</b>
2.3.1 NUMB AND ENDOCYTOSIS .....	16
2.3.2 NUMB AND THE NOTCH PATHWAY .....	20
2.3.3 NUMB AND HEDGEHOG PATHWAY .....	25
2.3.4 NUMB AND THE p53-MDM2 CIRCUITRY.....	28
2.3.4.1 THE ROLE OF THE TUMOR SUPPRESSOR p53.....	28
2.3.4.2 p53 STRUCTURE AND MECHANISMS OF REGULATION .....	31
2.3.4.3 MDM2 BIOLOGY.....	36
2.3.4.4 REGULATION OF THE p53-MDM2 PATHWAY .....	39
2.3.4.5 p53 IN CANCER.....	42
2.3.4.6 TARGETING OF THE p53-MDM2 PATHWAY FOR CANCER THERAPY .....	47
2.3.4.7 THE ROLE OF NUMB IN THE REGULATION OF THE p53-MDM2 PATHWAY .....	49
2.3.5 NUMB IN CELL ADHESION, CELL MIGRATION AND EPITHELIAL-TO-MESENCHYMAL TRANSITION	51
2.3.6 INCREASING THE COMPLEXITY: THE ROLE OF NUMB ISOFORMS.....	53
<b>2.4 NUMB AND CANCER .....</b>	<b>57</b>
2.4.1 NUMB INVOLVEMENT IN CANCER: THE ROLE IN THE DETERMINATION AND MAINTENANCE OF THE STEM CELL COMPARTMENT.....	60
<b>3 AIM OF THE PROJECT .....</b>	<b>64</b>
<b>4 MATERIALS AND METHODS.....</b>	<b>66</b>
<b>4.1 CELL CULTURE PROCEDURES AND REAGENTS .....</b>	<b>66</b>
4.1.1 CELL LINES.....	66
4.1.2 PRIMARY MAMMARY EPITHELIAL CELLS (MECs) .....	67
4.1.3 PLASMIDS AND REAGENTS .....	67
4.1.4 GENE EXPRESSION SILENCING BY siRNA TRANSFECTION .....	68
4.1.5 CELL TRANSFECTION .....	69
4.1.6 VIABILITY ASSAY .....	69
<b>4.2 SELECTION OF BREAST CANCER PATIENTS AND STATISTICAL ANALYSIS .....</b>	<b>69</b>
<b>4.3 PROTEIN PROCEDURES.....</b>	<b>72</b>
4.3.1 CELL LYSIS.....	72

4.3.2	SDS POLYACRYLAMIDE GEL ELECTROPHORESIS (SDS-PAGE) AND IMMUNOBLOTTING .....	73
4.3.3	PROTEIN ASSAYS .....	74
4.3.3.1	IMMUNOPRECIPITATION .....	74
4.3.3.2	IMMUNOFLUORESCENCE .....	74
4.3.3.3	IHC CHARACTERIZATION OF p53 MUTATIONAL STATUS ON BC SAMPLES .....	75
<b>4.4</b>	<b>NUCLEIC ACID TECHNIQUES.....</b>	<b>78</b>
4.4.1	mRNA PURIFICATION AND cDNA SYNTHESIS .....	78
4.4.2	GENE PREAMPLIFICATION AND RT-qPCR ANALYSIS .....	78
4.4.3	DIGITAL PCR .....	80
4.4.4	DNA POLYMERASE-MEDIATED PCR AMPLIFICATION AND AGAROSE GEL ELECTROPHORESIS. ....	81
4.4.5	p53 GENE SEQUENCING .....	82
<b>5</b>	<b>RESULTS .....</b>	<b>83</b>
5.1	EVALUATION OF THE EXPRESSION OF NUMB ISOFORMS IN BREAST CELL LINES .....	83
5.2	ONLY PTBi-CONTAINING NUMB ISOFORMS ARE ABLE TO EFFICIENTLY BIND MDM2..	87
5.3	ONLY PTBi-CONTAINING NUMB ISOFORMS ARE ABLE TO REGULATE P53 PROTEIN LEVELS	89
5.4	PTBi-CONTAINING NUMB ISOFORMS AFFECT THE P53-DEPENDENT RESPONSE TO GENOTOXIC STRESS .....	91
5.5	LOW LEVELS OF PTBi-CONTAINING NUMB ISOFORMS PREDICT RESISTANCE TO GENOTOXIC TREATMENT IN PRIMARY BCs. ....	95
5.6	NUMB ISOFORMS PREDICT PROGNOSTIC OUTCOME IN HUMAN BCs .....	98
<b>6</b>	<b>DISCUSSION .....</b>	<b>107</b>
6.1	THE ROLE OF NUMB ISOFORMS IN THE REGULATION OF THE p53 PATHWAY. ....	107
6.2	PROGNOSTIC VALUE AND RELEVANCE OF THE NUMB ISOFORM EXPRESSION IN BREAST TUMORIGENESIS. ....	109
6.3	THE MULTIPLE WAYS LEADING TO NUMB DYSFUNCTION IN TUMORS AND THE POSSIBLE THERAPEUTIC INTERVENTIONS.....	112
<b>7</b>	<b>ACKNOWLEDGEMENTS .....</b>	<b>115</b>
<b>8</b>	<b>BIBLIOGRAPHY.....</b>	<b>116</b>

# FIGURES LEGEND

**FIG. 1** NUMB ASYMMETRIC DIVISION IN DROSOPHILA SOP AND NEUROBLASTS.....11

**FIG. 2** PAR COMPLEX ORCHESTRATES NUMB ASYMMETRIC PARTITION AT MITOSIS.....13

**FIG. 3** SCHEMATIC DIAGRAMS SHOWING NUMB ISOFORMS STRUCTURE.....16

**FIG. 4** NUMB IN ENDOCYTOSIS AND RECYCLING.....19

**FIG. 5** TWO, NOT ALTERNATIVE, MODELS OF NOTCH INHIBITION BY NUMB.....24

**FIG. 6** NUMB-MEDIATED REGULATION OF THE HEDGEHOG PATHWAY.....27

**FIG. 7** MECHANISMS OF P53 TUMOR SUPPRESSION.....30

**FIG. 8** SCHEMATIC STRUCTURE OF P53 PROTEIN HIGHLIGHTING ITS MAIN FUNCTIONAL DOMAINS.....33

**FIG. 9** MODEL OF P53 ACTIVATION.....36

**FIG. 10** MECHANISMS OF MDM2 REGULATION OF ACTIVATED P53.....37

**FIG. 11** SCHEMATIC REPRESENTATION OF THE FULL-LENGTH MDM2 STRUCTURE.....38

**FIG. 12** DUAL SITE MECHANISM OF MDM2-P53 INTERACTION.....41

**FIG. 13** HOTSPOT MUTATIONS IN THE *TP53* GENE IN HUMAN CANCERS.....43

**FIG. 14** MULTIPLE STRATEGIES TO ACTIVATE THE P53 PATHWAY IN CANCER.....46

**FIG. 15** POSSIBLE MODEL OF NUMB INTERACTION IN A NUMB/HDM2/P53 TRICOMPLEX..49

**FIG. 16** THE EX3-ENCODED SEQUENCE REPRESENTS A NOVEL SURFACE IN THE NUMB PTB DOMAIN DYNAMICALLY INVOLVED IN MDM2 BINDING.....50

**FIG. 17** NUMB ISOFORMS STRUCTURE AND ROLE IN NOTCH REGULATION.....54

**FIG. 18** NUMB REGULATED SIGNALING PATHWAYS AND THEIR DEREGULATION IN CANCER CONDITION.....59

**FIG. 19** ROLE OF NUMB IN THE MAINTENANCE OF THE STEM AND PROGENITOR CELL POOLS IN THE MAMMARY EPITHELIUM.....61

**TAB. 1** PATIENTS CLINICAL-PATHOLOGICAL CHARACTERISTICS IN THE BREAST CANCER COHORTS ANALYSED.....71

**FIG. 20** PROGNOSTIC RELEVANCE OF P53 STATUS EVALUATED BY IHC IN THE IEO COHORT OF BCS.....77

<b>FIG. 21</b> NUMB ISOFORMS 1, 2, 3 AND 4 ARE THE MOST ABUNDANT IN THE BREAST CELL LINES MCF-10A AND BT-474.....	84
<b>FIG. 22</b> NUMB ISOFORMS 1, 2, 3 AND 4 ARE THE MOST ABUNDANT IN TUMORAL AND NORMAL PRIMARY BREAST CELLS.....	86
<b>FIG. 23</b> PTBi-CONTAINING NUMB ISOFORMS 1 AND 2 ARE ABLE TO BIND STRONGLY TO MDM2.....	88
<b>FIG. 24</b> SPECIFICITY OF ANTI-MDM2 PRIMARY ANTIBODY TESTED BY IB.....	89
<b>FIG. 25</b> ONLY PTBi-CONTAINING NUMB ISOFORMS ARE ABLE TO REGULATE P53 LEVELS..	90
<b>FIG. 26</b> PTBi-CONTAINING NUMB ISOFORMS ARE ABLE TO REGULATE THE P53 RESPONSE TO GENOTOXIC STRESS.....	93
<b>FIG. 27</b> NUMB PTBi-CONTAINING ISOFORMS REGULATE P53-MEDIATED DNA DAMAGE REPAIR UPON GENOTOXIC STRESS.....	93-94
<b>FIG. 28</b> RT-QPCR ANALYSIS OF THE MRNA LEVELS OF TOTAL NUMB, NUMB 1/2 OR NUMB 3/4 IN 13 PRIMARY BREAST TUMORS.....	96
<b>FIG. 29</b> THE RESPONSE OF PRIMARY BC CELLS TO GENOTOXIC TREATMENT CORRELATES WITH THE MRNA LEVELS OF NUMB 1/2.....	97
<b>FIG. 30</b> ANALYSIS OR SPECIFICITY OF THE TAQMAN ASSAYS USED FOR NUMB ISOFORM AMPLIFICATION .....	99
<b>FIG. 31</b> COMPARISON OF RELATIVE EXPRESSION LEVELS OF NUMB ISOFORMS DETECTED BY DIGITAL PCR AND RT-QPCR ON MRNA EXTRACTED FROM FFPE SAMPLES OF BCS.....	101
<b>FIG. 32</b> LOW TOTAL-NUMB STATUS CORRELATES WITH HIGHER RISK OF DISTANT RELAPSE.....	102
<b>FIG. 33</b> EXPRESSION OF NUMB 1/2 IS AN INDEPENDENT PREDICTOR OF PROGNOSIS IN LUMINAL-TYPE BCS WITH A P53 WT STATUS.....	104
<b>FIG. 34</b> LOW LEVELS OF NUMB ISOFORMS 1/3 AND OF NUMB ISOFORMS 2/4 CORRELATE WITH ADVERSE PROGNOSIS.....	106

# LIST OF ABBREVIATIONS

**aa** amino acids  
**ACD** Asymmetric cell division  
**AD** acidic domain  
**AJ** adherens junctions  
**AP1/ AP2** activating protein 1/ activating protein 2  
**aPKC** atypical protein kinase C  
**Arf 6** ADP- ribosylation factor 6  
**Aur-A** Aurora A  
**AVG** average  
**BC** Breast cancer  
**bp** base pairs  
**BSA** bovine serum albumin  
**CBF** C promoter binding factor 1  
**CBP** CREB-binding protein  
**CNS** Central Nervous system  
**Co-A** coactivator; Co-R corepressor  
**CSC** Cancer stem cell  
**CSL** CBF1/Suppressor of hairless/LAG1  
**Ctr** Control  
**DBD** DNA binding domain  
**DC** Daughter cell  
**ddPCR** droplet digital polymerase chain reaction  
**Disp** Dispatched  
**Dll4** Delta-like 4  
**DMEM** Dulbecco's modified Eagle medium  
**dNUMB** *Drosophila* Numb  
**DPF** aspartic acid-proline-phenylalanine  
**ECM** extracellular matrix  
**EGF** Epidermal growth factor  
**EH** Epsin15 homology  
**EHD** Epsin15 homology domain  
**EMT** Epithelial-to-mesenchymal transition  
**EPS15** Epidermal growth factor receptor substrate 15  
**FFPE** Formalin-fixed paraffine-embedded  
**FGF** Fibroblast growth factor  
**Forw. or fw** Forward primer  
**GMC** Ganglion mother cell  
**Hh** Hedgehog  
**HR** hazard ratio  
**HRP** horseradish peroxidase  
**IB** immunoblot  
**IEO** European Institute of Oncology  
**IF** Immunofluorescence  
**IHC** immunohistochemistry  
**LAG 1** Longevity assurance gene 1  
**LDLR** low density lipoprotein receptor  
**LGL** lethal giant larvae

**KD** knockdown  
**Mdm2** Murine double minute  
**MEC** Mammary epithelial cell  
**MEMB** mammary epithelial basal medium  
**Mut** mutated  
**NA** North American  
**NES** Nuclear export signal  
**NICD** Notch intracellular domain  
**NLS** Nuclear localization signal  
**NPF** asparagine-proline-phenylalanine  
**NPM** nucleophosmin  
**NSCLC** Non-small cell lung cancer  
**PAR** Partytioning-defective  
**PBS** Phosphate-buffered saline  
**aPKC** atypical Protein kinase C  
**P** p-value  
**PDX** patient derived xenograft  
**PIP** phosphoinosides  
**PM** Plasma membrane  
**PML** Promyelocytic leukemia protein  
**PNS** Peripheral nervous system  
**PRR** Prolin-rich region  
**pSer-276** Phosphorylated Serine 276  
**PTB** Phosphotyrosine binding domain  
**PTC** patched  
**PTM** Post-translational modification  
**Rbm** RNA binding motif  
**Rev. or rv** reverse primer  
**RITA** reactivation of p53 and induction of tumor apoptosis  
**RT** Room temperature  
**RT-qPCR** Real time quantitative Polymerase Chain Reaction  
**SA** South American  
**SC** Stem Cell  
**SCD** Symmetric cell division  
**SDS** Sodium dodecyl sulfate  
**SH3** Src homology 3  
**SHH** Sonic Hedgehog  
**SF** scaling factor  
**siRNA** silencing RNA  
**SOP** Sensory organ precursor cell  
**Smo** Smoothened  
**TAD** transactivation domain  
**TAE** Tris-Acetate EDTA  
**TBS** Tris-buffered saline ; TBS-T Tris-buffered saline tween  
**TD** tetramerization domain  
**TIC** tumor-initiating cell  
**TJ** tight junctions  
**Tm** melting temperature  
**TMA** tissue microarray  
**WT** wild type

# 1 ABSTRACT

Numb was originally identified as a determinant of cell fate in *Drosophila*, and more recently as a tumor suppressor in different human cancers. Our lab, in particular, has contributed to the characterization of Numb as a tumor suppressor. Indeed, we showed that Numb protein expression is lost in ~30% of breast cancers (BCs) and associates with an adverse prognostic outcome. At the cellular level, Numb loss results in uncontrolled proliferation, impaired response to genotoxic treatments and emergence and amplification of the cancer stem cell pool, while at the molecular level, it leads to enhanced Notch oncogenic signaling and reduced expression of the tumor suppressor protein p53.

Under physiological conditions, Numb acts to stabilize p53 protein by binding to and inhibiting the activity of Mdm2, the E3 ligase that mediates p53 ubiquitination and subsequent degradation. A detailed structural characterization of the Numb:Mdm2 binding interface, recently performed in our lab, has revealed that a short Numb region encoded by the alternatively spliced exon 3 was necessary and sufficient to bind to Mdm2 and prevent p53 degradation. This region is only present in two out of the four main Numb isoforms (Numb 1 and 2, hereafter referred to as Numb 1/2).

Based on these findings, we hypothesized that the tumor suppressor role of Numb might be mediated specifically by isoforms 1 and 2, and that altered splicing could represent a novel mechanism responsible for the functional loss of Numb in tumors.

To test these possibilities, we performed a series of experiments aimed at elucidating the specific roles of Numb isoforms in cancer and their contribution to tumorigenesis. In particular, we characterized Numb isoforms expression in BC cells and investigated the involvement of the expressed isoforms in the regulation of the p53 pathway. Our results

point to the exclusive role of Numb 1/2 isoforms in the regulation of the Mdm2-p53 circuitry. Loss of Numb 1/2 in p53-WT BCs leads to reduced p53 levels and activity and an accumulation of DNA damage upon genotoxic stress. Accordingly, primary BC cells, displaying reduced levels of Numb 1/2, exhibited increased chemoresistance, indicating that Numb splicing patterns could influence therapy response in BC patients.

Moreover, we performed a large-scale RT-qPCR-based screening of a case-cohort of 890 breast tumors to uncover the impact of the different Numb isoforms on clinical outcome. We unmasked an increased risk of distant metastasis in patients expressing low levels of Numb 1/2, which was more evident in the p53-WT BCs, in accordance with our results on the role of Numb 1/2 in p53 regulation. A similar prognostic effect was also observed in BCs displaying low levels of total Numb mRNA, revealing that, alongside the well-characterized mechanism of Numb hyperdegradation, also pre-translational mechanisms contribute to Numb loss in BC. Our analysis also revealed worse prognosis in BC patients displaying low levels of Numb isoforms 1/3 and 2/4 (with or without the exon 9 coded-region, respectively), suggesting a more complex scenario, in which the differential role of Numb isoforms in pathways other than p53, such as the Notch pathway, might contribute to tumorigenesis. Together, our results indicate that the aberrant alternative splicing of Numb towards exon 3 skipping events (leading to a reduction in Numb 1/2 levels), could increase chemoresistance and contribute to tumor progression in p53-WT BCs. Moreover, additional layers of Numb deregulation, independent of hyperdegradation, could account for loss of Numb in BCs. These findings offer new strategies for stratifying BC patients according to Numb status, and possibly new therapeutic options to re-establish the Numb-p53 physiological circuitry in breast tumors.

## 2 INTRODUCTION

This thesis explores the role played by the different isoforms of the protein Numb and, in particular, their involvement in tumorigenesis. In this introduction, I will provide an overview of the different Numb functions, starting from its discovery as a cell fate determinant in *Drosophila* (Section 2.1) and ending with its well-characterized role as an endocytic adaptor protein and, more recently, as a tumor suppressor (section 2.4). A particular focus will be placed on the latter point and the Numb-Mdm2-p53 circuitry (section 2.3.4), considering the key role that this circuitry plays in the cell and how its deregulation has a profound impact on tumorigenesis (section 2.3.4.5). Finally, the last part of the introduction will be focused on the consequences of loss of Numb in cancer to provide the rationale for possible therapeutic interventions in Numb-deficient tumors (section 2.3.4.6).

### **2.1 NUMB FROM ITS DISCOVERY...THE LESSON FROM *DROSOPHILA***

Numb was originally identified as a cell fate determinant during *Drosophila* nervous and muscle system development<sup>1</sup>. Loss of functional protein in *Drosophila* mutants causes flies to become “numb”, since it dramatically affects sensory neuron maturation during peripheral nervous system (PNS) development<sup>2</sup>. The complex molecular mechanisms involved in the generation of the bristle sensory organ is organized as a hierarchical pattern of asymmetric cell divisions (ACD) from a sensory organ precursor (SOP) cell to give rise to all the differentiated cells that constitute the architecture of the external sensory organ, a component of the PNS<sup>3</sup>.

Numb is uniformly distributed in the cytosol of the SOP cell during interphase and then is asymmetrically distributed towards one of the spindle poles during cytokinesis. This event drives the acquisition of alternative developmental fates in the daughter cells (DCs)<sup>4</sup> (Fig. 1). Alteration of this asymmetry, by either overexpression or depletion of Numb in *Drosophila* results in cells acquiring the same cell identity.

Also at the level of the stem cell (SC) compartment, it has been shown that Numb segregates asymmetrically during cell mitosis and this event ultimately has an impact on the DC fates, both in *Drosophila*<sup>5,6</sup> and in mammal neuroblasts<sup>7</sup> (see paragraph 2.4.1) (Fig. 1).

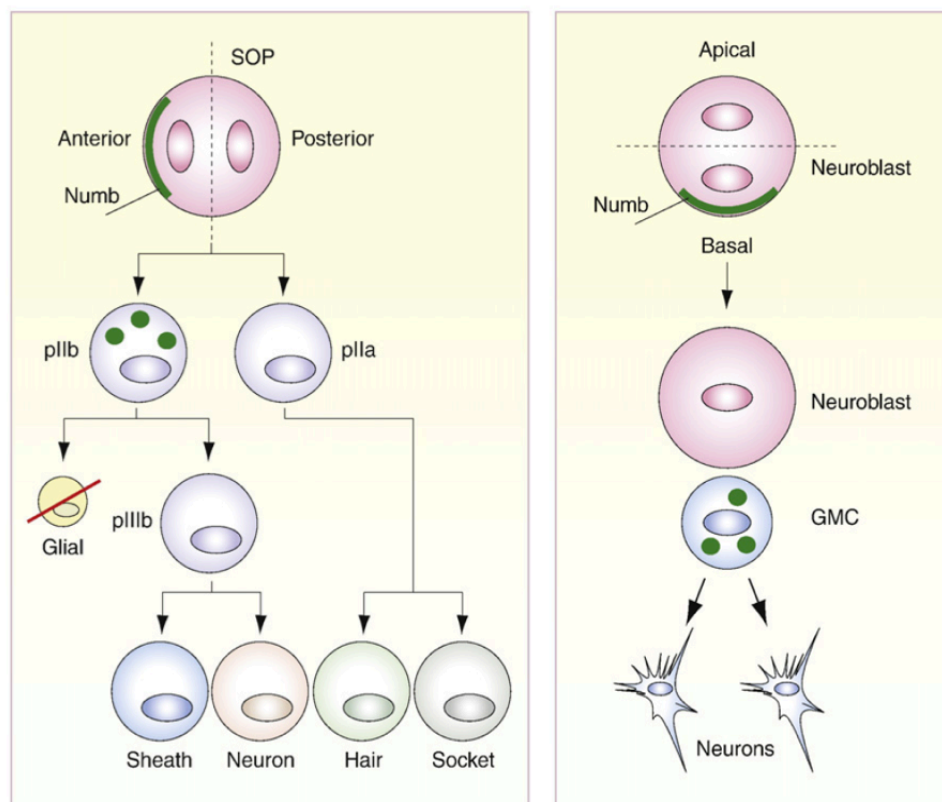


**Fig. 1 Numb asymmetric division in *Drosophila* SOP and neuroblasts**

The figure shows Numb asymmetric partition in *Drosophila* SOP cell (left) and central nervous system (CNS) neuroblast (right) cell division. The orientation of the plane of division is indicated. Numb is depicted in green, as a crescent in the dividing SOP and in the neuroblast, or as spheres in the pIIb cell (one of the daughter cells derived from SOP division) and in the ganglion mother cell (GMC) where it accumulates after the first asymmetric cell division (ACD). For simplicity, only the first ACD in both lineages is depicted in detail. However, all other divisions are asymmetric and, at least in the SOP lineage, involve asymmetric partitioning of Numb. Details are in the main text. Figure from<sup>2</sup>.

Despite the initial focus on the role of Numb in neurogenesis and in SC regulation, another aspect that emerged early in Numb studies in *Drosophila* is its molecular counteraction of Notch (see paragraph 2.3.2) that affects the differentiative-proliferative balance in nervous system and partially justifies Numb being labeled as a tumor suppressor gene.

In conclusion, the extensive research on the neurogenic function of Numb highlighted the critical role of Numb in the regulation of cell fate in SC compartments, and its inhibition over Notch, two roles that also open important questions: i) how is the asymmetric localization of Numb determined, and ii) how does Numb work at the molecular level?

Concerning the first point, great interest was placed in clarifying how Numb partition is generated. The major components of the polarity machinery involved in the asymmetric partition of Numb at mitosis, during ACD, were intensively studied and are conserved between flies and mammals. The process seems to be orchestrated by PAR (par-titioning – defective) proteins. In *Drosophila*, as in mammalian neurons, this complex includes the proteins Par3 (Bazooka in *Drosophila*) Par6 and aPKC (atypical protein kinase C) that localize asymmetrically in correspondence with one of the spindle poles: posteriorly in SOP cells, apically in neuroblasts of the *Drosophila* central nervous system (CNS) (Fig. 1), and basally in neuroblasts of mammals CNS<sup>2</sup>. At the onset of mitosis, Aurora A is activated, which triggers a kinetic cascade that leads to the phosphorylation of Numb by aPKC<sup>8,9</sup> (Fig. 2A). Direct phosphorylation of Numb by aPKC is sufficient to displace Numb from the pole where aPKC is localized<sup>10</sup>. In this way Numb accumulates at the opposite pole together with other intrinsic cell fate determinants, such as Mira, Prospero and Pon<sup>11,12,13,14</sup> (Fig. 2B). Phosphorylation of Pon by Polo kinase is also involved in Numb localization, but the

mechanisms need to be better elucidated<sup>15</sup>.

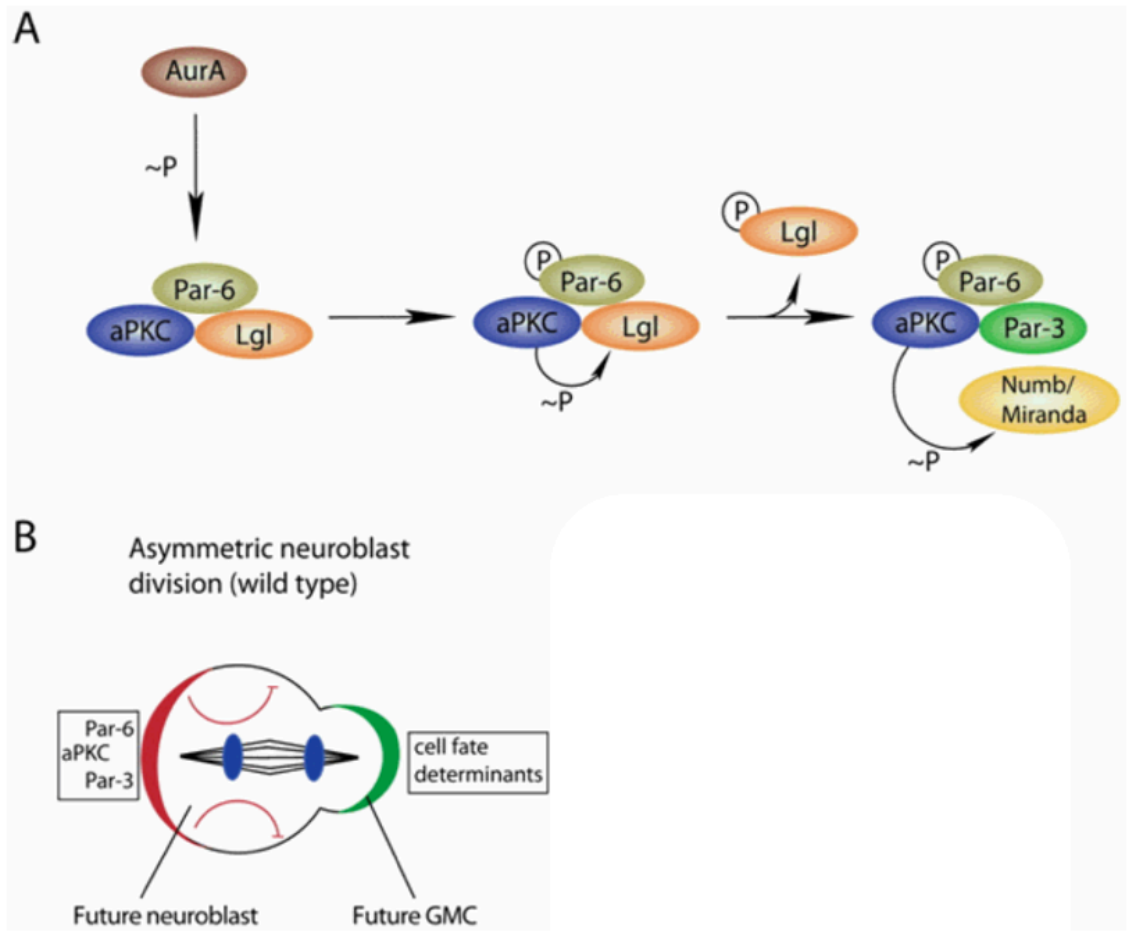


**Fig. 2 PAR complex orchestrates Numb asymmetric partition at mitosis.**

**A)** At mitosis, Aurora-A (AurA)–mediated phosphorylation of Par-6 leads to activation of aPKC kinase activity on Lethal giant larvae (Lgl). Phosphorylated Lgl is excluded from the complex, which allows entry of Par-3 into the Par complex. This complex remodeling is associated with an alteration of the aPKC substrate specificity towards Numb and Miranda, which are phosphorylated by aPKC. **B)** In neuroblasts, phosphorylated Numb is excluded from the cell side occupied by aPKC (red crescent) and accumulates on the opposite site of the plasma membrane (green crescent) with other cell fate determinants. The ratio of apical/basal determinants specifies identity in each daughter cell (DNA, blue). Figure adapted from<sup>12</sup>.

Deregulation of the expression of PAR complex components can alter physiologic developmental decisions and tissue morphogenesis by compromising Numb segregation at cell mitosis and consequently the fates in stem/progenitor cells. The exact elucidation of

these mechanisms and the molecular players that crosstalk with Numb to trigger the cell fate choice requires further studies. Nevertheless, it is clear that a number of pathways that control stem/progenitor cell development have been described to involve Numb and they will be the object of an in-depth analysis in paragraphs 2.3.2, 2.3.3, 2.3.4.7.

## 2.2 NUMB STRUCTURE

The vertebrate homologues of *Drosophila* Numb (dNumb) are represented by Numb and Numb-like proteins<sup>16</sup>. These proteins belong to an evolutionary conserved protein family and show some redundant roles during early neurogenesis<sup>17</sup>. The structural similarity between Numb and Numb-like is present throughout the protein, with a strong sequence similarity, particularly, in the N-terminal region, which displays also strong similarity with the N-terminal portion of dNumb.

The structure of Numb resembles a scaffold protein composed of different protein-protein interactor domains. Mammalian Numb protein is composed of an N-term phosphotyrosine binding (PTB) domain, followed by a proline-rich region (PRR) containing different putative Src homology 3 (SH3) domain-binding sites, along with an NPF (asparagine-proline-phenylalanine) and two DPF (aspartic acid-proline-phenylalanine) motifs at the C-terminal responsible for binding to the EH (Eps homology) domain of endocytic proteins<sup>16</sup>.

In general, looking at Numb domain composition, Numb displays a structural similarity to the *bona fide* cargo selective adaptors, DAB2 and ARH. In particular, these proteins share a highly related PTB domain supporting the concept that Numb belongs to the same protein functional family<sup>2</sup>. The PTB domain is highly represented in protein domain structures, has a globular folding and is highly conserved in the two mammalian homologue proteins. In

particular, Numb PTB is able to interact *in vivo* with multiple target proteins involved in several biochemical roles. Moreover, Numb PTB is able to recognize ligand peptides that differ in primary amino acid sequence and secondary structure<sup>18</sup>.

Differently from other PTB domains, such as those of Shc and IRS-1, Numb PTB does not require tyrosine phosphorylation for high affinity peptide binding and seems to display a wide interaction specificity mediated by a flexible hydrophobic groove. This allows the backbone structure of PTB to be able to adopt different tertiary conformations adapted by a wide range of intermolecular binding partners<sup>18</sup>.

These structural considerations provide insights into the broad involvement of Numb in signaling regulation and in coordination of the biochemical network of protein-protein interactions.

An additional layer of complexity in Numb structure is related to the different lengths of the Numb PTB displayed in the four most abundantly expressed Numb splice variants expressed in mammals as a result of alternative splicing events. Although nine Numb isoforms have been described, only the four main isoforms are well-characterized since they are expressed in different tissue models. These four isoforms differ in their retention or skipping of exon 3, comprised of 33 nucleotides (11 amino acids), in the N-terminal PTB domain-encoding region of Numb, and of exon 9, comprised of 144-nucleotides (48 amino acids), in the C-terminal PRR-encoding region<sup>19,20</sup> (see paragraph 2.3.6 and Fig. 3).

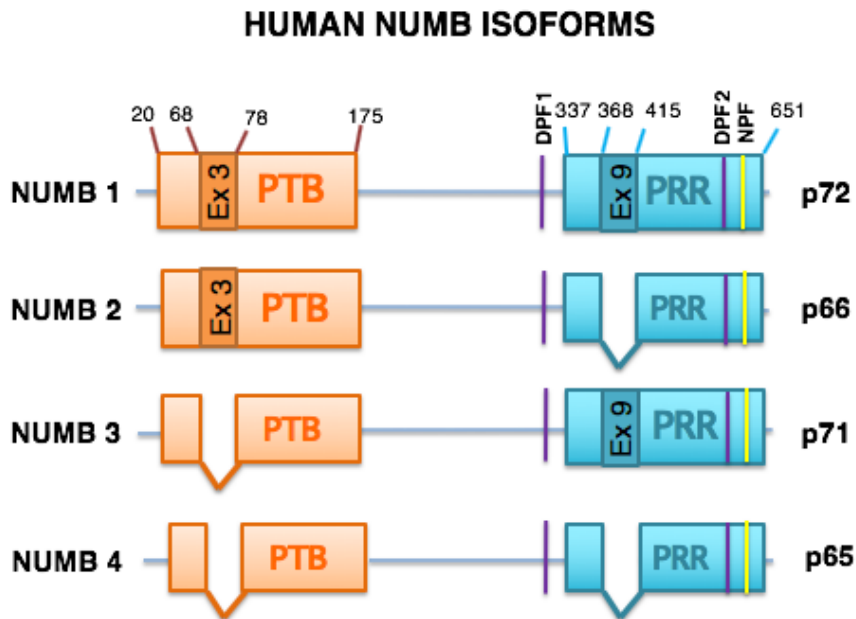


**Fig. 3 Schematic diagrams showing Numb isoforms structure**

Human Numb isoforms 1/2/3/4 (p72, p71, p66, p65 respectively) structure showing the main protein-protein interactor domains: phosphotyrosine binding domain (PTB, light orange), the proline-rich region (PRR, light blue), and the DPF1, DPF2, and NPF motifs. Exon numbering starts from the first Numb codifying exon. In dark orange, the alternatively spliced exon 3 within PTB domain. In dark blue, the alternatively spliced exon 9 within PRR domain. DPF1 and DPF2: aspartic acid-proline-phenylalanine motifs. NPF: asparagine-proline-phenylalanine motif.

## 2.3 THE MULTIPLE NUMB FUNCTIONS

### 2.3.1 NUMB AND ENDOCYTOSIS

Although the majority of research on Numb has focused on its role in cell fate specification and signaling regulation (see paragraphs 2.3.2, 2.3.3, 2.3.4.7), the wide pattern of Numb expression in almost all tissues suggests a general role of Numb in cell homeostasis. Clues about a more general role of Numb in basic cellular processes come from observations on

i) the Numb protein modular domain structure and ii) Numb subcellular localization in endocytic organelles, described in detail below. Both observations suggest the possibility that Numb acts as an endocytic adaptor protein interacting with several components of the endocytic machinery.

*i) Numb protein modular domain structure.* The Numb motifs, DPF and NPF (Fig. 3), have been shown to mediate interactions with endocytic proteins. Specifically, Numb DPF motifs at the C-terminal of the protein mediate the interaction with the main clathrin adaptor AP2 (specifically, the  $\alpha$ -adaptin subunit) in endocytic clathrin-coated pits<sup>21</sup>, while the NPF motif is important for binding to Epsin15 homology domain (EHD) containing proteins, Eps15 and Eps15R, which act as adaptors in clathrin-dependent and -independent endocytosis, as well as in vesicle transport<sup>22,23</sup>. The Numb NPF motif is also required for the interaction with the endocytic proteins, Epsin 15 homology domain 1 and Epsin 15 homology domain 2 (EHD1 and EHD4), which are involved in recycling vesicles back to the plasma membrane, in order to return their cargo (membrane proteins or receptors) to the cell surface<sup>24</sup>. By affecting vesicles recycle, Numb is involved in spatial regulation of signaling<sup>25</sup>. Moreover, the Numb PTB domain has been shown, both in *Drosophila* and mammalian proteins, to bind to the intracellular domains of transmembrane proteins, promoting receptor recruitment<sup>2</sup>. Via these domains/motifs, Numb has been shown to interact with, and be involved in the regulation of transferrin receptor<sup>26</sup>, LDLR (low density lipoprotein receptor)<sup>26</sup>, cell adhesion molecules (e.g., L1 in neurons)<sup>27</sup>, integrins (B1 and B2)<sup>28</sup>, and Notch<sup>29,30</sup>, being co-trafficked with these internalized receptors and membrane proteins<sup>2</sup> (Fig. 4).

ii) *Numb subcellular localization in endocytic organelles.* The role of Numb at various stages of endocytosis is suggested by its temporally coordinated co-localization with AP2 and Eps15 in clathrin-coated pits and early endosomes<sup>21</sup>, and by its localization in Arf6 GTPase-containing vesicles, which are known to represent recycling endosomes<sup>24</sup>. These subcellular localizations have suggested a role of Numb as a cargo selective adaptor, acting at the internalization step of endocytosis and in endosomal trafficking of transmembrane receptors<sup>2</sup>. Moreover, Numb has been characterized as a negative modulator of Arf6-dependent endocytic recycling<sup>24,25</sup>

The first indications of an endocytic function of Numb were linked to its role as a cell fate determinant in the SOP system. The identified mechanism also explains Numb-mediated inhibition of Notch signaling (see paragraph 2.3.2). Similarly to Numb, the AP2 subunit,  $\alpha$ -adaptin, was demonstrated to be asymmetrically segregated in the SOP lineage<sup>31</sup>. Mutation of  $\alpha$ -adaptin phenocopies loss of Numb, similarly affecting the bristle morphology in *Drosophila*<sup>31</sup>. Moreover, in the SOP system, Numb was required for the internalization of Sanpodo, a membrane protein important for Notch activity<sup>32,16</sup>(Fig. 4). These results suggested that the retention of the Numb/ $\alpha$ -adaptin axis could have an impact on Notch polarized endocytosis and on its signaling asymmetry in DCs.

Of note, also Numb negative regulation of receptor and ligands recycling might also explain Numb-mediated counteraction of Notch<sup>33</sup>. It has been shown that in myoblast cells, Numb seems to promote the sorting of Notch receptor to late endosomes for degradation, thus, inhibiting its signaling. The downmodulation of Numb, instead, directs Notch to recycling vesicles, thus, enhancing Notch signaling<sup>34</sup> (see paragraph 2.3.2 and Fig. 4).

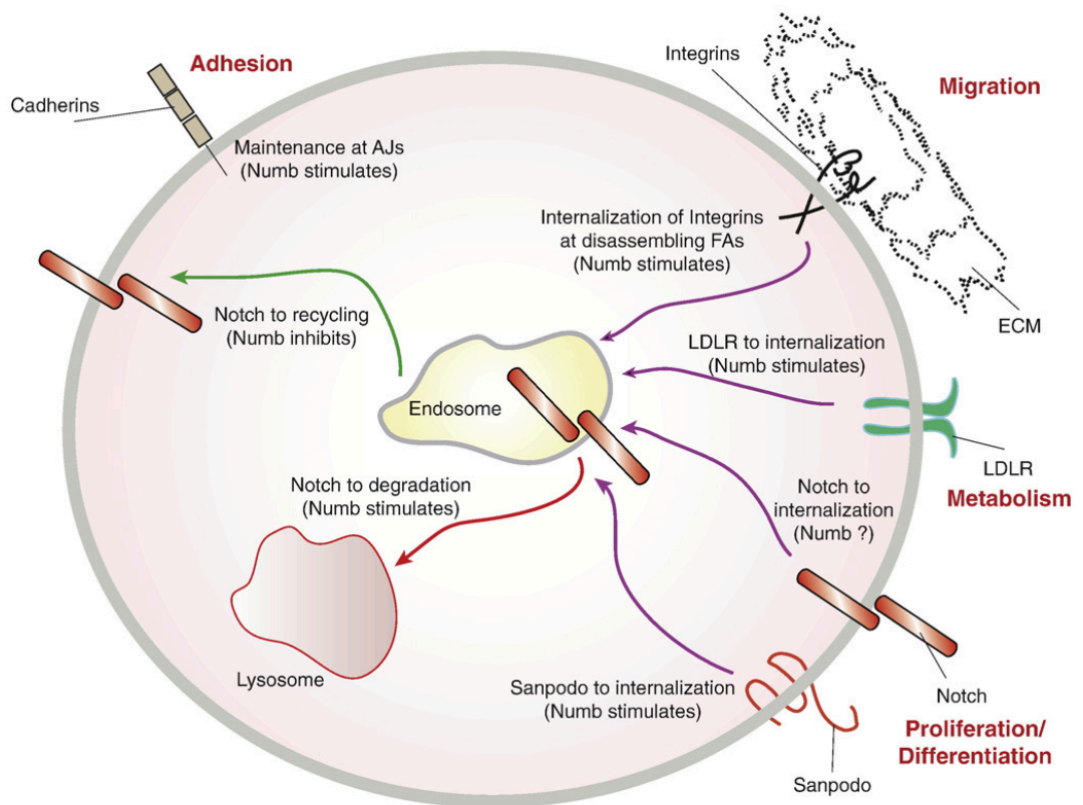


**Fig. 4 Numb in endocytosis and recycling.**

The figure shows examples of cellular phenotypes controlled by Numb endocytic functions (in red: migration, adhesion, proliferation/differentiation, metabolism). Internalization (violet arrows), degradative (red arrows) and recycling routes (green arrows) highlight the multiple roles of Numb in vesicular intracellular traffic. AJs, adherens junctions; FAs, focal adhesions; ECM, extracellular matrix; LDLR, low-density lipoprotein receptor. Figure from <sup>2</sup>.

To summarize, Numb function in the endocytic machinery seems to be at the basis of its role in signaling, especially in Notch regulation (see paragraph 2.3.2), and to explain several Numb-related phenotypes affecting cell fate specification, proliferation, differentiation, survival and stem cell homeostasis.

## 2.3.2 NUMB AND THE NOTCH PATHWAY

The Notch signaling pathway is a highly conserved developmental network involved in cell fate determination, homeostasis of the SC compartment, and regulation of the proliferative/differentiative balance during development and in adult tissue homeostasis<sup>35</sup>.

Notch signaling functions as an essential mechanism to direct cell fate decisions of neighboring cells through cell-cell physical interactions. Trans-interaction between receptors and ligands, present on opposing cells, represent activating events of the Notch signaling pathway.

Notch is an evolutionary conserved transmembrane receptor localized on the signal-receiving cell. It binds directly to ligands of the DSL family (Delta, Serrate, Lag-2 in mouse; DLL1, DLL2, DLL3, Jagged 1/2 in human) located, as integral membrane proteins, on the opposing signal-sending cell<sup>2</sup>. Receptor-ligand engagement triggers a cascade of proteolytic cleavage events that concludes with the cleavage of Notch itself by  $\gamma$ -secretase. These steps are critical for Notch maturation and signal transmission, and culminate in the cleavage of the entire Notch intracellular domain (NICD) from the cell membrane and its translocation into the nucleus, where it acts with the CSL transcription complex composed by C promoter binding factor 1 (CBF-1)/Suppressor of Hairless/Longevity assurance gene-1 (LAG-1), Mastermind and other coactivators to drive the expression of the Notch target genes<sup>36</sup> (Fig. 5). The biological outcome of Notch signaling is far from being fully understood and results from different model systems are often contradictory.

In the regulation of Notch signaling, a central role has been assigned to Notch endosomal processing and trafficking at different stages of the signaling pathway. Of the proteins that guide endocytic trafficking of Notch receptor upon activation in signal-receiving cells, Numb and Sanpodo interplay to directly regulate Notch availability and activity.

Numb was originally identified as an inhibitor of Notch signaling in *Drosophila*. Indeed, Numb loss-of-function phenocopies Notch gain-of-function and this confirms their epistatic relationship<sup>37</sup>. The Numb-Notch axis is important in both *Drosophila* and mammals, in CNS development and in ACD of SCs. During ACD of SCs, Numb is asymmetrically partitioned at mitosis: the DC that receives Numb is unresponsive to Notch signaling, while the DC that loses Numb retains responsiveness to Notch and adopts the cell fate associated with Notch activation. A broad model of the molecular mechanisms governing this Numb-mediated inhibition of Notch has been deduced.

The first clues to the mechanism came from the characterization of the SOP system in which the endocytic function of Numb accounts for its biological antagonism of Notch (see paragraphs 2.3.1). Numb can indeed suppress Notch function by controlling Notch intracellular trafficking and consequently its potential activation. In the *Drosophila* neural system, this effect is mediated by Sanpodo. Sanpodo is a transmembrane protein expressed only in asymmetrically dividing cells<sup>38</sup>. It is required for Notch signaling activation, and it interacts with both Notch and Numb. Numb, on the other hand, interacts with the endocytic proteins, AP2 and Eps15, and by doing so it works as an adaptor protein mediating endocytosis of Sanpodo<sup>39</sup>. Numb asymmetrically distributes at cytokinesis of the SOP cell. This results in Sanpodo removal from plasma membrane, through internalization, in the SOP daughter cell that retains Numb (Fig.4)<sup>38,29</sup>, causing inhibition of Notch signaling, and preventing the acquisition of a neuroblast cell fate<sup>2</sup>. In contrast, in the stem daughter cell, Numb is excluded and, consequently, Sanpodo is stabilized at the level of the plasma membrane and Notch is highly expressed, leading to the acquisition of a neuroblast cell fate. Inhibition of Notch signaling in the SOP system results in neuroblast depletion, while its overexpression in progenitor daughter cells leads to their de-differentiation back to a

neuroblast fate. Thus, in this system, the Numb/Notch axis is decisive in committing cells to specific fates.

Although mammalian cells do not express Sanpodo, the general mechanism of Numb-mediated inhibition of Notch is conserved. Mammalian Notch is constitutively internalized and either recycled back to the plasma membrane or trafficked to the late endosomal compartment for degradation<sup>40</sup> (Fig.5). It has been demonstrated that changes in Numb expression alter the dynamics of late endocytic trafficking of Notch. Overexpression of Numb promotes Notch sorting to late endosomes/lysosomes for degradation, whereas its depletion facilitates its recycling to plasma membrane<sup>34</sup>. These observations suggest that Numb behaves like a molecular sensor that modulates the responsiveness of cells to Notch ligand. Thus, under pathological conditions, loss of Numb could impose Notch hyper-activation due to increased receptor recycling and enhanced cell responsiveness to Notch activating signals (see paragraph 2.4)

In mammals, Numb antagonizes Notch also by controlling the intracellular trafficking and stability of the Notch ligand, Delta-like 4 (Dll4). It acts as a post-endocytic sorting switch, negatively controlling recycling to the plasma membrane through AP1 and, instead, increasing Dll4 delivery to lysosomes for degradation<sup>33</sup>. In this way, Numb limits Notch signal transmission from the signal-sending cell. In this complex scenario, the endocytic role of Numb is fundamental to remove or recycle molecules from specific plasma membrane domains for the execution of polarized functions. Numb is involved in creating multiple levels of asymmetry relevant for directional signaling (in the case of Notch signaling, at the level of cell-cell interface) or for asymmetric activation of cell fate determinants following ACD.

These findings about the endocytic function of Numb in Notch signaling regulation have been complemented by several lines of evidence suggesting an additional tier of Numb regulation on Notch signaling via the ubiquitin-proteasome degradation pathway. Numb interacts with NICD and promotes its ubiquitination driving its proteasomal degradation, thus, resulting in attenuation of Notch signaling <sup>41</sup> (Fig. 5). Numb recruits Itch (HECT domain-containing E3 ligase), a component of the ubiquitination machinery to the cell membrane-tethered Notch 1 receptor, thereby cooperatively enhancing Notch ubiquitination and degradation, ultimately, leading to downregulation of Notch signal transduction <sup>41</sup>.

Inappropriate activation of Notch has been reported as oncogenic signal associated with various types of cancer, including colon, pancreatic, lung and breast cancer, acute myeloid leukemia and glioblastoma <sup>42,43,44,45</sup>. Of note, the role of Notch as an oncogene conceptually underlines that, at the molecular level, its upstream regulator Numb, has a tumor suppressor role in different cancer contexts (see paragraph 2.4).

In conclusion, tight regulation of the Numb-Notch axis is essential for preventing potential pro-tumorigenic events that could result from its deregulation. Although the main mechanisms of Numb inhibition of Notch have been depicted here, the overall, context-dependent scenario is still far from being completely unraveled.

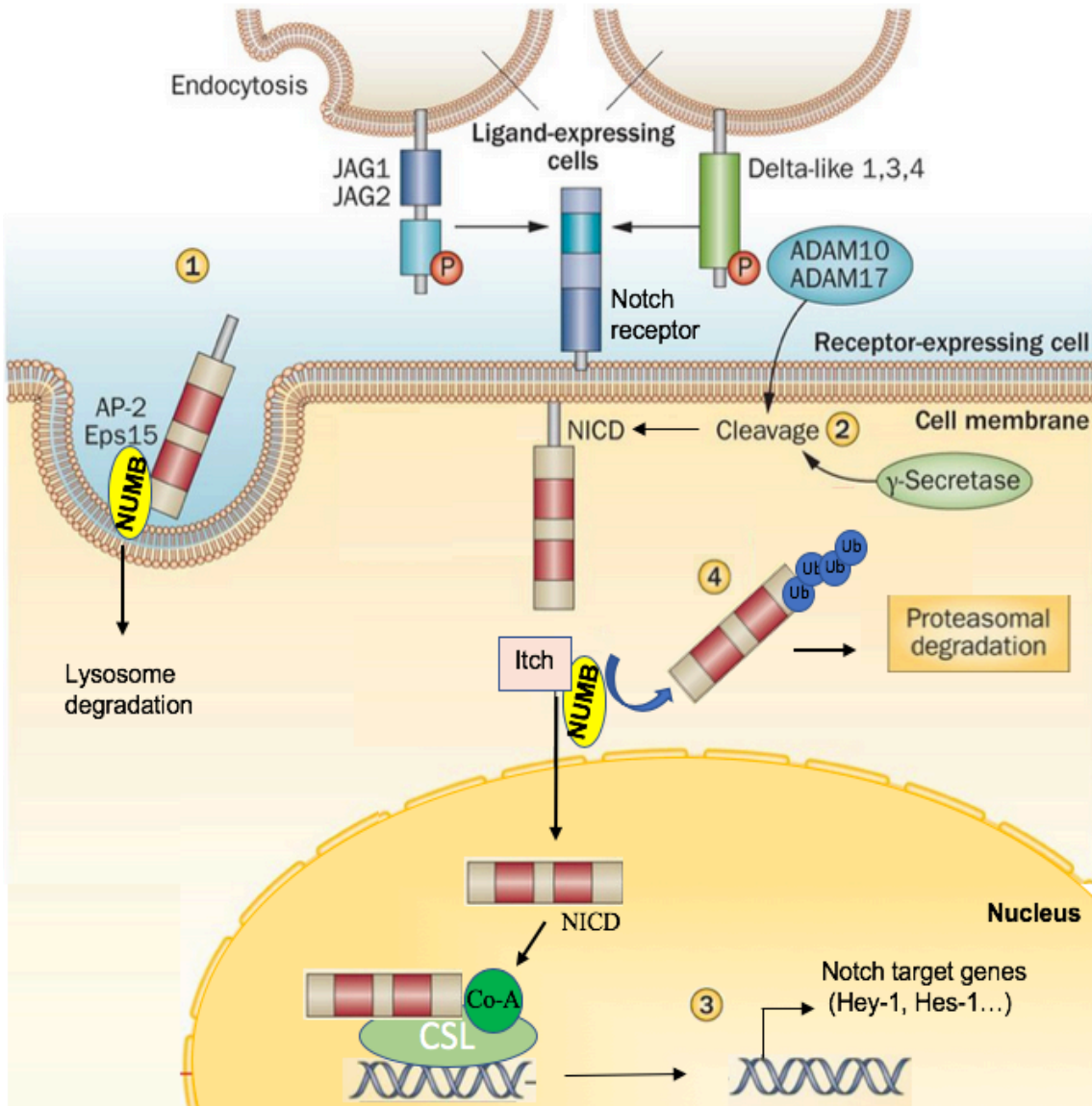


**Fig. 5 Two, not alternative, models of Notch inhibition by Numb.**

Numb interacts with AP-2 and Eps15 to downregulate Notch receptor signaling by clearing Notch from the surface of receptor-expressing cells. In the same way, Numb targets Sanpodo, required for Notch activation, for endocytic removal from the plasma membrane (not shown)(1). Notch signaling activation is initiated by the binding of Notch ligands (Delta-like 1-3-4, Jagged [JAG1, JAG2]) to Notch transmembrane receptors 1–4, which undergo a series of proteolytic cleavages, by ADAM family proteins (ADAM 10, ADAM 17) and a  $\gamma$ -secretase complex, which lead to the release of the Notch intracellular domain (NICD) (2). The NICD translocates to the nucleus, where it interacts with CSL and converts the complex from a repressor (Co-R CSL) to an activator of Notch target genes (Co-A CSL), such as Hes-1 and Hey-1 (3). Numb prevents translocation of NICD into the nucleus targeting NICD for Itch-mediated ubiquitination and consequent proteasomal degradation (4). Figure adapted from <sup>46</sup>.

### 2.3.3 NUMB AND HEDGEHOG PATHWAY

The Hedgehog (Hh) signaling pathway (which takes its name from the Hh ligand, rather than the receptor) plays an important role in tissue patterning, SC regulation and cancer<sup>47</sup>. Hh is a morphogenic molecule that is necessary for the development of different tissue types, including bone, brain, skin, gonads, and lungs. Consequently, its cell distribution and pathway activation need to be strictly regulated<sup>48,49,50</sup>. In *Drosophila*, Hh mutants display an abnormal development and give rise to unusually hairy and stumpy larvae compared to wild-type, resembling the hedgehog animal from which it derives its name<sup>51,47</sup>. In mammals, Hh exists as 3 variants: Sonic (SHH), Indian and Desert<sup>51</sup>. Despite some differences in the signaling effectors between *Drosophila* and mammals, the main core components of the Hh pathway remain quite conserved.

Hedgehog ligand are composed by two main domains: the N-terminal "Hedge" domain that functions as a signal-transmitting domain and a processing C-terminal "Hog" domain, involved in the autocatalytic intramolecular cleavage of the Hedgehog ligand. The Hedge domain is modified by the addition of a cholesterol moiety at its C-terminal<sup>52</sup> and by palmitate addition to the N-terminal by an acetyl transferase enzyme. These modifications allow the interaction of Hedge with lipoproteins. The modified fully active "Hedge" domain is then released from cell membrane of signal producing cell thanks to the activity of Dispatched (Disp) and acts as signaling molecule (Hh, from hereafter) in the extracellular space<sup>50</sup>.

Hh interaction with its membrane receptor, Patch, in signal receiving cell, abrogates Patch inhibition of Smoothed (Smo), a G-coupled protein receptor. Smo, in turn, undergoes a conformational change that allows the activation of a signaling cascade that converges on

increasing transcription factor activity of Ci, in *Drosophila*, or of its mammalian homologues, Gli proteins (Gli1, Gli2, Gli3). Gli activity is regulated in a very similar way to that observed in *Drosophila*. In absence of Hh ligand, Gli proteins are phosphorylated and processed, and in their truncated form result inactive. Addition of Hh leads to inhibition of processing of Gli proteins and their accumulation as full-length active form of proteins. Of note, Gli1 e Gli2, upon activation, act as transcriptional activators of Hh target genes, while Gli 3 acts as a transcriptional repressor<sup>50,53</sup>. The strength and duration of Hh signaling is strictly regulated by the ubiquitin-dependent proteolytic processing of Gli proteins. The Hh cascade induces different set of target genes encoding secreted signaling protein involved in cell growth and division and many transcription factors that are essential for developmental processes.

The role of Numb in this context is to suppress Hh signaling, thereby arresting cell growth and promoting cell differentiation. Numb interacts with the E3-ubiquitin ligase, Itch, promoting its ubiquitination of Gli1<sup>54,55</sup> (Fig. 6A). This results in Gli1 degradation and consequently decreased transcriptional activity leading to downregulation of Gli1 target genes, such as cyclin D2, IGF-2, N-Myc and Bmi-1<sup>54,55</sup> (Fig. 6A). This mechanism is reminiscent of that already discussed for the inhibition of Notch signaling in mammals (see paragraph 2.3.2)

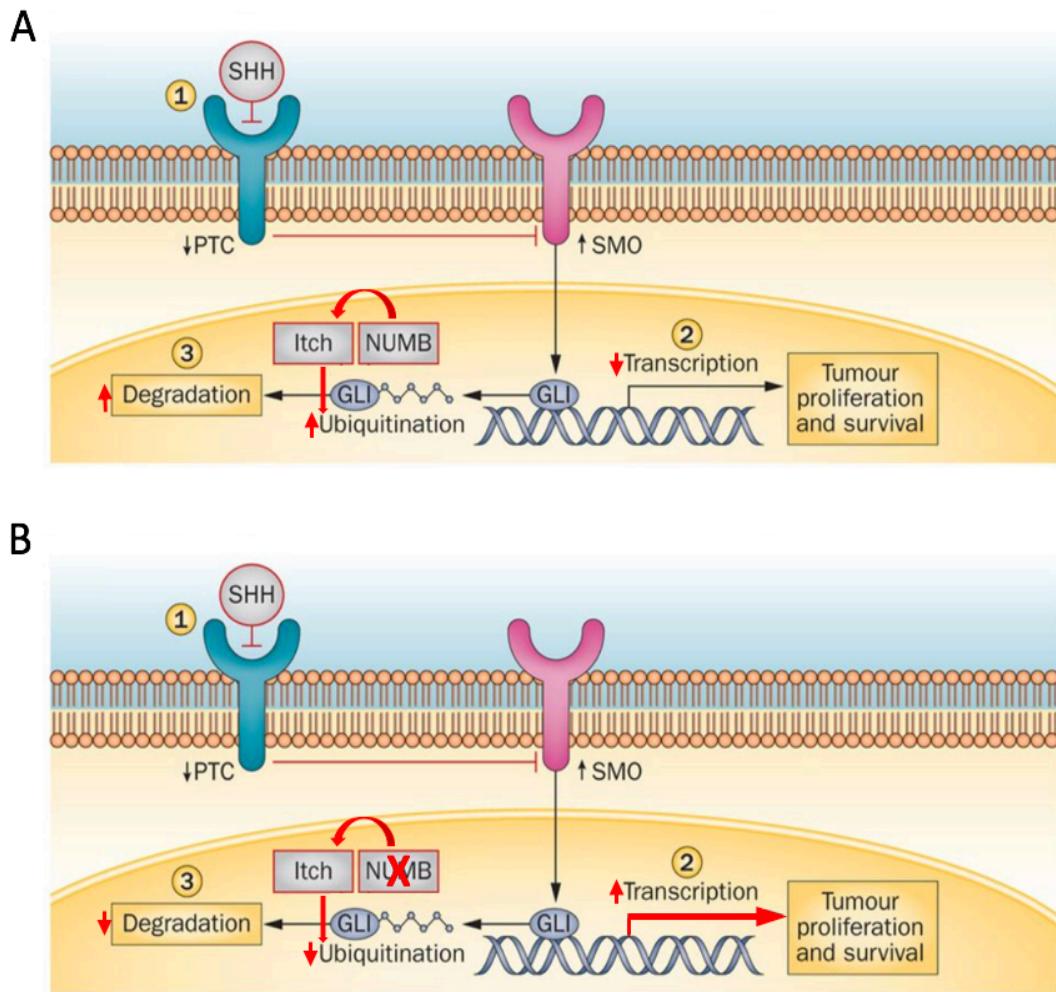


**Fig. 6 Numb-mediated regulation of the Hedgehog pathway.**

Sonic hedgehog (SHH) binds to the receptor Patched (PTC) and inhibits its repression of Smoothed (SMO)(1). Activated SMO translocates to the nucleus and triggers the nuclear activity of the GLI transcription factors. GLI proteins regulate Hh target gene expression, promoting tumor proliferation and survival (2). **A**) Numb activates Itch ubiquitin-ligase activity on GLI proteins, targeting them to proteasomal degradation (3). **B**) Numb downregulation negatively affects Itch activation, leading to increased GLI protein half-life and increased transcriptional activation of Hh target genes. Figure adapted from <sup>46</sup>.

The described mechanism highlighted a pro-differentiation, anti-proliferative effect of Numb in tumor cells due to suppression of functional Gli activity (Fig. 6B). Aberrant activation of the Hh signaling can enhance survival and proliferation of cells, inducing tumorigenesis and metastasis formation <sup>56-60</sup>. Aberrant activation of the Hh pathway is indeed associated with different solid cancers <sup>57,58,59,61</sup> and can be induced by ligand-

independent constitutive activation or hyper-expression of Hh pathway players<sup>62</sup>. Numb deregulation is an additional regulator of Hh signaling activation. Therefore, the subversion of the Numb-Hh axis could be relevant to tumorigenesis. Moreover, since a signaling crosstalk between Notch and Hh is involved in normal developmental processes, as well as in tumorigenesis, an interesting scenario emerges in which Numb might act as a master regulator of two fundamental and intimately integrated morphogenetic systems. The obvious consequence of this is a profound and concomitant alteration of these mechanisms in tumors displaying Numb dysfunction (see paragraph 2.4).

## **2.3.4 NUMB AND THE p53-MDM2 CIRCUITRY**

A previous work in our lab has demonstrated the involvement of Numb in the regulation of the tumor suppressor p53, by the ability of Numb to bind and inhibit the ubiquitin ligase Mdm2<sup>63</sup>. This has profound implications in BC tumorigenesis, where a reduction of the p53 activity was observed in Numb-deficient BCs<sup>63</sup>. In the next paragraphs will be discussed the key role that p53 plays into the cell and the complex circuitry involved in its regulation, the alterations of this pathway in cancers and what is known about the function of Numb in the p53 regulation.

### **2.3.4.1 THE ROLE OF THE TUMOR SUPPRESSOR p53**

While the tumor suppression function of p53 has long been recognized, the mechanisms underlying this biological role and its regulation are still under intense investigation. p53 is known as the “cellular gatekeeper”<sup>64</sup> or the “guardian of the genome”<sup>65</sup>, because of its central role in orchestrating specific cellular responses to a broad range of stress factors

encountered by cells<sup>66</sup>. p53 acts like a cellular stress sensor that can be activated in response to different stimuli, such as DNA damage, hyper-proliferative signals as consequence of oncogene activation, hypoxia, oxidative stress, ribonucleotide depletion and nutrient starvation<sup>67</sup>. Many of these stimuli are encountered by tumor cells in the tumor microenvironment and are therefore important for triggering p53 tumor suppression function *in vivo*. Depending on the type of stimulus, p53 activation can lead to different cellular outcomes, such as transient cell cycle arrest, senescence, DNA repair, autophagy or apoptosis<sup>66</sup>. As a transcription factor, p53 can activate and repress a broad range of transcriptional targets that mediate these different cellular outcomes. The fine tuning of the activation/repression of p53 target genes according to the cell's necessities relies on a complicated network of signaling interactions.

According to the traditional model, p53 activity under basal conditions, or induced by mild stress or DNA damage, elicits a protective response that supports cell survival and promotes the repair of genotoxic damage<sup>68</sup>. Under these conditions, p53 engages an entire suite of responses that contribute to the inhibition of cell proliferation (temporary induction of a G1 block) and DNA repair. In contrast, high levels of sustained stress, accompanied by irreparable damage, induce the killer functions of p53 that consist in p53-mediated activation of cell death or senescence<sup>68</sup> (Fig. 7). Both these response modes help to prevent progression towards malignancy, either by preventing the accumulation of oncogenic lesions or by eradicating damaged cells.

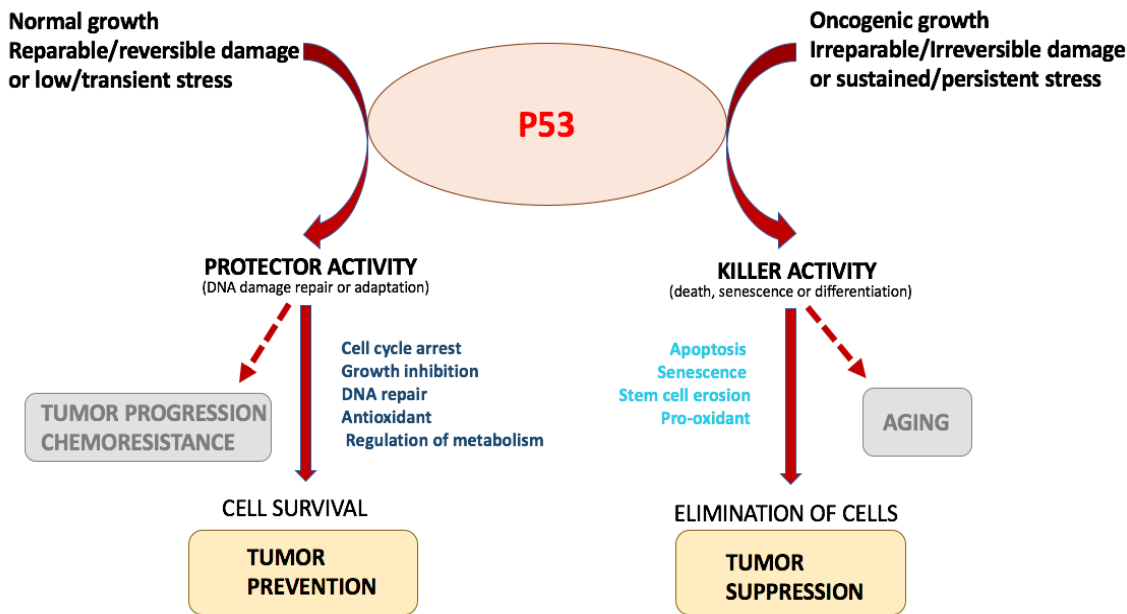


**Fig. 7 Mechanisms of p53 tumor suppression.**

Under normal conditions, p53 is present at very low concentrations in the cell, while under stress conditions, it accumulates and acts as a point of integration of signals from different stress stimuli, thereby resulting in the appropriate biological response. Under conditions of low/transient stress and damage, p53 has a protector activity supporting DNA repair, adaptation and survival of cells (mechanisms in dark blue), thus acting in tumor prevention. Under sustained stress conditions, p53 has a killer activity that drives the elimination of cells that cannot be repaired (mechanisms in light blue) leading to suppression of tumor growth. p53 functional deregulation could disrupt both of these activities leading to tumorigenesis, tumor progression, chemoresistance or aging. Figure adapted from <sup>68,69</sup>.

The emerging role of p53 in the regulation of SC homeostasis introduces another layer of complexity in p53-mediated tumor suppression, linked to its ability to regulate SC self-renewal by ensuring an asymmetric mode of division (see paragraph 2.4.1) <sup>70</sup>. In tumors where p53 is inactivated, cancer progression is associated with expansion of the SC pool as result of increased self-renewal, a symmetric mode of cell division, and reprogramming of progenitors to a SC-like state <sup>70,71</sup>.

To summarize, with the characterization of the multiple roles of p53 it has become clear that this protein is critical for the regulation of almost every aspect of cell behavior. Being a

highly connected node, p53 could be seen as an Achille's heel: the most effective way for a cell transformation to occur is to destroy the network by attacking its hub <sup>72</sup>. Therefore, it is not surprising that a growing complexity within the p53 pathway and its regulation is emerging, as described in the next paragraph 2.3.4.2.

### **2.3.4.2 p53 STRUCTURE AND MECHANISMS OF REGULATION**

Unraveling the structural biology of p53 is a good starting point to understanding its functional complexity and to developing a structure-guided approach to rescuing p53 function in tumors. The p53 protein is composed of three different functional domains separated by short linker regions (Fig. 8):

i) The N-terminal transactivation domain (TAD, residues 1-70), which activates transcription and regulates p53 stability and activity <sup>73</sup>. The transcriptional co-activator proteins p300/CREB-binding protein (CBP) and the p53 inhibitor murine double minute (Mdm2) (see paragraph 2.3.4.3, 2.3.4.4) have overlapping binding sites within the TAD of p53 and compete for its binding. Phosphorylation events, triggered by DNA damage, at p53 N-terminal residues (Thr18 and Ser20) decrease its affinity for Mdm2 and, concomitantly increase its binding with p300/CBP, which induce the transactivation activity of p53 <sup>73</sup>. In the absence of Mdm2, the p53 TAD is intrinsically disordered and it has been proposed that it has a flexible conformation allowing it to adapt for binding with multiple proteins; this is known as the “induced fit model” <sup>73</sup>.

ii) The sequence-specific DNA-binding core domain (DBD, residues 94-293), which consists of secondary structural elements able to establish multiple contacts with the DNA major and minor grooves. This central region of p53 is globular in shape and has a low thermodynamic stability that confers structural plasticity to allow both the binding to different interactors and affect p53 susceptibility to deleterious mutations <sup>74</sup>. These mutations have an impact on the p53-folded status and, thus, on the overall protein function.

iii) The C-terminal p53 tetramerization domain (TD, residues 324-355) allows protein interactions between the p53 monomer subunits. These interactions are extensive and mainly hydrophobic and are critical for both proteins folding and homotetramer formation. p53 homotetramerization allosterically regulates the DNA binding activity of p53. p53 tetramers display a higher affinity for the p53 DNA response sequence than p53 monomers and, consequently, shows an increased ability to act in the nucleus as a transcriptional regulator of p53 target genes <sup>75</sup>. Mutations in the TD impair the correct formation of homotetramers, leading to dominant-negative phenotypes and cellular transformation.

iv) Two linker proline-rich regions (PRR) spanning residues 71-93 and 294-323. The first PRR contributes to functional activity binding to SH3 proteins and facilitating p53 folding. This latter function is also maintained by the second PRR, which also accommodates the different symmetries of the flanking domains <sup>73</sup>.

v) C-terminal basic region spanning amino acids 356-393, which, as suggested from the name, is rich in basic residues. Its conformational flexibility allows the region to adopt alternative conformations and provides binding specificity. Moreover, it is subjected to post-translational modifications (PTMs) that affect p53 DNA-binding activity and transcriptional activity since it allows the recruitment of co-activators involved in opening the chromatin structure <sup>73</sup>.

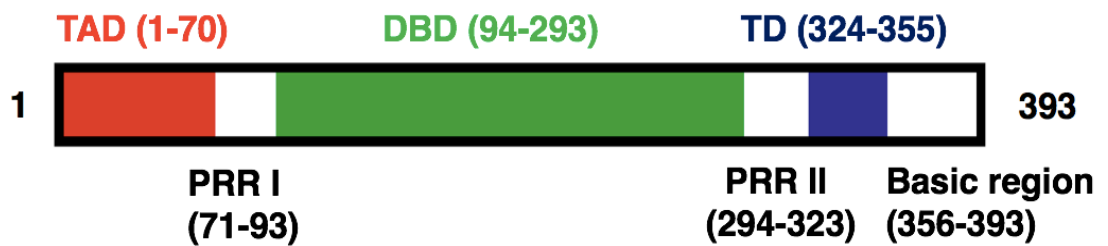


**Fig. 8 Schematic structure of p53 protein highlighting its main functional domains.**

Three main domains of p53 (TAD, red; DBD, green; TD, blue), the proline-rich linker regions (white) and the C-terminal basic region (white) are indicated. Residue numbers indicate the boundaries between these different structural elements. TAD: transcriptional activation domains; DBD: DNA binding domain; TD: transactivation domain. Figure from <sup>73</sup>.

The traditional model of stress-induced p53 activation consists of three rate limiting steps <sup>66</sup>: i) p53 stabilization ii) DNA binding and iii) transcriptional activation of p53 target genes (Fig. 9).

i) *p53 stabilization*. The tight control of p53 levels and function is mainly achieved by the regulation of its turnover by ubiquitin-mediated proteasomal degradation. Mdm2 has been described as the main E3 ligase that mediates the ubiquitination of p53, committing it to proteasomal degradation <sup>76,77</sup>. Mdm2 can also directly inhibit p53 activity by binding the p53 TAD. Since Mdm2 is also a known p53 transcriptional target, the absolute balance of p53 and Mdm2 in the cell is maintained in an auto-regulatory feedback loop between these two proteins whose equilibrium is essential to preserve the necessary p53 activity <sup>72</sup>. Multiple layers of Mdm2 regulation are therefore able to affect p53 levels and stability. In response to stress signals, p53 is displaced from its negative regulator Mdm2 and in that way p53 is stabilized. A growing number of proteins that affect the levels, localization or activity of MDM2 (MDMX, ARF, YY1, HAUSP, RASSF1A, NUMB), thus, influencing p53 levels have been identified. In addition, Mdm2 activity can also be regulated by phosphorylation and acetylation at different sites, resulting in its activation or inhibition depending on the

precise site and on the modifying kinase (ATM, cAbl) or acetylase (CBP/p300) (see paragraph 2.4.4.3) <sup>66</sup>.

In the same way, p53 activation is regulated by an array of PTMs. Regulatory redundancy among p53 PTMs might ensure that p53 is regulated appropriately in a tissue-specific manner in response to different stimuli and different strength of signals <sup>78</sup>. Genetic and biochemical studies emphasize the notion that p53 stabilization *in vivo* requires a sophisticated regulatory network. Different kinases (ATM, ATR, DNAPK, CHK1, CHK2) can affect the p53-Mdm2 interaction by phosphorylating N-terminal TAD of p53 and stabilizing the protein in response to various stress signals. Recent work has demonstrated that acetylation of p53 C-terminal lysine residues by CBP/p300 is required for p53 stabilization since it blocks some of the major Mdm2-targeted ubiquitination sites <sup>66</sup>. p53 PTMs in concert with the interaction of p53 with a wide variety of protein binding partners, help to regulate its subcellular localization, stability and conformation, ultimately controlling p53 transcription-dependent and -independent functions.

ii) *DNA binding*. The second step in the regulation of p53 activation is at the level of binding to the DNA consensus sequence of specific response elements within promoters of target genes. p53 binding to DNA occurs through the central conserved DBD that provides sequence specificity. The p53 C-terminal region recognizes instead structural features of target DNA and folds back acting as a negative modulator of DNA binding domain. Additional p53 PTMs interfere with this folding and, at the same time, regulate the recruitment of other cofactors (coactivators or corepressors) to allow sequence-specific DNA binding <sup>66</sup>.

iii) *Transcriptional activation of p53 target genes.* The third step in the regulation of p53 activation involves the recruitment of the general transcription machinery and additional cofactors. Different p53 PTMs are recognized by transcription factors to achieve promoter specific transactivation. Evidence suggests that both Mdm2 and its homologue MdmX are generally recruited at the promoter region of target genes and inhibit their transcription <sup>79</sup>. In light of recent studies, it appears that p53 activation *in vivo* requires the release from this repression state mediated by MdmX e Mdm2 <sup>66</sup>. Moreover, the timing of p53 acetylation of different regions in the protein might be important for selection of target genes to transactivate. Also methylation, sumoylation, and neddylation also occur at specific sites in p53 and the many possible combinations of PTMs might act like a barcode, resulting in specific and sometimes contradictory p53 responses <sup>80</sup>. The exact combination of recruited cofactors and p53 PTMs is likely to determine the activation of specific sets of target genes and direct specific cellular responses.

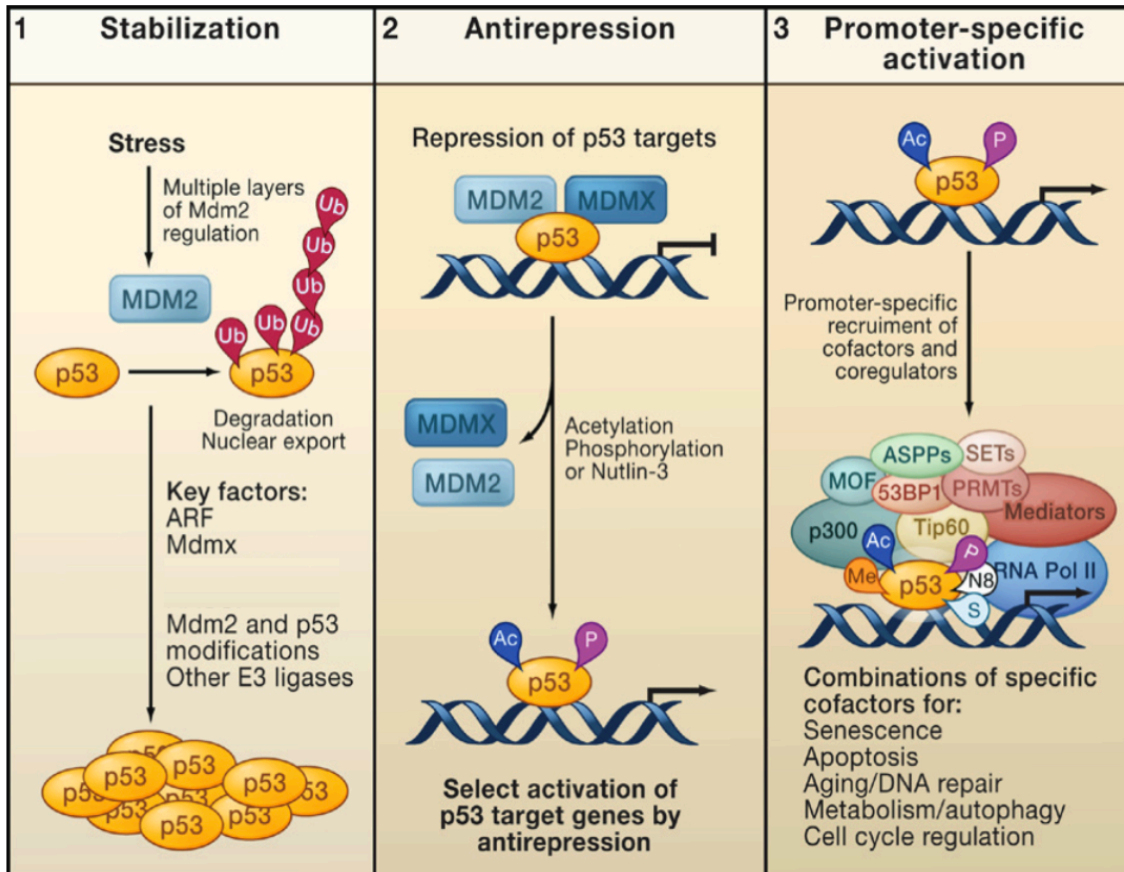


**Fig. 9 Model of p53 activation**

p53 activation involves three key steps: 1) stabilization, 2) anti-repression, 3) promoter-specific activation. Details are discussed in the main text. Figure adapted from <sup>66</sup>.

### 2.3.4.3 MDM2 BIOLOGY

Under physiological conditions, p53 protein is tightly maintained at low steady state levels since high levels of pro-apoptotic and anti-proliferative p53 might be detrimental for normal cell growth and development. Low cellular p53 levels in unstressed cells are mainly maintained by Mdm2, a p53 target gene that is able, in turn, to quench p53 activity. Low levels of Mdm2 activity promote monoubiquitination of p53, responsible for its shuttling from the nucleus to the cytoplasm. High levels of Mdm2 instead induce polyubiquitination of p53 that triggers its degradation (Fig. 10). Moreover, Mdm2 is able to inhibit p53 trans-

activation of target genes both by preventing p53 interaction with coactivators (it competes with p300 binding to the p53 N-terminal TAD) and recruiting transcriptional repressors<sup>81</sup> (Fig. 10).

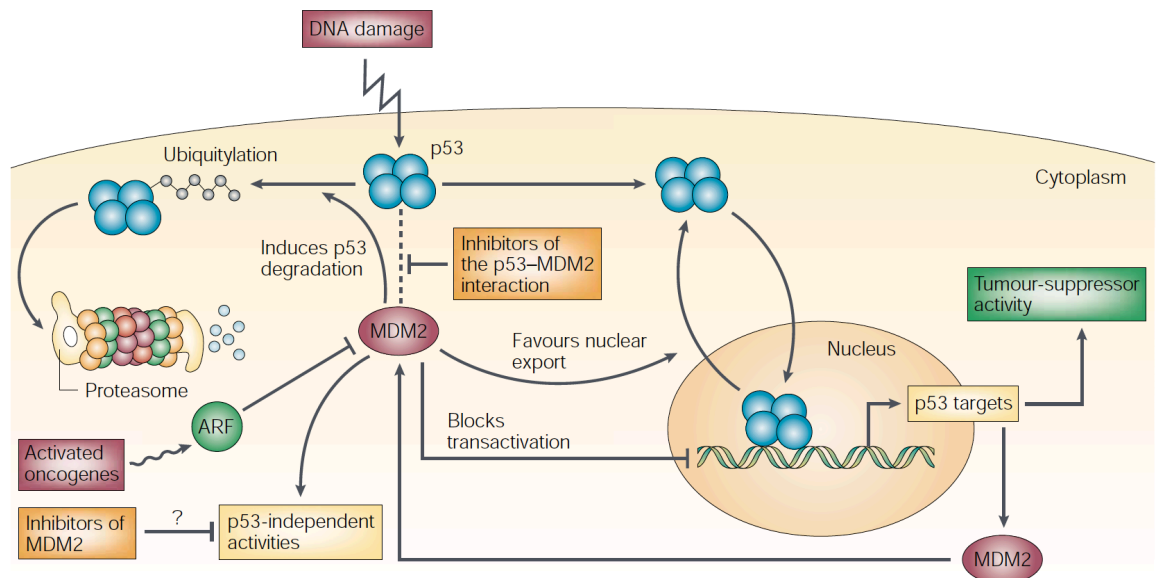


**Fig. 10 Mechanisms of Mdm2 regulation on p53.**

Several stress conditions such as acute DNA damage or oncogene activation (by stimulating ARF-mediated Mdm2 inhibition) induce p53 activation. Activated p53 is released from its negative regulator Mdm2. Mdm2 physiologically interacts with p53 promoting its ubiquitination and consequent degradation, favoring p53 nuclear export and blocking p53 transactivation activity on target genes. Transcription of these genes is ultimately important for mediating tumor suppressor functions of p53. Among p53 target genes, p53 stimulates Mdm2 transcription forming a p53 /Mdm2 auto-regulatory feedback loop. Inhibitors of Mdm2 or Mdm2/p53 interaction should stabilize p53. Figure from<sup>82</sup>.

In addition to this well-characterized function of Mdm2, increasing evidence has demonstrated several p53-independent roles of Mdm2. In fact, Mdm2 is able to regulate several cellular proteins, and is thus involved in pathways ranging from DNA repair and synthesis to control of cell cycle progression, apoptosis, cell fate, differentiation, cell motility and invasion<sup>83</sup>. The mapping of Mdm2 structural domains has helped to dissect the mechanisms underlying its biological functions and its expression regulation.

Mdm2 contains four functionally independent structural domains: i) an N-terminal p53-binding domain (aa 18-111) that binds the p53 N-terminal Box I domain, ii) a central region rich in acidic amino acids also referred to as the acidic domain (AD, aa 237-288), iii) a zinc-finger domain (aa 289-331) and iv) a C-terminal RING finger domain (aa 436-482), where the E3-ubiquitin ligase activity resides<sup>84</sup> (Fig. 11). The primary amino acid sequence of the Mdm2 AD is evolutionarily conserved in mammals and provides the binding sites for many Mdm2 positive regulators (transcription activator YY1, co-activator p300) and negative regulators as ADP ribosylation factor (ARF), Promyelocytic leukemia protein (PML) and ribosomal proteins, Rb<sup>85</sup>. Moreover, the Mdm2 AD is involved in several processes, such as ubiquitination-independent inhibition of the DNA-binding function of p53 or negative regulation of p300-mediated p53 acetylation and other p53-independent functions<sup>81</sup>.



**Fig. 11 Schematic representation of the full-length Mdm2 structure.**

Mdm2 domains include the N-terminal p53-binding domain (yellow, residues 18–101); the centrally located acidic domain that binds ARF and is involved in p53 ubiquitination (green, residues 237–288); and the zinc-finger motif (blue, residues 289–330). The Mdm2 C-terminal contains a RING domain that displays E3-ubiquitin ligase activity (orange, residues 436–482). Numbers indicates amino acid residues at the borders between these domains. NLS = nuclear localization signal; NES = nuclear export signal. Figure adapted from<sup>84</sup>

Recent evidence highlights a previously unexpected role of endogenous Mdm2 in mitochondria (mtMdm2) that is independent of p53. It was shown that Mdm2 is actively imported into mitochondria and localizes at the level of the mitochondrial matrix where it

appears to control respiration and mitochondrial dynamics independently of p53 in a lung cancer cell line model system<sup>86</sup>. High levels of mtMdm2 prompt an increased motility in cancer cells, suggesting an additional role of mtMdm2 in tumorigenesis<sup>86</sup>.

Mdm2 gene expression is regulated by two transcriptional promoter elements: P1, where basal transcription is initiated and P2, which is activated upon p53-induced transcription<sup>87</sup>. Other transcription factors (NF- $\kappa$ B, IRF-8, FliETS, SP1), pathways (Rad-Raf-MEK-MAPK) and several microRNAs (143,145,29,18b) are involved in modulation of Mdm2 mRNA expression and protein translation<sup>81</sup>. Moreover, PTMs, including phosphorylation of Mdm2 protein by several kinases, can affect its stability, activity and localization<sup>88,89</sup>. Once expressed, Mdm2 translocates to the cytoplasm where it mediates the proteasomal degradation of many of its targets<sup>81</sup>.

An enhanced expression of Mdm2 is tumorigenic, thus, establishing it as an oncoprotein. Indeed, amplification of the *MDM2* gene is a common event occurring in over 17% of tumors<sup>90</sup>. This event accounts for Mdm2 overexpression and contributes to p53 inactivation in many p53-WT tumors<sup>91-93</sup>. In human tumors, Mdm2 overexpression is associated with poor prognosis and correlates with more aggressive and metastatic tumor phenotypes, especially in solid tumors<sup>81</sup>.

#### **2.3.4.4 REGULATION OF THE p53-MDM2 PATHWAY**

Different therapeutic strategies aim to overcome p53 attenuation in cancer cells. One possibility is to rescue p53 levels by directly targeting the Mdm2-p53 interaction. Thus, there

have been several studies focused on characterizing this interaction at the structural and functional level. Although the main interaction, originally mapped between N-terminal domains of p53 and Mdm2 blocks the p53-mediated transactivation of target genes, it alone is not sufficient to promote Mdm2-catalyzed p53 ubiquitination <sup>94</sup>. A second interaction site has been identified between a specific DNA-binding site in the p53 DBD that harbors a ubiquitin signal (Box V) and the Mdm2 AD and part of the zinc-finger domain <sup>95</sup> (Fig.12). This latter region is located between residues 211 and 321 and is critical for Mdm2-mediated ubiquitin ligase activity towards p53 <sup>95</sup>. In particular, deletion of Mdm2 residues 247-258 and 270-274 was shown to severely impair its ability to ubiquitinate p53 <sup>85</sup>. Moreover, this activity can be affected by phosphorylation events at multiple sites in Mdm2. Different kinases (PLK1, HGSK3, GK2, c-ABL) target Mdm2 residues within these cluster regions (247-258 and 270-274) or in close proximity to them, thereby modulating Mdm2 E3-ligase activity <sup>85</sup>.

Further experimental results support the idea that the N-terminal domain and the AD of Mdm2 bind to p53 in a cooperative way. In this model, the interaction between the p53 Box I and the Mdm2 N-terminal domain acts to induce conformational changes in Mdm2 that facilitate the binding between the p53 Box V and the Mdm2 AD <sup>94</sup> (Fig. 12).

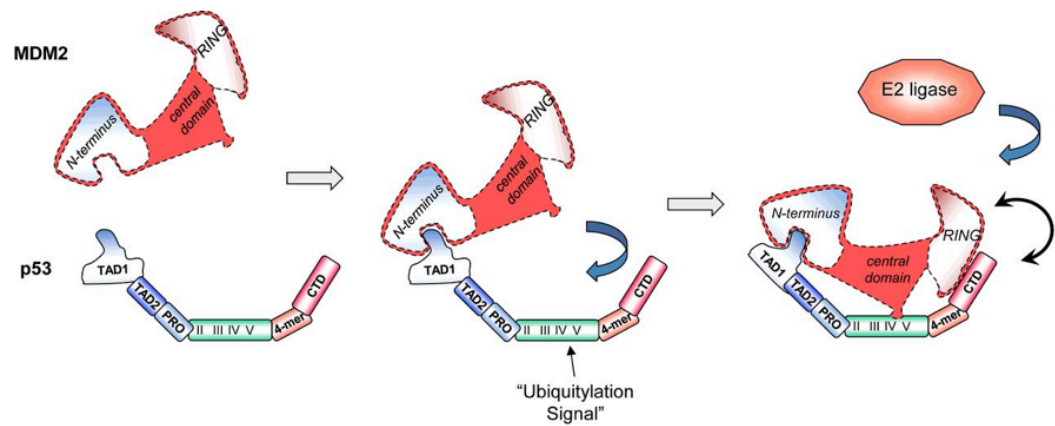


**Fig. 12 Dual site mechanism of Mdm2-p53 interaction.**

The p53 and Mdm2 proteins are shown in schematic modular format. Interaction of the N-terminal TAD1 of p53 with the N-terminal hydrophobic pocket of MDM2 leads to a conformational shift that facilitates the association between the acidic domain of MDM2 with the so-called ‘ubiquitylation signal’ within the Box V region of p53. This brings the C-terminal domain (CTD) of p53 into contact with the RING domain of MDM2 together with the E2 ligase, leading to ubiquitylation of p53. TAD1 and TAD2 = two functional portions of the transcriptional activation domains; PRO=proline-rich domain. II,III, IV, V = highly conserved Box regions of the p53 DNA binding domain. Figure adapted from <sup>96</sup>

Currently, the vast majority of the inhibitors were screened or designed in order to bind the N-terminal regions of Mdm2 and p53 (e.g., Nutlin family of inhibitors has been the first to be characterized). Further characterization of the second structural interaction between the p53 DBD and the Mdm2 AD could be extremely helpful for designing inhibitor molecules that are able to modulate this second interaction surface to therapeutically reactivate p53 tumor suppressor activity.

There is also a wide “supporting cast” of interacting factors that are involved at multiple levels in Mdm2-p53 regulation. The following proteins are the main interactors that can affect Mdm2 localization, binding and expression, reviewed in <sup>81</sup>:

- MdmX shows significant homology and shares domain structural architecture with Mdm2<sup>97</sup>. It inhibits p53 transactivation activity but does not directly induce p53 degradation since its RING domain lacks E3-ligase activity. However, by heterodimerizing with Mdm2, MdmX also directly contributes to p53 turnover<sup>98</sup>.
- ARF interacts with Mdm2, sequestering it into the nucleolus, thereby, indirectly stabilizing p53 by preventing its Mdm2-mediated cytosolic degradation<sup>99</sup>. A similar mechanism is mediated by PML that confines Mdm2 to the nuclear compartment<sup>100</sup>. Nucleophosmin (NPM) instead competes with Mdm2 for p53 binding, thus stabilizing p53<sup>101</sup>.
- 14-3-3 is a p53 target gene that stabilizes p53 by increasing Mdm2 auto-ubiquitination and inhibits Mdm2-mediated p53 nuclear export to the cytoplasm<sup>102</sup>
- Ribosomal proteins bind to the Mdm2 AD inhibiting its E3-ligase activity towards p53. -Subset of Polycomb proteins bind and destabilize Mdm2 leading to increasing p53 stability<sup>103</sup>.

The above-mentioned interactors could be indirect targets to rescue p53 levels or decrease Mdm2 activity to prevent p53 degradation.

### **2.3.4.5 p53 IN CANCER**

The prominent role of p53 in many aspects of cell physiology makes it a primary target for alterations promoting malignant transformation. p53 deficiency can enhance the initiation and progression of cancer. Tumors with p53 dysfunction are characterized by genomic instability and more aggressive features, such as increased invasiveness and metastatic potential, lack of cellular differentiation, increased vascularization, indefinite proliferation and resistance to anti-cancer therapies<sup>67</sup>.

In about half of spontaneous cancers, p53 protein does not function correctly. In a great

number of cases, p53 dysfunction is due to mutations of the *p53* gene or in genes that encode for p53 upstream or downstream regulatory proteins that interact with p53 or transmit signal information to and from p53. Most p53 mutations are missense and cluster in 86% of cases in the p53 DBD (Fig. 13). Hotspot mutations involve residues important for correct architecture folding of the flexible DNA binding surface or critical for contacts with p53-responsive element on promoters of target genes. The functional impact of these mutations is dysregulated p53 transactivation activity. Transcriptional activity requires the formation of p53 tetramers (dimers of dimers). Incorporation of a mutant p53 monomer, due to mutation in a single p53 allele, in these structures may preclude their activity resulting in a dominant-negative phenotype<sup>104</sup>.

In some human cancers, the frequency of the p53 mutations is not as high as in the vast majority of cancers. In breast cancer, p53 mutations are detected in only 20-30% of patients. However, the percentage of tumors displaying p53 dysfunction is higher, due to the fact that p53 can be inactivated also by indirect mechanisms, such as altered expression of Mdm2 (due to amplification of the locus) and loss of ARF protein expression, as mentioned above

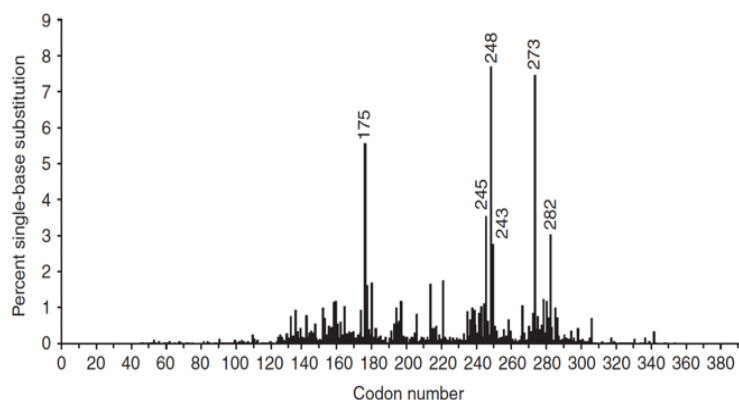


**Fig. 13 Hotspot mutation in the TP53 gene in human cancer.**

Height of the peaks is proportional to the relative frequency of cancer associated missense mutations of each p53 residues (see figure 8 as reference) according the TP53 mutation database of the Agency for Research on Cancer<sup>105,104</sup>. Figure adapted from<sup>104</sup>.

From a therapeutic perspective, p53 reactivation is hailed as an obvious goal to halt tumor progression. The emerging theme is that p53 has a pivotal role in maintaining organism fitness through two mechanisms: first, by supporting the adaptation and repair of cells under conditions of stress and damage, and second, by driving the elimination of cells that cannot be repaired or are under constant stress conditions<sup>69</sup>. Although there is still much to learn, experimental evidence clearly indicates that manipulating the p53 pathway could bring considerable therapeutic benefits.

The goal is to try to re-establish the growth inhibitory function of p53 in cancer cells where it is impaired or defective. The main approaches (Fig. 14) include<sup>106</sup>:

i) gene therapy consisting of adenoviral delivery of p53 WT (Ad-p53) into cancer cells to rescue p53 activity. *In vitro* and *in vivo* studies demonstrated that Ad-P53 delivery correlates with tumor regression in several cancer contexts including head and neck cancer<sup>107</sup>, lung cancer<sup>108</sup>, prostate<sup>109</sup>, glioma<sup>110</sup>. This strategy has shown a satisfactory safety profile thus promoting its testing in phase I to IV clinical trials for the treatment of different tumor types, such as recurrent malignant gliomas<sup>111</sup>, head and neck cancer<sup>112</sup>, hepatocellular carcinoma<sup>113</sup>, and significantly increased patient survival when combined to radiotherapy.

ii) inhibition of Mdm2 or Mdm2-p53 interaction using small molecule inhibitors<sup>114</sup>, (see paragraph 2.3.4.6), such as Nutlin<sup>115</sup>.

iii) restoration of the p53 WT conformation in mutated cases<sup>116</sup>. Mutant p53 often accumulates in cancer cells and therefore represents a tumor-specific biomarker<sup>117,118</sup>. *In silico* high-throughput screenings of chemical libraries and computational analyses have

identified several small molecules that are able to restore physiological p53 WT functions and conformation, leading to massive apoptosis in tumor cells and thus antitumor activity. These compounds include PRIMA-1, MIRA-3, STIMA-1, PhiKan083, ellipticine, P53R, NSC319726, CP31398 [reviewed in <sup>106</sup>].

iv) targeting mutant p53 to degradation <sup>119</sup>. An alternative strategy in tumors addicted to mutant p53, involves targeting p53 mutants to degradation by administration of p53 siRNA or small molecules that induce degradation of mutant p53 (e.g., HSP90 inhibitors, SAHA inhibitor, arsenic trioxide) <sup>120,121</sup>.

v) p53-based immunotherapy (e.g., vaccines: p53 SLP, INGN25). Mutant p53 expression in cancer cells can be used as tumor-specific antigen to target with immunotherapy. p53 vaccines against mutant p53 synthetic peptides have entered phase I/II clinical trials, and were well-tolerated and able to activate a specific anti-mutant p53 immune response <sup>122</sup>.

Considering the above, it is clear that the evaluation of p53 status in tumors is of great importance in deciding the appropriate treatment strategy. Many p53 mutations lead to abnormal p53 nuclear accumulation <sup>118</sup>. Mutant p53 protein probably accumulates as a result of compromised p53-mediated transcription of its modulator Mdm2. As a result, mutant p53 has a longer half-life compared to the relatively unstable WT protein. Based on this observation, a large number of studies have used immunohistochemistry (IHC) detection of accumulated p53 as a surrogate marker for p53 mutational status <sup>123</sup>. In this IHC analysis, a semi-quantitative score is attributed according to the percentage of positive nuclear-stained cells in the analyzed tissue section <sup>118,123</sup>. Data from several breast cancer cohorts demonstrated that p53 accumulation is an independent parameter of poor

prognosis<sup>124</sup>. It has emerged, however, that also undetectable p53 nuclear staining is a likely indicator of null-mutations in the *p53* gene and poor prognosis<sup>118</sup>. *p53* gene sequencing clearly remains the most reliable technique to assess p53 mutational status in a tumor sample. However, its application is lab intensive and time-consuming, thus, currently not suitable in clinical settings.

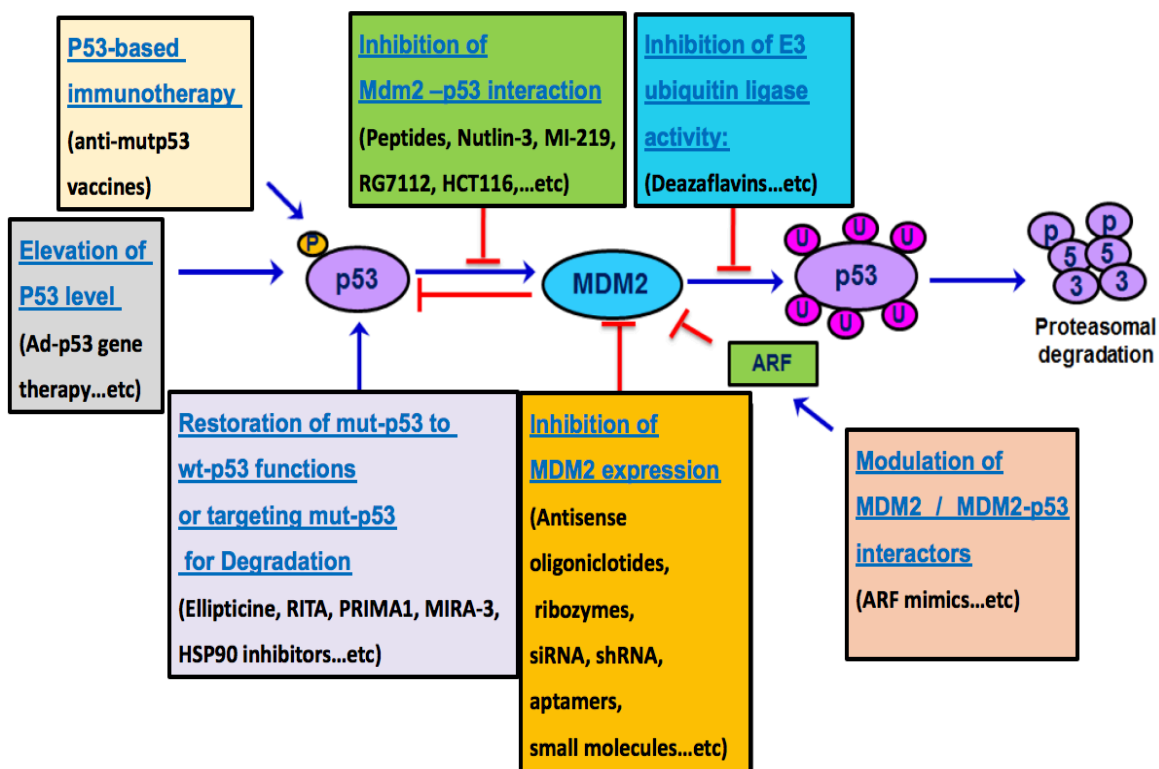


**Fig. 14 Multiple strategies to reactivate the p53 pathway in cancer.**

According to the mechanism of p53 dysfunction, different approaches can be used to restore p53 function in tumors<sup>125-127</sup>, in order to halt tumor growth. The main strategies used to directly or indirectly recover p53 tumor suppressor activity include; i) direct elevation of p53 protein levels, p53-based immunotherapy; ii) inhibition of Mdm2 expression, of its ubiquitin ligase activity or of the Mdm2-p53 interaction; iii) restoration of mutant p53 (mut-p53) to wild-type p53 (wt-p53) function or promotion of mut-p53 degradation; iv) modulation of Mdm2/Mdm2-p53 interactors. RITA = Reactivation of p53 and induction of tumor apoptosis. Figure adapted from<sup>81</sup>.

## 2.3.4.6 TARGETING OF THE p53-MDM2 PATHWAY FOR CANCER THERAPY

The MDM2-p53 pathway has been widely studied and presents an attractive target for cancer therapy. Inhibition of Mdm2 or of the Mdm2-p53 interaction represent indirect approaches to re-establish p53 function and are thus considered as viable therapeutic strategies to negatively affect tumor progression. The following approaches were tested *in vitro* to prove their efficacy and feasibility and some of them are proceeding their path towards therapeutic application in the clinical setting<sup>81</sup> (Fig. 14):

- i) *Mdm2 inhibition*. This strategy exploits silencing techniques using antisense oligonucleotide delivery, Mdm2 ribozymes or aptamers. All these techniques showed pro-apoptotic and anti-proliferative effects *in vitro* in a panel of cancer cell lines<sup>128</sup> but, only recently, has their use in the clinic been promoted by the successful smart delivery of Mdm2 siRNA<sup>129,130</sup>.
- ii) *Direct inhibition of Mdm2-p53 binding*. Small molecule Mdm2 inhibitors were designed to target the hydrophobic pocket on the surface of Mdm2 protein, where the main residues critical for p53 binding are present. The most promising candidates came from the screening of chemical libraries to identify molecules that bind the N-terminus of Mdm2 (e.g., Nutlin, RG7112, HCT116, spiro-oxindoles, isolindones, chalcone, MI219, HLI98, benzodiazepinedione) and analogues of these lead compounds are being developed and optimized for clinical use<sup>114</sup>. The most prominent example is that of the Nutlin family of compounds, which, in p53 WT tumors, is able to activate tumor suppressor functions of p53

allowing transactivation of downstream target genes<sup>131</sup>. Nutlin has been proved to be effective in the preclinical setting, and a related compound, RG7388 is better tolerated in patients, although long-term effects in a clinical setting should be still evaluated<sup>132,133</sup>.

The aforementioned compounds only weakly inhibit E3-ligase activity. They likely disrupt the interaction between the N-terminal domains of Mdm2 and p53, but are unable to fully dissociate the complex, since a second Mdm2 AD-p53 Box V binding persists. Concerning this issue, an alternative approach to induce p53 activation involves the physical or allosteric inhibition of Mdm2 E3-ligase activity by targeting this second Mdm2-p53 docking site with small molecules inhibitors or peptide ligands (e.g., ARF-mimicking compounds)<sup>134</sup>.

Despite the intensive efforts aimed at identifying or synthetically designing novel inhibitors targeting the Mdm2-p53 interaction, no such drugs have been approved in the clinic. However, some of these compounds (e.g., RG7388, R05503781, SAR405838, CGM097, MK-8242) are already being tested in advanced clinical trials and appear to be promising for p53 WT cancer treatment<sup>135</sup>.

It is important to remember that multiple levels of regulation by a wide and dynamic protein-interaction network, impose restrictive parameters and conditions that should be kept in consideration when stratifying patients for a successful precision medicine. In this context, exploiting Numb inhibition of the Mdm2-p53 circuitry for the rational design of Numb mimetic molecules could be an interesting parallel strategy to reactivate p53 in p53 WT tumors.

## 2.3.4.7 THE ROLE OF NUMB IN THE REGULATION OF THE p53-MDM2 PATHWAY

Previous work from our lab has highlighted a tumor suppressor role of Numb in breast cancer related to its sustainment of the p53 pathway under physiological conditions. Numb enters into a trimeric complex with p53 and Mdm2, directly interacting with both proteins to inhibit Mdm2-mediated ubiquitination of p53, thereby stabilizing p53 protein levels<sup>63</sup> (Fig. 15).

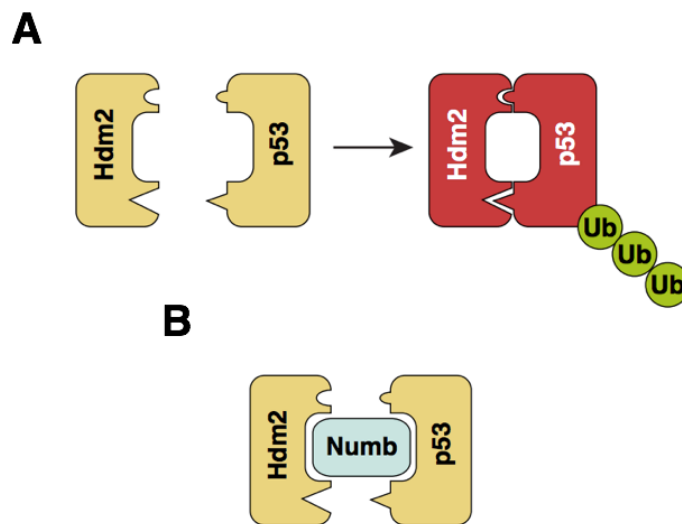


**Fig. 15 Possible model of NUMB interaction in a Numb/Hdm2/p53 tricomplex.**

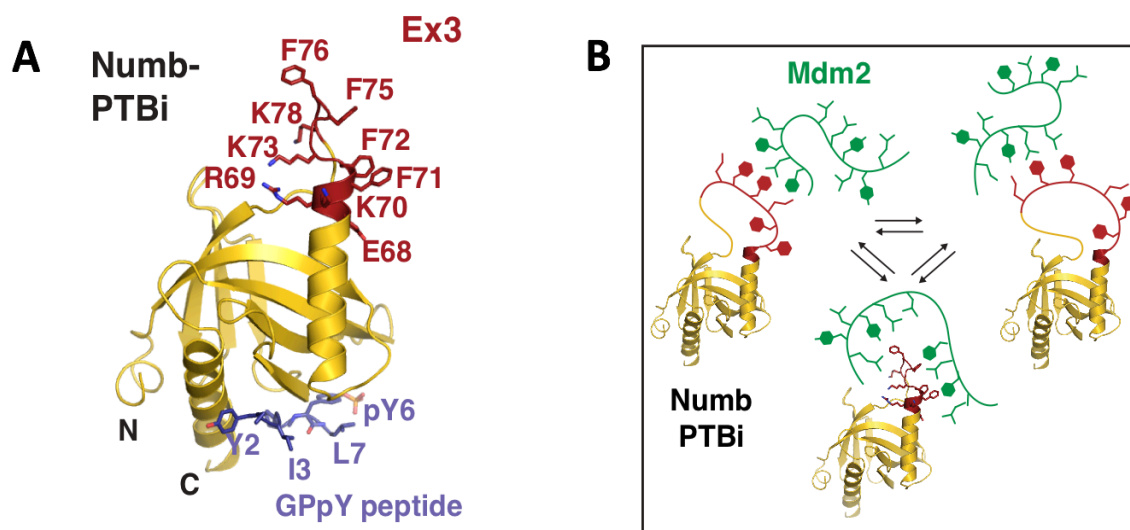
**A)** Mdm2 targets p53 for ubiquitination. The p53-Mdm2 interaction is mediated by at least two different docking sites: 1) between the N-terminal BOX-I region of p53 and the N-terminal domain of HDM2; 2) between the p53 DNA binding region and HDM2 acid domain (AD). **B)** Possible model of NUMB action. NUMB prevents the physical interaction between p53 and HDM2 AD, by intercalating between the two proteins.

Figure adapted from<sup>63</sup>

Consequently Numb-deficient tumor cells (see paragraph 2.4) display reduced p53 levels and activity, and impaired ability to respond to genotoxic treatment and to efficiently repair DNA damage<sup>63</sup>. A more detailed biochemical and structural characterization of the Numb-Mdm2 interaction from our lab has further illuminated the mechanism of the action of Numb on Mdm2<sup>136</sup>. In particular, a region encompassing the Numb exon 3 encoded

sequence within the PTB domain (PTBi; aa 54-91) seems to be necessary and sufficient for high affinity binding of Numb to Mdm2. Since exon 3 is alternatively spliced, this region is present only in Numb isoforms 1 and 2 (see paragraph 2.2). The crystallographic resolution of the Numb PTBi reveals that the exon 3-containing Numb region (11 aa) is arranged as a dynamic loop able to adopt at least three different conformations. This flexible loop is enriched in aromatic and positively charged amino acids<sup>136</sup>. Nuclear magnetic resonance (NMR) chemical shifts and mutational analysis suggested that Numb PTBi residues contribute to the formation of a large hydrophobic and positively charged patch that dynamically engages an intrinsically flexible, hydrophobic and negatively charged Mdm2 region at the level of its AD (aa 250-290), giving rise to a “fuzzy” complex<sup>136</sup> (Fig. 16).

**Fig. 16** *The Ex3-encoded sequence represents a novel surface in the NUMB PTB domain dynamically involved in MDM2 binding.*



**A)** Ribbon model of the crystallographic structure of Numb-PTBi in complex with a GPpY phosphopeptide (violet). GPpY is a phosphopeptide that derives from a canonical PTB-binding protein. The 11 aa exon3-encoded sequence is depicted in red. **B)** Schematic representation indicating that the PTBi:Mdm2 interaction interface represents a fuzzy complex, where two intrinsically disordered regions in both binding partners interact and retain dynamic and intrinsic disorder in the complex. The Numb-Mdm2 interaction is based on multiple polar and hydrophobic interaction between the negatively charged Mdm2 acidic domain and the positively charged Numb PTB domain. Figure adapted from<sup>136</sup>

Interestingly, as previously discussed, the Mdm2 AD is important for its E3-ligase activity and is also targeted by other Mdm2 inhibitors, such as ARF. The Mdm2 AD is regulated by different PTMs, in particular, phosphorylation of different residues, which contribute to maintain the interaction with p53 under 'unstressed' conditions when the cell needs to maintain low levels of p53. Phosphomimic mutants of Mdm2 that mimic the phosphorylation occurring *in vivo*, were able to increase the binding to Numb, indicating that probably also some PTMs might contribute to the Numb-Mdm2 interaction. The crystallographic resolution of the Numb PTBi region might open the way to future therapeutic interventions in breast cancer, envisioning the possibility to identify new small molecules or peptides that mimic Numb action on Mdm2 to inhibit its E3-ligase activity and thus rescue p53 levels in Numb-deficient tumors. The characterization of the Numb-Mdm2 interaction and, in particular, of the exclusive role of the exon 3-coded region of Numb in this interaction, prompted us to investigate whether exon 3-containing Numb isoforms have a specific role in p53 regulation, as will be described in the results section of this thesis (see paragraph 5.3).

### **2.3.5 NUMB IN CELL ADHESION, CELL MIGRATION AND EPITHELIAL-TO-MESENCHYMAL TRANSITION**

The role of Numb in endocytosis and recycling of transmembrane receptors unveils additional functions in the regulation of cell adhesion. Numb was indeed reported to physically interact with the E-cadherin/catenin complex at the level of cells adherens junctions (AJs)<sup>137</sup>. AJs are multi-protein complexes that provide a strong mechanical attachment between

adjacent epithelial cells, and are thus, involved in the regulation of plasma membrane dynamics, cell shape and motility<sup>138</sup>. AJs consist of the transmembrane E-cadherin protein responsible for i) trans-pairing intercellular contacts on opposing cells and ii) intracellular interactions with cytoplasmic p120-catenin,  $\beta$ -catenin and  $\alpha$ -catenin that are connected to the actin cytoskeleton, locally regulating its dynamics<sup>139</sup>. In this context, Numb contributes to continuous internalization and recycling at plasma membrane of E-cadherin-containing vesicles, within Rab11 containing endosomes, for the maintenance of AJ stability<sup>137</sup>.

To acquire migratory traits, cells need to undergo epithelial-to-mesenchymal transition (EMT). EMT is a process in which epithelial cells acquire pro-metastatic migratory traits by expressing mesenchymal markers while losing their cell-cell contacts and polarity. Numb dysfunction, by ablating its role in cell adhesion maintenance, triggers the EMT process connected with tumor progression and metastasis<sup>140</sup>.

Another role of Numb is in cell-extracellular matrix adhesion regulation, controlling integrin endocytosis. Numb is able to control the directional trafficking of integrin at the leading edge of cell protrusions in migrating cells. Numb binds to beta-integrins and localizes to clathrin-coated pits at the substratum-facing cell surface. These interactions allow the control of integrin endocytic trafficking, from their internalization to their route back to plasma membrane to make new adhesion sites at the leading front<sup>28</sup>.

Numb is also involved in the EMT process by regulating cell polarity in epithelial cells. Cell polarity is established by the asymmetrical organization of several cellular components. Polarity complex proteins (PAR) are involved in coordinating this process and have a role also in the establishment of tight junctions (TJs). TJs seal neighboring epithelial cells thus functionally separating the apico-basolateral surfaces and limiting liquid flux between cellular interspace. TJs consist of a network of transmembrane proteins, occludin and claudin,

and the cytoplasmic scaffolding proteins ZO-1,-2, and -3<sup>141,139</sup>. By interacting and affecting the localization of PAR3 (members of PAR polarity complex) it seems that Numb might also be involved in regulation of TJs dynamics<sup>2</sup>.

Moreover, Numb seems to prevent EMT by being a negative regulator of Notch. The Notch signaling cascade promotes EMT by inducing Snail and Slug that, in turn, transcriptionally repressing the expression of E-cadherin<sup>142,143</sup>.

In the context of cancer, the downmodulation of Numb can causally drive an enhanced tumor invasion by prompting the EMT phenotype<sup>142,143</sup>. Taken together, these data suggest a role of Numb in driving all the steps of the EMT process, from loss of cellular polarity and cell-cell contacts (dynamic remodeling of AJs and TJs), actin remodeling and cell-to-extracellular matrix dynamics for cell migration.

## **2.3.6 INCREASING THE COMPLEXITY: THE ROLE OF NUMB ISOFORMS**

Recent evidence has highlighted another level of complexity in the regulation of Numb biochemical functions concerning the differential role of Numb isoforms. As previously described, there are four main Numb isoforms in mammals, resulting from alternative splicing events that occur at the level of exon 3 and exon 9 of the *NUMB* gene. To date, the different functional roles of these isoforms is not fully understood. However, some studies have focused on dissecting the role of the exon 9 alternative splicing event and highlighted a differential role of Numb isoforms in Notch activation<sup>19</sup>.

### ***Numb Ex9 alternative splicing***

The expression of exon 9-containing isoforms (1 and 3) vs. exon 9 lacking isoforms (2 and 4) is developmentally regulated<sup>144</sup>. Alternative splicing is skewed towards isoforms 1 and 3 in progenitor cells, whereas isoforms 2 and 4 are predominantly expressed in differentiated cells<sup>145</sup>. This pattern of expression is observed in the embryonic mouse brain and in the developing pancreas and retina, where isoforms 1 and 3 are expressed in early developmental stages and decrease upon lineage differentiation. In mammalian neurogenesis, this pattern is compatible with distinct Numb isoform functions in promoting either neuronal differentiation (isoforms 2 and 4) or enhancing cell proliferation (isoforms 1 and 3)<sup>20</sup>. Neuronal differentiation implies a switch in Numb isoform expression towards an increase in exon 9-lacking isoforms 2 and 4<sup>144</sup>. The mechanism underlying the differential effect of Numb isoforms 1/3 vs. 2/4 on the cell proliferation/differentiation balance has been linked to the Notch signaling regulation. Indeed, increased expression of exon 9-containing isoforms 1 and 3 seems to result in enhanced Notch activation, while the prevalence of exon 9-lacking isoforms 2 and 4 results in Notch signaling attenuation<sup>144</sup> (Fig. 17) However, it is not clear how Numb isoforms mediate this dual and opposite effect on Notch signaling.

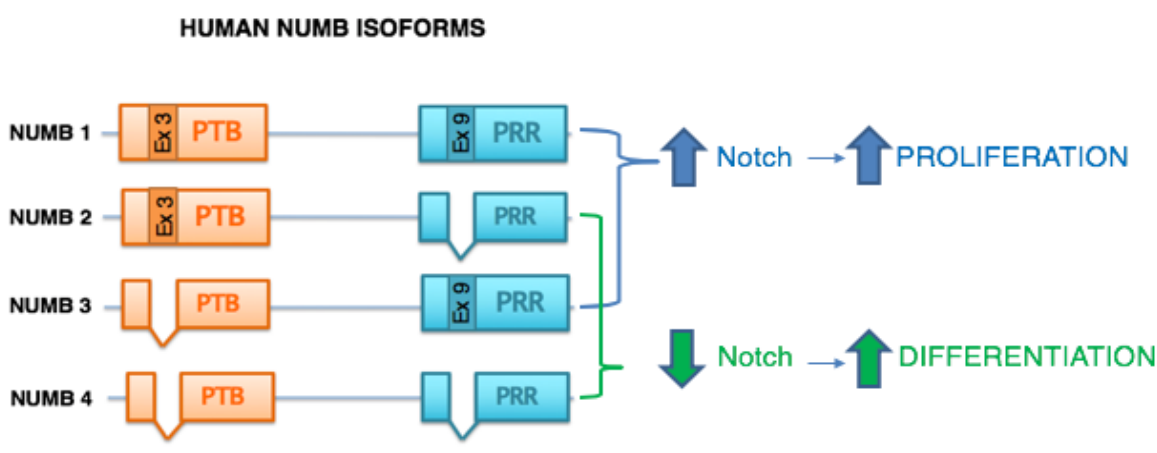


**Fig. 17 Numb isoforms structure and role in Notch regulation.**

Numb isoform 1/3 activate Notch signaling thus affecting cell proliferation, while Numb isoform 2/4 seem to negatively impact on Notch pathway prompting cell differentiation.

Alternative splicing is a tightly regulated process in development, as well as in adult tissues, and aberrant alternative splicing has been proposed to influence all the hallmarks of cancer<sup>146</sup>. The production and abundance of splice variants, which exert sometimes opposing functions, is dynamically regulated in a temporal and spatial manner<sup>147</sup>. Notably, deregulation of the alternative splicing of Numb, leading to alterations in Numb isoform expression, has been observed in different cancers, suggesting a role of aberrant alternative splicing in the tumorigenic processes. Indeed, increased expression of exon 9-containing isoforms have been observed in breast, colon and lung cancer compared to the normal tissue counterpart<sup>148,149,150</sup>.

Some alternative splicing factors have been shown to be involved in Numb exon 9 splicing, such as Rbm10, Rbm5, Rbm6, and Rbfox3. Rbm5 and Rbm6 seem to promote exon 9 inclusion, while Rbm10 induces exon 9 skipping<sup>151</sup>. By regulating the ratio of Numb isoforms, the expression levels of Rbm proteins can affect the cell proliferation rate, thus recapitulating the differential function of Numb isoforms 1/3 vs. 2/4 on the regulation of the Notch signaling pathway<sup>151</sup>. In addition, other pre-mRNA splicing regulators have been described to affect Numb exon 9 alternative splicing. Rbfox3 promotes exon 9 skipping<sup>152</sup> and RBM4 has been described to suppress exon 9 inclusion, while promoting the retention of exon 3<sup>153</sup>. Deregulation of the Numb splicing pattern due to mutations or altered expression of these regulators is frequently associated with cancer progression.

### ***Numb Ex3 alternative splicing***

In contrast to Numb exon 9 alternative splicing, little is known about the functional consequences of Numb exon 3 alternative splicing. Some information about its functional consequences in the context of neurodegenerative disease has emerged. In Alzheimer's disease, Numb isoforms differentially affect amyloid precursor protein subcellular trafficking and processing to generate amyloid B peptide, the main component of neuritic amyloid plaques<sup>154</sup>. In neural cells, the expression of exon 3-containing isoforms 1/2 or of exon 3-lacking isoforms 3/4, differentially directs sorting of amyloid precursor protein towards degradative or recycling compartments, respectively<sup>155</sup>.

Another strong indication of differential roles of exon 3-containing vs. -lacking isoforms derives from the fact that the subcellular localization of these isoforms is different. The Numb PTB domain, which presents as either the long version containing the exon 3 codified sequence (PTBi) or the short version lacking the exon 3 sequence (PTBo) (Fig. 3), appears to control the targeting Numb to the cortical plasma membrane. In particular, exon 3-containing Numb isoforms 1 and 2, possessing the longer PTBi domain, are mainly localized at the level of the cell membrane probably because of their interaction with acidic membrane phospholipids (e.g., phosphoinositides, PIP)<sup>19</sup>. In contrast, exon 3-lacking Numb isoforms 3 and 4 are mainly distributed in the cytoplasm. The region encompassing the Numb PTBi domain is rich in basic residues, which might explain its higher binding affinity for PIP lipids compared to PTBo<sup>156</sup>.

It is not clear yet the precise mechanism that regulates the subcellular localization of Numb isoforms; however, it is known that Numb phosphorylation plays a role. Numb hyperphosphorylation seems to disrupt Numb interactions with  $\alpha$ -adaptin, Eps15, E-cadherin and integrin, thus, affecting its endocytic functions and its localization<sup>10,28,157</sup>. Numb cortical

plasma membrane localization has also been shown to be dynamically regulated by GPCR-activated phospholipid hydrolysis and aPKC-dependent phosphorylation events<sup>156</sup>. aPKC activation has been described to cause redistribution of Numb from the cortical membrane to the cytosol<sup>10</sup>, but nothing has been described so far concerning isoform-specific mechanisms of Numb localization.

## 2.4 NUMB AND CANCER

Numb regulation of signaling pathways lies at the heart of its function as a tumor suppressor in cancer development<sup>2</sup>. The tumor suppressor role of Numb was highlighted in several types of solid tumors, including breast cancer, lung cancer, malignant pleural mesothelioma and hepatocellular carcinoma<sup>2,158,63</sup>. The clinical relevance of Numb in tumorigenesis can be appreciated considering that loss of Numb protein is detected in around 30% of breast and lung tumors (Numb-deficient) and it is correlated with poor prognosis (higher tumor grade) and more aggressive neoplastic disease<sup>44,63</sup>. The lack of mutations in the *NUMB* gene in tumors<sup>44</sup>, excluded this alteration as causally linked to loss of Numb protein. Evidence from our lab demonstrated that Numb-deficient breast and lung tumors, the molecular mechanism responsible for loss of Numb protein is due to enhanced ubiquitination and ensuing proteasomal degradation of the protein. Low Numb levels in primary culture cells from Numb-deficient tumors can be rescued by treatment with the proteasome inhibitor MG132, resulting in a growth inhibitory effect<sup>44</sup>. However, loss of Numb function in tumors is not only due to enhanced proteasomal degradation but appears to involve diverse mechanisms that converge on Numb deficiency. A recent study in prostate cancer

highlighted transcriptional deregulation of the *NUMB* gene as an additional mechanism underlying the downregulation of Numb<sup>159</sup>. Downmodulation of Numb mRNA levels in these tumors was associated with an advanced tumor stage<sup>159</sup>.

PTMs of Numb protein can also account for decreased Numb physiological functions. Numb phosphorylation by atypical protein kinase C (aPKC) destabilizes its interaction with p53, thus, enhancing p53 proteolysis. Consequently, decreased p53 protein levels and activity result in pro-tumorigenic phenotypes. aPKC-mediated Numb phosphorylation, also alters the subcellular distribution of Numb and promotes self-renewal and proliferation of tumor initiating cells (TIC), thus, playing a crucial role in promoting tumorigenesis<sup>160</sup>.

Several lines of evidence have demonstrated that Numb loss, independent of the mechanism underlying its deficiency, can confer a tumor growth advantage by two main mechanisms: i) activation of Notch and ii) decreased levels of p53 (Fig. 18).

i) In normal breast parenchyma, the Numb/Notch circuitry is relevant to the control of the proliferative/differentiative balance. Numb expression levels inversely correlate with Notch activation<sup>158</sup>. Numb loss-of-function phenocopies Notch gain-of-function and is linked to a hyper-proliferative phenotype. Restoration of Numb levels by overexpressing the protein, or attenuation of Notch activity by pharmacological inhibition, is able to revert the hyper-proliferative status of Numb-deficient breast tumors<sup>44</sup>.

ii) Ablation of Numb induces a reduction in p53 protein levels and activation upon DNA damage<sup>63</sup>. This is linked to increased resistance of Numb-deficient tumors to genotoxic agents compared with Numb-proficient tumors<sup>63</sup>. Loss of Numb and consequent downmodulation of p53 has been associated with the development of poorly differentiated tumors, impaired mammary gland morphogenesis in mice, and increased tumor cell proliferation<sup>161</sup>. Restoration of Numb levels by overexpressing the protein or pharmacological

inhibition of Mdm2 activity by Nutlin-3 rescues p53 levels and the chemosensitivity of Numb-deficient tumor cells <sup>162</sup>.

The complete elucidation of all the mechanisms involved in Numb deregulation in cancer is crucial for the identification of novel therapeutic targets and strategies for the treatment of the Numb-deficient tumors.

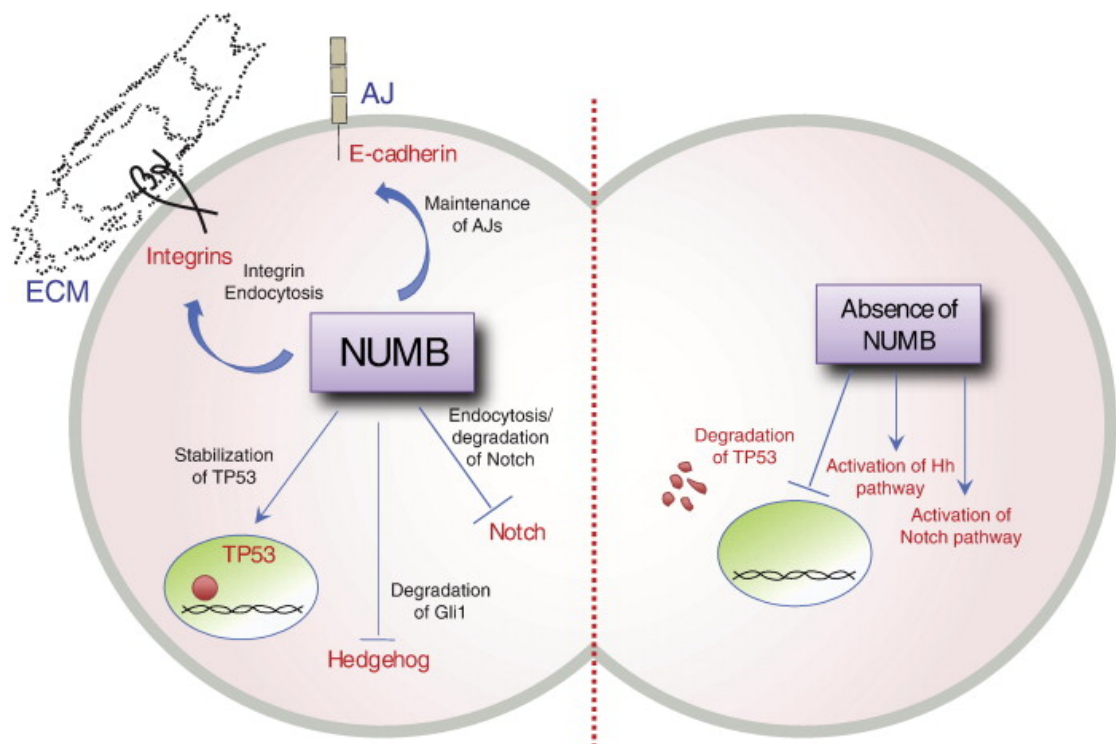


**Fig. 18 Numb regulated signaling pathways and their deregulation in cancer.**

On the left, Numb regulation on Integrin, adherens junction (AJs) dynamics and on downstream signaling pathways (p53, Notch, Hedgehog) and, on the right, their deregulation upon loss of Numb in cancer.

## 2.4.1 NUMB INVOLVEMENT IN CANCER: THE ROLE IN THE DETERMINATION AND MAINTENANCE OF THE STEM CELL COMPARTMENT

The physiological maintenance of the SC compartment is ensured by the ability of a SCs to perform ACD. Following this division mode, a SC generates two DCs with different cell fates: one DC retains the parental SC fate and withdraws into quiescence, while the second DC undergoes mitotic expansion and progressive lineage-specific differentiation. ACD thus ensures the preservation of the SC pool while allowing the proliferation of differentiated cells<sup>163</sup>. The correct execution of ACD likely represents a mechanism to prevent tumor development. This latter point is supported by evidence showing that uncontrolled symmetric division of SCs is associated with tumorigenesis<sup>70</sup>. The symmetric mode of division, indeed, gives rise to two DCs with identical SC fate, thereby expanding the population of pluripotent cells, thus, facilitating cancer development.

The mode of SC division is tightly regulated in development and tissue regeneration, as well as in adult SC homeostasis. Intrinsic and extrinsic determinants can have an impact on cell fate choices. These determinants consist of unequal segregation of molecular fate proteins between the two DCs or of polarized signaling triggered by “niche” local microenvironment cues or by neighboring cells, respectively<sup>164</sup>.

The dual role of Numb in the inhibition of Notch signaling and simultaneous stabilization of the p53 pathway has been linked to its role in the regulation of adult SC homeostasis. Numb asymmetric partitioning at SC mitosis causes functional asymmetry of the Numb-p53 and Numb-Notch circuitries that impart distinct developmental and proliferative fates to the

two DCs<sup>161</sup>. In the mammary gland, retention of Numb in one of the DCs imposes a SC fate. This can be explained because, in this cell, Numb positively regulates p53 activity, which results in withdrawal into quiescence, a stemness marker<sup>161</sup>. Thus, differential p53 activity in the two DCs, as result of diverse Numb levels, imposes an asymmetric mode of SC division<sup>161</sup>.

In the progenitor daughter cell, Numb progressively re-accumulates and appears to be critical for differentiation and the correct maturation of progenitors (Fig. 19). To resolve some of these apparent incongruences, a unifying scenario takes into account the role of Numb during the progressive steps of lineage specification. In immature SC division, Numb seems to segregate in stem daughter cell, while as maturation proceeds, instead, the re-expression of Numb confers a differentiative fate in committed progenitors<sup>161</sup>.

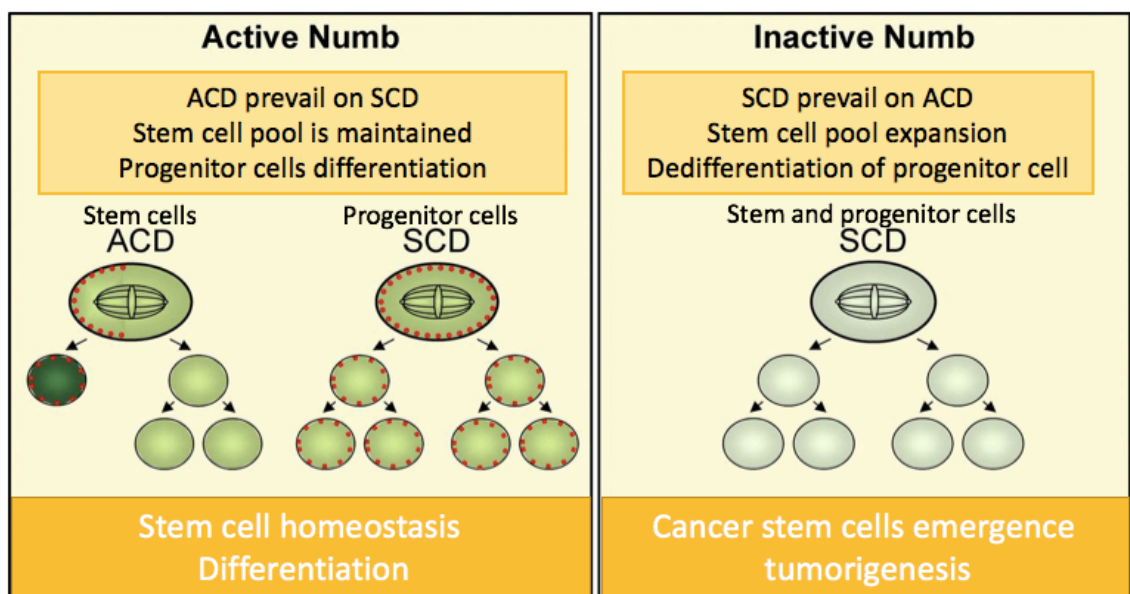


**Fig. 19 Role of Numb in the maintenance of the stem and progenitor cell pools in the mammary epithelium.**

Left, during normal mammary stem cell mitosis, ACD prevail, maintaining the stem cell pool and gland homeostasis. In stem cells, Numb (red dots) is retained in one daughter cell, where it stabilizes p53 (dark green), leading to quiescence and the adoption of a stem cell fate. In progenitor cells, Numb gets re/accumulated and is partitioned equally between the

two daughter cells, which have identical proliferative and developmental characteristics. Right, when Numb function is lost, p53 activity is decreased favouring expansion of the stem cell pool due to SCD, and dedifferentiation of progenitors thus facilitating tumour formation. Figure adapted from <sup>165</sup>.

Some studies have investigated the effects of loss of Numb in cancer <sup>63,44,161</sup>. Loss of Numb expression and consequently of p53 activity at the level of the SC compartment in the mammary gland results in a skewing in the mode division towards a symmetric mode and in the acquisition of unlimited self-renewal potential, causing the expansion of the SC population. In contrast, at the level of the progenitors, loss of Numb causes the activation of the EMT program associated with dedifferentiation and the *de novo* acquisition of SC traits <sup>161</sup> (Fig. 19). Together, these effects result in abnormal tissue morphogenesis and the emergence of CSCs <sup>161</sup>. CSCs from Numb-deficient breast cancers display an increased self-renewal potential compared to normal mammary SCs or Numb-proficient CSCs <sup>161</sup>

The effects of loss of Numb have also been shown to contribute directly to breast cancer tumorigenesis. The selective ablation of Numb in the mouse mammary gland results in morphological alterations and development of preneoplastic lesions. Thus, Numb regulation of p53 stability represents physiologically a tumor suppressor barrier that, by maintaining SC homeostasis, safeguards against their uncontrolled expansion.

Notably, the restoration of the Numb/p53 circuitry in Numb-deficient tumors can override all the phenotypes linked to the dysregulated p53 levels and furthermore it appears to represent an effective CSC targeted therapy <sup>162</sup>. Restoration of Numb by ectopic expression in primary Numb-deficient breast cancer cells results in a reduction of their tumorigenic potential *in vivo* <sup>161</sup>. Moreover, it has been demonstrated that *in vivo* treatment of patient-derived xenografts (PDX) of Numb-deficient breast cancer with the Mdm2 inhibitor, Nutlin-3a, a Mdm2 inhibitor, restores p53 levels in these breast tumors and decrease the self-

renewal properties of their CSCs <sup>162</sup>. Moreover, upon re-transplantation of MECs derived from Numb deficient PDX treated with Nutlin-3a, cells are able to induce the formation of smaller tumors in NOD/SCID mice compared to the corresponding not treated control <sup>162</sup>. Moreover, the effect of Nutlin-3a was even more striking when combined with paclitaxel, a standard-of-care chemotherapy drug used in treatment of many cancer, including breast cancer <sup>166</sup>; the combined treatment was shown to prevent tumor regrowth following interruption of chemotherapy treatment <sup>162</sup>.

### 3 AIM OF THE PROJECT

Since the discovery of the tumor suppressor function of Numb in our lab in 2004<sup>44</sup>, additional evidence has been produced supporting the role of Numb in the tumorigenesis process<sup>63,158,167</sup>. The first molecular pathway that was discovered to be deregulated in tumors upon loss of Numb was the Notch pathway, which is hyperactivated when Numb is lost<sup>44</sup>. Subsequently, it was discovered that Numb is also able to regulate the p53 tumor suppressor pathway<sup>63</sup>, whose inactivation is one of the most frequent events in human cancers<sup>168</sup>.

With a view to developing therapeutic strategies for Numb-deficient tumors, our lab has focused efforts on how to interfere with mechanisms acting upstream of Numb loss (i.e., on the machinery promoting Numb degradation), or downstream, in particular, at the level of Notch and p53 signaling.

With regards to the latter, our lab has performed an extensive structural study to elucidate the mechanism of action of Numb in the p53 pathway and, in particular, on its interaction with Mdm2<sup>136</sup>. From this study, it emerged that a region of Numb encompassing the alternatively spliced exon 3 is the main structural determinant mediating the interaction with the Mdm2 acidic domain and the consequent inhibition of the Mdm2 E3 ligase activity<sup>136</sup>. Since exon 3 is present in Numb isoforms 1 and 2, and not in isoforms 3 and 4, this finding raised the possibility of a differential role of Numb isoforms in cancer.

Thus, the founding hypothesis of this thesis, is that the exon 3-containing Numb isoforms 1 and 2 are responsible for the p53 regulation by Numb and thus they might play a role in BC tumorigenesis.

To test this hypothesis, we first tried to elucidate whether in some selected breast cell lines, the Numb isoforms 1 and 2 have specific and differential roles in the control of the p53 pathway and consequently on regulation of p53-dependent phenotypes, such as the response to genotoxic stress. We then investigated whether the deregulation of the Numb isoforms levels is an event present in primary BCs and whether the alteration of the alternative splicing of *Numb* might predict resistance to genotoxic stress and differential prognostic outcome in human BCs.

Together, the results of this thesis try to clarify if the deregulation of *Numb* alternative splicing could be a new pre-translational mechanism responsible for the functional loss of Numb in some BCs paving the way for the identification of novel molecular targets for the treatment of Numb-deficient tumors.

## **4 MATERIALS AND METHODS**

### **4.1 CELL CULTURE PROCEDURES AND REAGENTS**

#### **4.1.1 CELL LINES**

We used the following human cell lines: HEK-293 (from embryonic kidney), and two breast cell lines BT-474 (ductal carcinoma) and MCF-10A (not-tumorigenic mammary epithelial cells), all from the American Type Culture Collection (ATCC). HEK-293 cells were cultured in DMEM medium (Lonza) supplemented with 10% South American fetal bovine serum (FBS SA, HyClone), 2 mM L-glutamine (Euroclone) and 100 µg/mL penicillin and streptomycin antibiotics (Sigma). BT-474 cells were cultured in DMEM, 10% FBS North American fetal bovine serum (FBS NA), 2 mM L- glutamine and 100 µg/mL penicillin and streptomycin antibiotics. MCF-10A cells were maintained in a 1:1 mixture of DMEM and Ham F12 medium (Invitrogen) supplemented with 5% horse serum (Invitrogen), 10 µg/ml human insulin (Boehringer-Mannheim), 0.5 µg/ml hydrocortisone (Sigma), 100 ng/ml cholera toxin (Sigma), 100 µg/mL penicillin and streptomycin antibiotics (Sigma) and 2 mM L-glutamine. 20 ng/ml human epithelial growth factor (hEGF, Vinci-Biochem) was added freshly each time.

### **4.1.2 PRIMARY MAMMARY EPITHELIAL CELLS (MECs)**

Human primary BC epithelial cells were isolated from tissue biopsies by mechanical dissociation and enzymatic digestion with 200 U/ml collagenase type 1A and 100 U/ml of hyaluronidase (both from Sigma), in DMEM/F12 1:1 medium supplemented with 2 mM glutamine, for 4-5 h at 37°C with rotation. Cell suspensions were further digested in 0.05% trypsin-EDTA, centrifuged (80g, 5 min), re-suspended in hypotonic 0.2% NaCl solution to lyse red blood cells and eventually filtered through a 40 µm cell strainer filter. Flow-through cells were collected in Mammary Epithelial Basal Medium (MEBM). Serum-free MEBM (Clonetics) was supplemented with 5 µg/ml insulin, 0.5 µg/ml hydrocortisone, 1 U/ml heparin (Wockhardt), 2 mM glutamine and 100 µg/mL penicillin and streptomycin antibiotics. The complete MEBM medium was obtained by adding EGF (20 ng/mL), FGF (20 ng/mL, Peprotech), and B-27 Supplement (2%, Gibco) immediately before use. The complete medium was sterilized by filtering through a 0.2 µm filter before using it to resuspend and plate cells on six-well plates. Primary cells were amplified in culture for only 7-10 days to avoid adaptation to cell culture conditions and, thus, be representative of the primary tumor.

### **4.1.3 PLASMIDS AND REAGENTS**

Nutlin-3a (Cayman Chemical) and MG-132 (Enzo Life Science) were used at 10 µM. Cisplatin was used at different concentrations according to the length of treatment and the sensitivity of the treated cells.

Mammalian expression constructs encoding the different Numb isoforms were engineered in a pcDNA vector in-frame with a FLAG-tag at the C-terminus. The mammalian vector for the expression of Mdm2 was a kind gift from Prof. K. Helin (Biotech Research and Innovation Centre, Copenhagen, Denmark).

#### **4.1.4 GENE EXPRESSION SILENCING BY siRNA TRANSFECTION**

Transient silencing of specific Numb isoforms was achieved by transfecting specific pre-designed siRNAs (see Fig. 25 and sequences below). A non-targeting universal control siRNA was used as a negative control. For the silencing experiments in MCF-10A cells, delivery of siRNA oligos was achieved using Lipofectamine RNAiMAX (Invitrogen). Briefly, for cells cultured in 6-well plates, we prepared siRNA/Lipofectamine RNAiMAX complexes by diluting single siRNA oligos (final concentration = 10 nM in 2.5 ml final culture volume) and 5 µl Lipofectamine RNAiMAX in 500 µl OPTIMEM. The mixture was incubated for 20 min at room temperature (RT). Cells were plated in a total volume of 2 ml of complete medium without antibiotics and the siRNA/Lipofectamine RNAiMAX mixture was added to the plated cells. 24 h post-transfection, we replaced the medium with 2 ml of complete medium. Cells were harvested 72 h post-transfection for IB, RT-qPCR or IF analysis.

The following siRNA oligos were used:

- i) Total Numb siRNA, 5'-CAGCCACUGAACAAGCAGA-3' (GE Healthcare);
- ii) ctrl siRNA, 5'-AGACGAACAAGUCACCGAC-3' (GE Healthcare);
- iii) Numb isoforms 1/2: 5'-AGGCUUCUUUGGAAAAACU-3' (GE Healthcare);
- iv) Numb isoforms 3/4: 5'-AGAUUGAAAGCUACUGGAA-3' (GE Healthcare);
- v) p53 siRNA VHS40367 (Invitrogen).

### **4.1.5 CELL TRANSFECTION**

Cells were plated in 10 cm dish the day before transfection to reach 50-70% confluency the day of transfection. DNA /CaPO<sub>4</sub> complexes were prepared by diluting 20µg DNA in serum free medium (final volume = 500 µl) and CaCl<sub>2</sub> in final concentration of 0,25 M. This mixture was added drop by drop in a second tube containing 2X HBS reagent. After incubating 5 min at room temperature (RT), the resulting 1 ml DNA/CaPO<sub>4</sub> complex mixture was added to the cell culture dish drop by drop and incubated for 15 h in a CO<sub>2</sub> incubator at 37 °C. Cells were collected and analyzed by IB after 48h.

### **4.1.6 VIABILITY ASSAY**

Primary tumor cells derived from tissue digestion of patient BC biopsy samples were plated as a single cell suspension in 6-well plates and treated with cisplatin (18 µg/ml) for 9 h, then released for 72 h in cisplatin-free medium (plus or minus 10 µM Nutlin-3a). For the evaluation of viability, cells were stained with 0.05% crystal violet (DNA intercalating dye), for 10 min and then extensively washed free of the dye. The crystal violet retained by live cells was leached in acetic acid (10%) and the dye absorbance (proportional to the number of living cells) was read at 595 nm.

## **4.2 SELECTION OF BREAST CANCER PATIENTS AND STATISTICAL ANALYSIS**

The RT-qPCR analysis of the expression levels of Numb isoforms, presented in Figures 32-34, was performed on a case-cohort of 890 BC FFPE samples. The case-cohort was built as

a subcohort of 672 patients randomly selected from the consecutive “IEO cohort” composed of 2453 BC patients (see paragraph 5.6). This subcohort (n=671) includes 585 patients free of distant metastasis and 87 patients who instead experienced distant relapse. We verified that the “subcohort”, representing ~27% of the entire cohort, was representative of the “IEO cohort” (see Table 1). No significant difference was scored considering patients’ features between the subcohort and the remaining patients not included in the subcohort. To yield the final case-cohort, the subcohort was enriched with all the remaining patients from the “IEO cohort” who experienced distant metastasis within 10 years of follow-up: this gave an additional 218 patients for whom RNA was available. Therefore, the final case-cohort included 305 patients with distant metastasis and 585 patients free of distant metastasis at 10 years after the excision of the primary tumor.

Variable	All	Not in subcohort	Subcohort	P <sup>a</sup>
<b>All</b>	2,453	1,781	672	
<b>Age at surgery</b>				0.06
<50	969 (39.5)	683 (38.3)	286 (42.6)	
≥50	1,484 (60.5)	1,098 (61.7)	386 (57.4)	
<b>Histology</b>				0.43
Ductal	1,960 (79.9)	1,430 (80.3)	530 (78.9)	
No Ductal	493 (20.1)	351 (19.7)	142 (21.1)	
<b>pT</b>				0.06
pT1	1,616 (65.9)	1,199 (67.3)	417 (62.1)	
pT2	756 (30.8)	521 (29.3)	235 (35.0)	
pT3	63 (2.6)	47 (2.6)	16 (2.4)	
pT4	18 (0.7)	14 (0.8)	4 (0.6)	
<b>Positive lymph nodes</b>				0.16
None	1,207 (49.2)	893 (50.1)	314 (46.7)	
1+	1,187 (48.4)	842 (47.3)	345 (51.3)	
NA <sup>b</sup>	59 (2.4)	46 (2.6)	13 (1.9)	
<b>Grade</b>				0.53
1-2	1,537 (62.7)	1,126 (63.2)	411 (61.2)	
3	859 (35.0)	619 (34.8)	240 (35.7)	
NA	57 (2.3)	36 (2.0)	21 (3.1)	
<b>PVI<sup>c</sup></b>				0.16
Absent	1,681 (68.5)	1,235 (69.3)	446 (66.4)	
Present	772 (31.5)	546 (30.7)	226 (33.6)	
<b>ER<sup>d</sup></b>				0.47
ER = 0	375 (15.3)	278 (15.6)	97 (14.4)	
ER > 0	2,078 (84.7)	1,503 (84.4)	575 (85.6)	
<b>ER/PgR<sup>e</sup></b>				0.56
Nonexpressed (both 0)	341 (13.9)	252 (14.1)	89 (13.2)	
Expressed (ER > 0 or PgR > 0)	2,112 (86.1)	1,529 (85.9)	583 (86.8)	
<b>HER2 status</b>				0.45
Negative	1,935 (78.9)	1,356 (76.1)	579 (86.2)	
Positive	264 (10.8)	191 (10.7)	73 (10.9)	
NA	254 (10.4)	234 (13.1)	20 (3.0)	
	<b>Mean (SD)</b>			<b>P<sup>f</sup></b>
<b>Ki-67</b>	24.0 (16.7)	23.8 (16.7)	24.5 (16.5)	0.34

**Table 1 Patient clinical-pathological characteristics in the breast cancer cohorts analyzed.**

Distribution of patient clinical-pathological characteristics in the random subcohort (n=672) compared with the entire IEO cohort (All, n=2453) and the Not-in-subcohort (n=1781) a) P-value derived from  $\chi^2$  test; b) not available c) perivascular invasion d) estrogen receptor e) progesterone receptor f) P-value derived from t-test

The association between Numb mRNA levels (quintile groups) and the risk of distant metastasis at 10 years post-surgery was evaluated with the univariate and multivariable “pseudolikelihood” modification of Cox proportional hazards regression model. These analyses were performed using widely available software (e.g., the `cch` function in the R survival package). All p-values are 2-sided with a significance level of 0.05.

## **4.3 PROTEIN PROCEDURES**

### **4.3.1 CELL LYSIS**

Adherent cells were rinsed twice with phosphate buffer saline (PBS 1X) and lysed directly in the cell culture plate in ice-cold RIPA lysis buffer [50 mM Tris-HCl (pH 7.5), 150 mM NaCl, 1 mM EDTA, 1% NP40, 0.5% sodium deoxycholate, 0.1% sodium dodecyl sulphate, protease inhibitor cocktail (Calbiochem, added freshly each time; 1:200) by scraping directly on the plate using a cell scraper. The volume of lysis buffer was proportional to the number of cells being lysed (around 300  $\mu$ l/10 cm dish or 50  $\mu$ l/well of a six well plate). Cell lysates were then incubated for 30 min on ice and then clarified by centrifugation at 13000 rpm at 4°C for 30 min. The supernatant was transferred to a new collection tube and the protein concentration was quantified using the Bradford assay (Biorad), according standard procedure. BSA calibration curves were used as standard reference for protein quantification. Laemmli sample buffer 4x [250 mM Tris-HCl, 40% glycerol, 8% SDS, 0.4% Bromophenol blue] supplemented with  $\beta$ -mercaptoethanol (120  $\mu$ /ml) was added to the lysate and samples were boiled at 95°C for 10 min before loading into a sodium dodecyl sulphate (SDS) polyacrylamide gel.

## **4.3.2 SDS POLYACRYLAMIDE GEL ELECTROPHORESIS (SDS-PAGE) AND IMMUNOBLOTTING**

Desired amounts of protein were loaded on polyacrylamide SDS denaturing gels (Mini-PROTEAN and Criterion Tris-Glycine Precast Gels). Electrophoresis was performed in Running buffer 1X (Running buffer 10X: 250 mM Tris-HCl, 192 mM Glycine, 1% SDS) at 200V. The electrophoretic transfer of proteins from polyacrylamide gels to nitrocellulose membrane was achieved by Trans-Blot Turbo semi-dry transfer system optimized for mixed molecular weight transfer (2.5 A, 25 V, 12 min).

Following transfer, the membrane was blocked 1 h (or overnight) in 5% non-fat dry milk in Tris-buffered saline (25 mM Tris-HCl pH 7.4, 137 mM NaCl, 2.7 mM KCl) supplemented with 0.1% Tween (TBS-T) and then incubated with primary antibodies diluted in 5% milk in TBS-T, for 1 h at RT, or at 4°C overnight, followed by 3 washes in TBS-T of 10 min each. The membrane was then incubated with different horseradish peroxidase (HRP)-conjugated secondary antibody (AbII) diluted in 5% milk in TBS-T for 45 min and washed again 3 times in TBS-T, 10 min each wash. The ECL (enhanced chemiluminescence) method (Amersham) was used to reveal proteins on Amersham Hyperfilm (GE Healthcare).

The following primary antibodies were used for immunoblotting (IB) : anti-Total Numb monoclonal antibody (generated in-house against amino acids 537–551 of human Numb<sup>63</sup>); anti-Numb 1/2 polyclonal antibody (generated in-house against amino acids 66-80 of human Numb isoform-1); anti-Mdm2 OP46 (EMD Millipore); anti-p53 DO-1 and FL-2393 (Santa Cruz Biotechnology); anti-phospho-p53–Ser 15 and anti-FLAG (2368; Cell Signaling); anti-Vinculin (V9131, Sigma).

### **4.3.3 PROTEIN ASSAYS**

#### **4.3.3.1 IMMUNOPRECIPITATION**

For co-immunoprecipitation experiments, HEK-293 cells overexpressing Numb-flagged isoforms were lysed in JS buffer [50 mM Hepes pH 7.5, 150 mM NaCl, 10% Glycerol, 1% Triton X100, 1.5 mM MgCl<sub>2</sub>, 5 mM EGTA, 1:200 Protease inhibitor cocktail added just before use]. Total lysate of HEK-293 cells was incubated with anti-FLAG M2-agarose Affinity Gel (Sigma) resin in JS lysis buffer for 2 h with rotation at 4°C. This resin consists of murine IgG1 anti-FLAG covalently attached to agarose. Beads were pulled down by centrifugation at 2000 rpm for 2 min and washed three times in JS buffer. Supernatant was collected before washing steps. Immunoprecipitated proteins were eluted in Laemmli loading buffer, boiled for 10 min at 95°C, centrifuged for 1 min and analyzed by IB.

#### **4.3.3.2 IMMUNOFLUORESCENCE**

For immunofluorescence (IF) experiments, cells, plated on glass coverslips, were washed twice with PBS, fixed by incubating with 4% paraformaldehyde for 10 min, washed again with PBS 1X and permeabilized in PBS 0.1% Triton X-100 for 10 min at RT. To avoid non-specific binding of the antibodies, coverslips were incubated for 1 h with goat serum as a blocking reagent. Cells were then incubated with primary antibody (anti-phospho-histone H2AX (Ser 139); Upstate) diluted in BSA 3% / PBS 1X, washed three times in BSA 1% / PBS 1X and then a secondary fluorochrome-conjugated (Cy3) antibody (Jackson ImmunoResearch Laboratory) was applied for 45 min in the dark. Cells were washed again three

times in PBS 1X before proceeding with 2 min DAPI staining (for nuclear visualization) followed by two additional washing steps. Coverslips were mounted in glycerol mounting medium and observed under a white-field microscope (Olympus) using a 20X 0.75 NA objective equipped with a digital camera for collection of cells and tissue section images. Digital images were computer processed using Fiji/ImageJ imaging software (National Institute of Health) and Photoshop (Adobe).

### **4.3.3.3 IHC CHARACTERIZATION OF p53 MUTATIONAL STATUS ON BC SAMPLES**

p53 functionality is often compromised in cancer, by direct mutations of the p53 gene or indirect mechanisms (see paragraph 2.3.4.5). To evaluate the p53 status of the BC FFPE cohort analyzed in Fig. 33-34, we took advantage of IHC analysis, that is largely recognized as a surrogate method for determining the p53 mutational status<sup>123,118</sup>.when sequencing is not possible or it is too time- and cost-consuming due to the high number of patients analyzed. The p53 IHC analysis was performed on the entire consecutive cohort of 2453 BC cases collected at the European Institute of Oncology (IEO, Milan) via standardized operative procedures, from BC patients who underwent surgery between years 1997 and 2000 (the “IEO cohort”). Informed consent was obtained for use of all clinical data connected with the related tissue sample.

3-µm thick sections prepared from formalin-fixed paraffin-embedded (FFPE) tissue microarray (TMA) blocks were deparaffinized, pre-treated with the Epitope Retrieval Solution 2 (pH 9) at 100°C for 20 min and then incubated for 30 min with the primary antibody (p53

DO-1, Santa Cruz Biotechnology) at a final concentration of 40 ng/ml. p53 IHCs were processed in a Bond Max Automated Immunohistochemistry Vision Biosystem (Leica Microsystems GmbH, Wetzlar, Germany) using the Bond PolymerRefine Detection Kit (DS9800, Leica Biosystems). TMA slides were scanned exploiting Aperio ScanScope system (Leica Microsystems) and then analyzed by a pathologist. For each sample, the percentage of cells with p53-positive nuclei was scored on a total of 500 cells counted. Patients were classified according to the percentage of p53-positive nuclei into three groups:

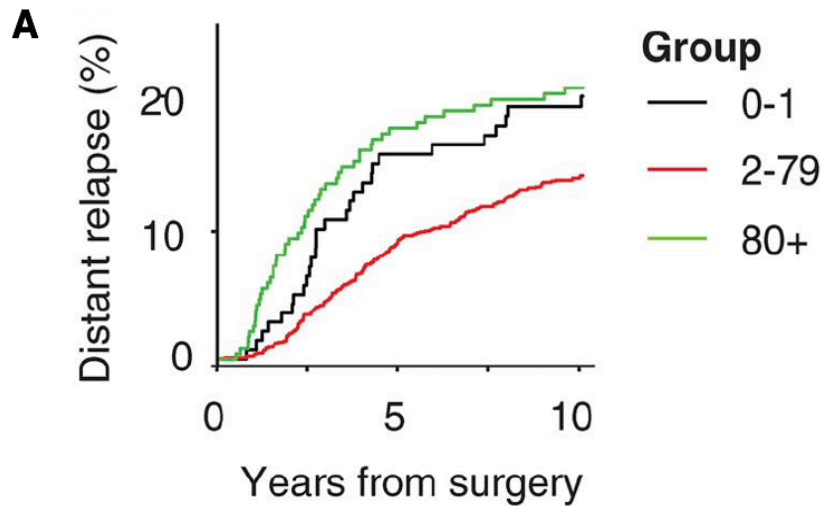
i) 0-1 (0-1% positive nuclei), indicative of loss of p53 protein due to missense mutations or mutations at the level of the p53 promoter <sup>118</sup>;

ii) 2-79 (2-79% positive nuclei), representative of p53 WT levels of p53;

iii) 80+ (over 80% positive nuclei), indicative of possible p53 missense mutations (generally involving the DNA-binding domain of p53), leading to p53 accumulation, as reported <sup>124 123</sup>.

This accumulation is probably due to mechanisms, such as the loss of the ubiquitin-ligase Mdm2, due to the impairment of the transcriptional p53 activity (Mdm2 is also one of the p53 target genes <sup>169,170</sup>).

We evaluated the cumulative occurrence of distant metastasis or death from BC in the entire cohort of BC patients, clustered into the three p53 IHC groups. Patients classified as 80+ and 0-1 displayed a worse prognosis compared to the 2-79% class of presumptive p53 WT samples, as expected for BCs with an alteration of the p53 pathway, suggesting that p53 IHC can be used as a surrogate to evaluate the p53 mutational status (Fig. 20A). Furthermore, the percentage of p53 presumptive mutated samples (groups "0-1" and "80+ combined) in the cohort (considering the samples with an available p53 IHC classification) is ~20%, in accordance with the published data reported on the incidence of p53 mutations in BC <sup>171,172</sup> (Fig. 20B).



**HR (95% CI)**

0-1 vs. 2-79 : 1.54 (1.04; 2.29),  $p=0.032$

0-1 vs. 80+ : 0.92 (0.58; 1.46),  $p=0.72$

80+ vs. 2-79 : 1.68 (1.23; 2.29),  $p=0.001$

**B**

p53 group	N	N. events
0-1	143	28
2-79	1463	204
80+	239	49
NA	608	38

**Fig. 20 Prognostic relevance of p53 status evaluated by IHC in the IEO cohort of BCs.**

**A)** The entire cohort of 2453 BC patients was analyzed and semi-quantitatively categorized into three groups based on the percentage of p53 nuclear stained cells: 0-1% (0-1 group, indicative of complete loss of p53), 2%-79% (2-79 group, indicative of WT p53) and >80% (80+ group, indicative of p53 missense mutations). Cumulative incidence of distant metastasis or death from BC is shown for each group. The hazard ratios (HR) comparing the different p53 groups (with P-values) is shown and was estimated with a univariate Cox proportional hazards model. 95% CI = confidence interval. **B)** Distribution of the 2453 BC patients into the p53 IHC groups. N: number of patients; “N. events”: number of patients with distant metastasis; NA: p53 IHC not available. Data published in <sup>136</sup>

## **4.4 NUCLEIC ACID TECHNIQUES**

### **4.4.1 mRNA PURIFICATION AND cDNA SYNTHESIS**

Total RNA including small RNAs was extracted from FFPE tumor sections included in the case-cohort, using the AllPrep DNA/RNA FFPE Kit (Qiagen). Patient samples were processed using on column semi-automated DNA/RNA purification including a RNase-free DNase treatment, exploiting QIacube technology according manufacturer's instructions. Two hundred nanograms of purified total RNA (measured using the NanoDrop ND-1000 Spectrophotometer) were used for first strand cDNA synthesis by Superscript VILO cDNA Synthesis Kit (Thermo Fisher Scientific) following the relative protocol scaled to a final reaction volume of 10  $\mu$ l. The reaction mix was incubated according to the following thermal conditions: 25°C 10 min, 42°C 60 min and 85°C 5 min.

### **4.4.2 GENE PREAMPLIFICATION AND RT-qPCR ANALYSIS**

The RT-qPCR screening was performed for the analysis of the relative mRNA expression levels of total Numb, Numb 1/2, Numb 3/4, Numb 1/3, Numb 2/4, Gapdh, Gusb, Hprt1, Tbp, using the specific TaqMan Gene Expression Assays. In brief, total Numb primers were chosen to amplify a portion of Numb protein (spanning Numb exon 5-6 boundary) common to all Numb isoforms (see Fig. 21, A assay). Hydrolysis probes spanning exon boundaries were designed to specifically detect and amplify Numb isoforms in which an exon skipping event occurs. Otherwise either one primer or the probe were designed partially on the exon in order to detect the exon inclusion event (see Fig. 30 for details).

Inventoried TaqMan gene expression assays used for the RT-qPCR screening were:

Hs01105433\_m1 for 'NUMB TOT' (NUMB isoform-1: NM\_001005743.1, -2: NM\_001005744.1, -3: NM\_003744.5 and -4: NM\_001005745.1), Hs01105434 for NUMB 1/3, Hs02800695\_m1 (HPRT1), Hs03929097\_g1 (GAPDH), Hs99999908\_m1 (GUSB), Hs01060665\_g1 (ACTB), Hs00963534\_m1 (ALAS1) and Hs00427621\_m1 (TBP) all purchased from Thermo Fisher Scientific.

The custom TaqMan gene expression assays to detect NUMB 1/2 (forw. GATGAATCAAGAG-GAATGCACATC; rev. TGAAGAACTTCCTTTCAGCTTTCAA; probe: TGAAGATGCTGTAAAAAG) and NUMB 2/4 (forw. TGGCACCACAATCTCCTACCT; rev. AGGCAGCACCAGAAGATTGAC; probe: CCAAGGGACCGAGTGG) were designed using the Primer Express Software V3.0 and purchased from Thermo Fisher Scientific. The custom TaqMan assay to detect NUMB 3/4 (forw. GAATGCACATCTGTGAAG; rev. ACTGCTTAACTGCTTTC; probe: TTCCAG-TAGCTTTCATCTTTT) was from Bio-Rad Laboratories.

Ten cycles of pre-amplification of cDNA were performed before RT-qPCR amplification, using a pooled mix of the aforementioned Taqman gene expression assay (0.2X each assays) and TaqMan Preamp Master Mix (Thermo Fisher Scientific), according to the following conditions (95°C 10 min, 10 cycles: 95°C 15 sec, 58°C 4 min). The preamplified reaction mix (final volume 50 µl) was diluted 1:5 before quantitative PCR amplification (5 µl were used for each RT-qPCR reaction).

RT-qPCR was performed in a volume of 10 µl in 384-well plate, analyzing each target gene as technical triplicates according to the following thermal cycling conditions: polymerase activation 1 cycle at 95°C for 10 min followed by 40 cycles: 95°C 15 sec, 55°C 1 min, on the Roche LightCycler® 480 Real-Time PCR System. The RT-qPCR output data for each gene were analyzed calculating the average Cq (AVG Cq) of the triplicate values when the standard deviation was < 0.4, or excluding the outlier value when the standard deviation was ≥

0.4. AVG Cq data were normalized on the geomean of 4 housekeeping genes (Hprt1, Gapdh, Gusb, Tbp). The normalized Cq (Cq normalized) of each target gene was calculated using the following formula:

$$\text{Cq normalized} = \text{AVG Cq} - \text{SF};$$

where: SF is the difference between the AVG Cq value of reference genes for each patient and a constant reference value K; K represents the mean of the AVG Cq of the 4 reference genes calculated across all samples (K = 24.148). This normalization strategy allows the retention of information about the abundance of the original transcript, as measured by RT-qPCR (i.e., in Cq scale), which is conversely lost when using the more classical  $\Delta\Delta\text{Ct}$  method. We defined Cq = 35 as the limit of detection and Cq values beyond this limit were set to 35. Normalized data were then processed for statistical analysis.

For gene expression analysis and p53 sequencing on primary breast tumors the DNA/RNA was extracted using the AllPrep DNA/RNA Mini Kit automated on QIAcube (QIAGEN). 500 ng of RNA was retrotranscribed in a reaction volume of 20  $\mu\text{l}$  as described before.  $\Delta\Delta\text{Ct}$  method was used to calculate relative fold-changes normalized against 5 reference genes (Gusb, Hprt1, Tbp, Alas1, Actb).

### **4.4.3 DIGITAL PCR**

We performed ONE STEP Droplet Digital PCR (ddPCR) on BC FFPE samples. For droplet generation, we placed 150 ng DNA/well for each sample and the appropriate ddPCR master mix (ONE STEP supermix or ddPCR buffer control) and the required assay, diluted in 20  $\mu\text{l}$  of final volume in the middle row of droplet generator cartridge (already preloaded in the DG8 cartridge holder) while 70  $\mu\text{l}$  of droplet generation oil were loaded into the bottom well. The prepared cartridge holder, placed within a Q-100 droplet generator, allowed the

sample to be partitioned in 20,000 nanoliter-sized droplets for each sample. 40 µl of water/oil emulsion droplet for each sample were transferred from the top well of the cartridge into a 96-well PCR plate. The PCR plate was placed in a thermal cycler using the following thermal cycling protocol: 57°C 30 min, 95°C 5 min, 40 cycles (each: 94°C 30 sec, 57°C 1 min, 98°C 10 min). Completed the PCR amplification, the plate was placed inside a QX100 droplet reader. Plate layout was set up according experimental design using QuantaSoft software. After QX100 droplet reader finished interrogating all well plate, this software was also used to analyzed data in each well reporting as output the concentration (copies/µl) of the related target within the sample. Data were normalized on the relative quantification of one of the samples. The following assays were used (see Fig. 21): A (Hs01105431), B (Hs01105433\_m1),C (forward primer: GCGGTCAAAGGAGCAAAACA; reverse primer: GGGACCTTTGGGATTAGTGAAAA; probe: ACTTTGTCTCCTGATTAGTAC ).

#### **4.4.4 DNA POLYMERASE-MEDIATED PCR AMPLIFICATION AND AGAROSE GEL ELECTROPHORESIS**

We extracted DNA and RNA from two distinct pools of primary normal breast cells (3 samples each), from MCF-10A non-tumorigenic breast epithelial cells and from seven primary BC samples using the AllPrep DNA/RNA Mini kit (Qiagen). Retro transcription of 0.5 µg RNA in 20 µl of final volume was performed using the Superscript VILO standard protocol. Once retrotranscribed, 2 µl of reaction volume were used for PCR amplification using the following primers (Fig. 22A):

Forw. gcttcccggttaagtaccttggc; Rev. tatgaccggcctggaagagac

PCR was performed using GoTaq DNA polymerase (Promega) according to manufacturer's guidelines and the thermal cycling protocol was adapted according to primer set melting temperatures ( $T_m$ ). Initial denaturation 95°C 2 min, 35 cycles (each cycle: denaturation 95°C 1 min, annealing 62°C 1 min, extension 72°C 3 min). After amplification, 15  $\mu$ l of PCR products mixed with 6X Blue/orange loading dye (Promega) were directly loaded, along with DNA marker (1 Kb DNA ladder, Promega) into the wells of a 1% agarose gel in 1X Tris-Acetate EDTA buffer (from 50X TAE: 250 mM Tris-HCl, 192 mM Glycine, 2 M Tris, 1 M acetic acid, 10 mM EDTA pH 8) and separated by gel electrophoresis. Gel Red (Biotium) was added 1:10000 to agarose as tracking fluorescent nucleic acid dye to visualize PCR products during electrophoresis separation. DNA bands were visualized under a UV lamp.

#### **4.4.5 p53 GENE SEQUENCING**

For p53 mutational status analysis of primary BCs, the *p53* gene (NM\_000546.4, 10 coding exons) was sequenced according to standard procedure. DNA was extracted through the AllPrep DNA/RNA FFPE Kit (Qiagen) from the FFPE BC samples, as described above (paragraph 4.4.1), and the *p53* gene was PCR amplified using specific PCR primers that cover the entire p53 coding sequence and all exon-intron boundaries. Every forward and reverse primer had a 5' universal tail (PE-21 forward; M13 reverse). The strategy allows sequencing all the different amplified fragments with only 2 sequencing primers that recognize the universal tail sequences of PCR primers. The primers were designed with a similar  $T_m$ , so that all the different regions could be amplified simultaneously in isothermal conditions. The PCR products were purified with EXO-SAP enzymes, sequenced with BigDye chemistry v3.1 and run onto a 3730xl Sequencer (Applied Biosystems). Data were analyzed with Mutation Surveyor (SoftGenetics).

## 5 RESULTS

### 5.1 EVALUATION OF THE EXPRESSION OF NUMB ISOFORMS IN BREAST CELL LINES

The aim of this thesis was to elucidate the role of the different Numb isoforms in the regulation of p53 and their relevance and contribution to breast carcinogenesis. We used two different human breast cell lines as model system to evaluate the Numb isoforms expression: the non-transformed mammary epithelial immortalized cell line, MCF-10A, and the tumor BT-474 cell line derived from a ductal carcinoma.

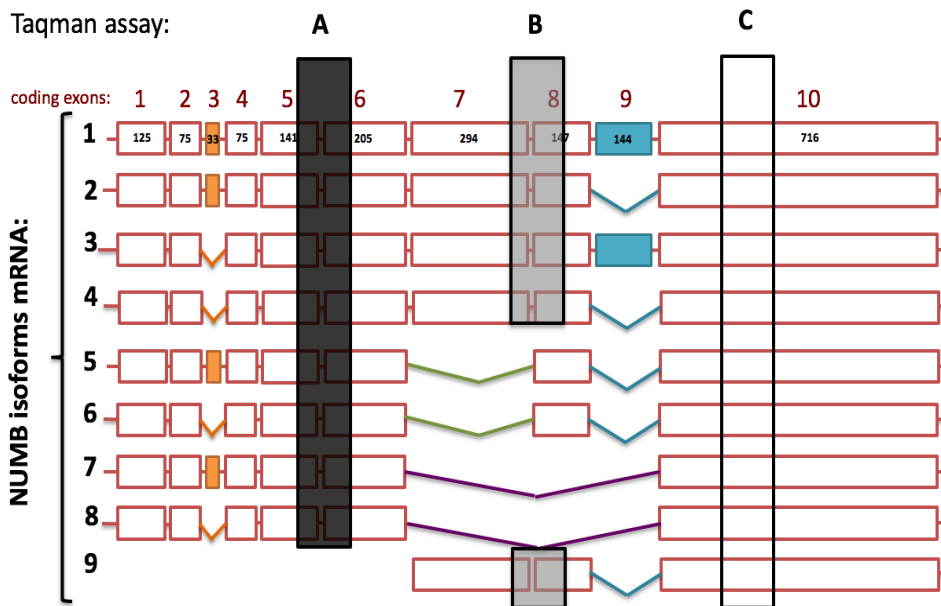
These cell lines are both p53-WT and represent breast cell line displaying an intermediate-high level of Numb expression compared to a panel of breast cell lines analyzed in the lab (not shown).

As a starting point, we evaluated the abundance of all Numb isoforms in these cell model systems. Nine different splice variants of Numb have been reported (Fig. 21A), but only isoforms 1 to 4 have been described in detail in the literature since they are expressed in many different tissues. To evaluate the levels of expression of the Numb isoforms, we used digital PCR and three different sets of Taqman assays able to recognize specific sets of Numb isoforms: Assay 'A' specific for Numb isoforms 1 to 8 designed across the coding exons 5-6; Assay 'B' recognizing Numb isoforms 1, 2, 3, 4 and 9 designed across the boundary of exons 7-8; Assay 'C' recognizing all nine isoforms designed across exon 10 (Fig. 21A). The digital

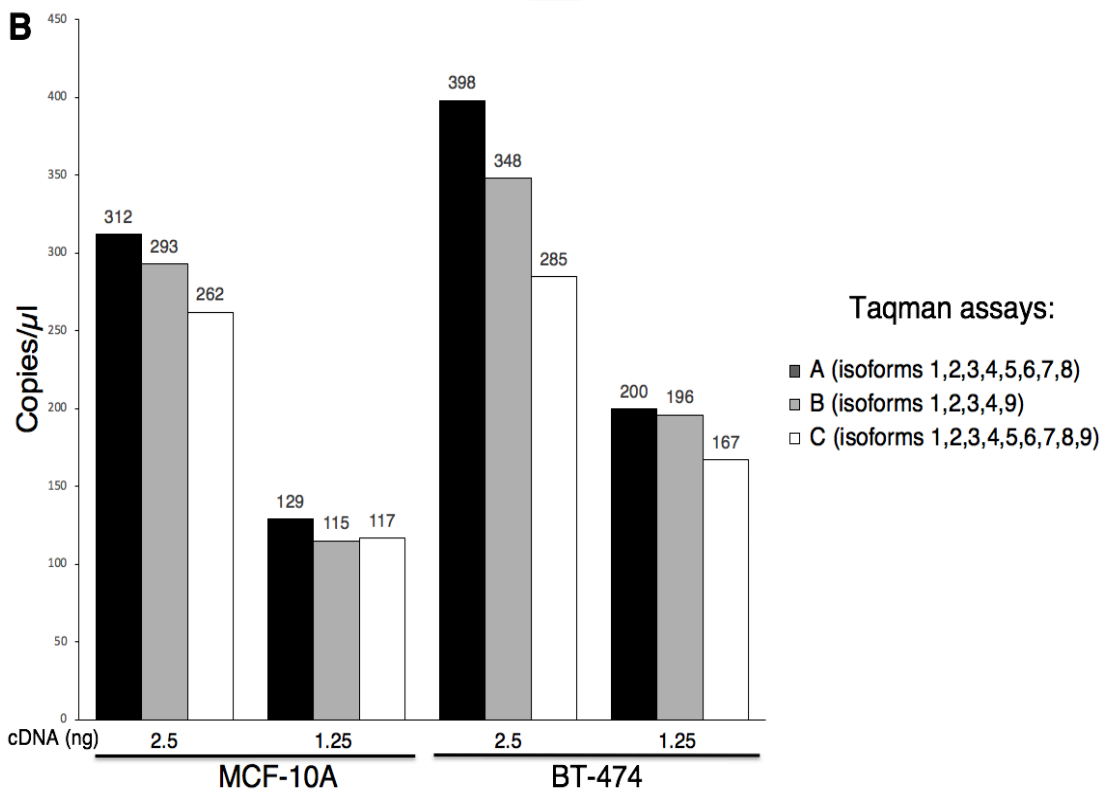
PCR analysis was performed on two different amounts of cDNA retrotranscribed from RNA

**A**

Taqman assay:



**B**



extracted from the two cell lines (Fig. 21B).

**Fig. 21 Numb isoforms 1, 2, 3 and 4 are the most abundant in the breast cell lines MCF-10A and BT-474.**

**A)** Schematic representation of all nine Numb isoforms described as products of alternative splicing events of the gene. Colored rectangles highlight the regions amplified by the Taqman assays (A, B, C) used in the digital PCR analysis. The coding exons are numbered in red and their length in bp is indicated in black inside the exon box. **B)** Digital PCR analysis

was performed on mRNA isolated from MCF-10A and BT-474 cells, using the Taqman assays indicated in A. The results show the number of copies/ $\mu\text{l}$  of each set of isoforms detected by the different assays. Two quantities of cDNA for each cell line was analyzed as indicated (ng). Results derive from a single experiment.

In both cell lines, the number of the molecules of isoforms 1 to 8 (assay A) is similar or slightly higher than the number of the molecules of all isoforms 1 to 9 (assay C) in the same cell line, indicating that isoform 9 is not present or is expressed in negligible amounts (Fig. 21B). Considering that also the number of molecules recognized by assay B (Numb 1, 2, 3, 4 and 9) is similar to the number of the molecules identified by the other two assays in each cell line (Fig. 21B), we can conclude that the isoforms 1 to 4 are the main Numb isoforms expressed in these breast cell lines, consistent with the literature.

To confirm the predominant expression of Numb isoforms 1 to 4 in human breast tissue, we amplified the cDNA retrotranscribed from RNA extracted from primary human normal and tumor breast tissue, using primers designed to amplify Numb isoforms 1 to 8 (Fig. 22A). The PCR products were analyzed on an agarose gel to discriminate the length of the amplified DNA (Fig. 22B). In all the samples, we observed two main bands  $>1000$  bp in length likely corresponding to Numb isoforms 1 to 4. Considering the very similar sizes of isoforms 1 and 3 and of isoforms 2 and 4 it was not possible to distinguish between these pairs. Indeed, in MCF-10A cells, in which we have confirmed at the protein level the expression of isoforms 1 to 4 (see Fig. 25C), we only observed two main bands in the PCR reaction.

In addition to the two main bands, other faint smaller bands were visible. These bands might indicate the expression at very low levels of other Numb isoforms (5 to 9) or they might represent incomplete or non-specific products from the PCR reaction (Fig. 22B).

To summarize, these results suggest that the four main Numb isoforms (1 to 4) represent the most abundant isoforms in tumor and normal breast cells. Although, we cannot exclude

that there might be some breast tumors displaying an enrichment of other Numb isoforms, we decided to focus our study only on the four major Numb isoforms.

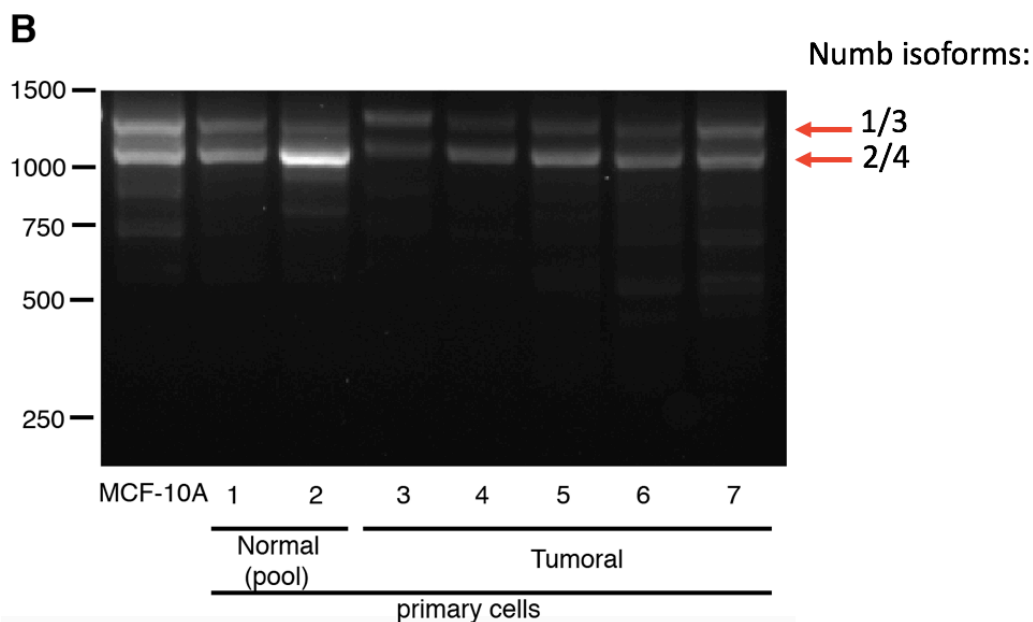
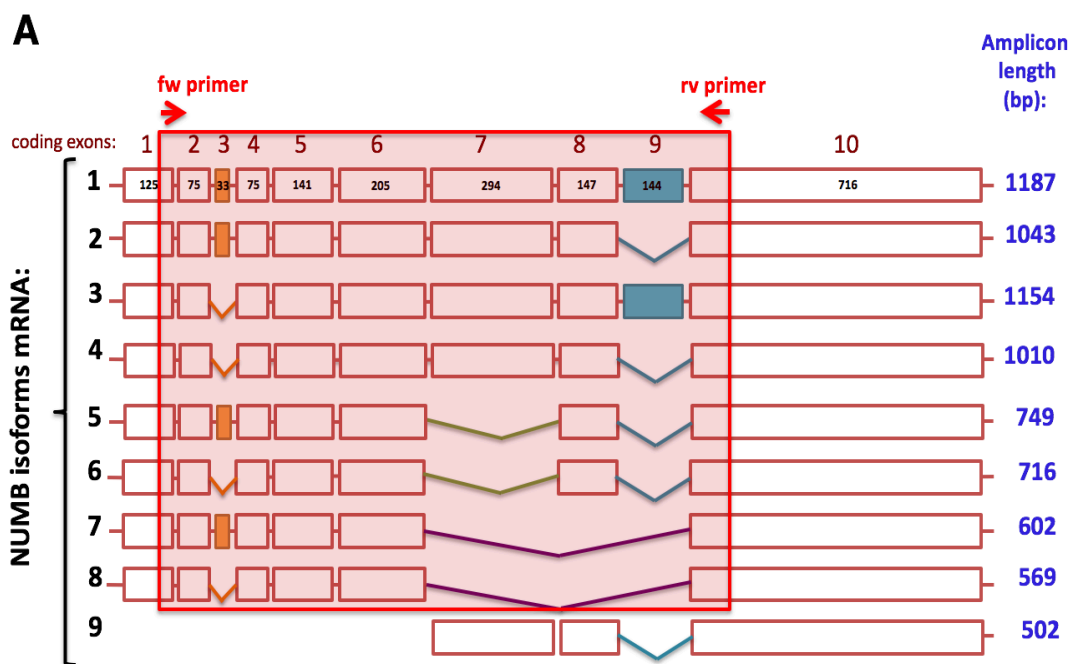


**Fig. 22** Numb isoforms 1, 2, 3 and 4 are the most abundant in normal and cancer primary breast cells.

**A)** Schematic representation of exon composition of all nine Numb isoforms, with the positions of the forward (fw) and reverse (rv) primers (red arrows) used for the PCR amplification shown in B. The corresponding length (bp) of the PCR products is shown on the right in blue. The ten Numb exons (numbered in red) and their corresponding size in bp

(indicated in black inside the exon boxes of isoform 1) are shown. **B)** Gel electrophoresis of the PCR products resulting from the reaction with primers shown in (A) on cDNA derived from MCF-10A cells and from primary normal breast cells (samples 1 and 2; each sample was a mix of cells derived from three different patients) and from primary breast tumor cells (samples 3 to 7 derived from individual tumors). Reference DNA lengths (bp) are shown on the left.

## **5.2 ONLY PTBi-CONTAINING NUMB ISOFORMS ARE ABLE TO EFFICIENTLY BIND MDM2**

Numb physiologically binds to and inhibits Mdm2, thereby, preventing Mdm2-mediated ubiquitination of p53 and stabilizing the p53 tumor suppressor protein<sup>63</sup>. Recent biochemical and structural studies performed in our laboratory on the Numb-Mdm2 interaction surface have demonstrated that only the long version of the Numb PTB domain containing the stretch of 11 aa coded by exon 3 (PTBi), which is present in isoforms 1 and 2, is able to bind to Mdm2 *in vitro*<sup>136</sup>. In contrast, the short version of PTB lacking the 11 aa sequence (PTBo) and present in isoforms 3 and 4, is not able to bind Mdm2<sup>136</sup>. Starting from these results, we reasoned that only the two PTBi-containing Numb isoforms 1 and 2 should be able to directly bind Mdm2 *in vivo*, and, thus, to inhibit p53 ubiquitination. To test this hypothesis, we performed co-immunoprecipitation experiments to investigate the physical interaction of the Numb isoforms with Mdm2. To overcome the problem of low basal protein expression and/or the poor affinity of commercially available antibodies, which often hinder co-immunoprecipitation experiments, we exogenously expressed FLAG-tagged Numb isoforms and WT Mdm2 in the human embryonic kidney cell line, HEK-293, which is known for its high transfection efficiency. We performed an anti-FLAG immunoprecipitation experiment and analyzed the immunoprecipitated proteins by immunoblotting (IB) with anti-FLAG and anti-Mdm2 antibodies. Results revealed that

Mdm2 co-immunoprecipitates preferentially with Numb isoforms 1 and 2, despite all isoforms being expressed and immunoprecipitated at very similar levels (Fig. 23).

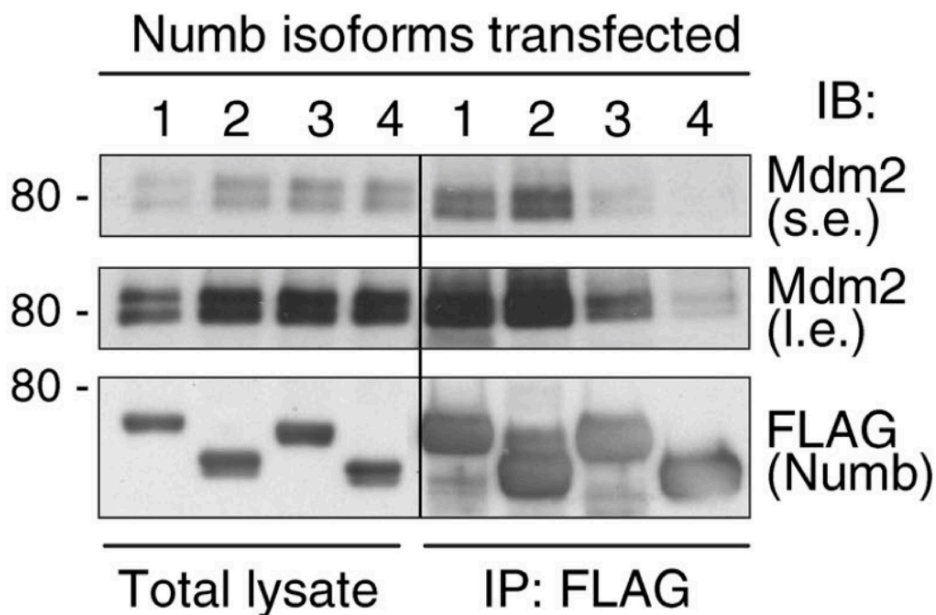


**Fig. 23 PTBi-containing Numb isoforms 1 and 2 are able to bind strongly to Mdm2.**

Lysates of HEK-293 cells transfected with the FLAG-tagged human Numb isoforms 1 to 4 and with WT Mdm2 were immunoprecipitated (IP) with the anti-FLAG antibody and immunoblotted (IB) as indicated. Total lysate was 0.005% of the IP. Reference molecular weight (MW) markers are indicated on the right. s.e.=short exposure; l.e.=long exposure. Data published in <sup>136</sup>.

In the IB, we observed a doublet for Mdm2 with a MW of ~90 kDa, compared with a theoretical MW of 55 kDa. While the slower migration of Mdm2 in polyacrylamide gels has been already described, we do not know exactly the nature of the doublet, although it is probably due to a post-translational modification (PTM) of the protein. However, we demonstrated that the Mdm2 antibody used is specific for the protein, by interfering Mdm2 expression in HEK-293 cells with siRNA oligos specific for Mdm2 and verifying in IB the disappearance of the band upon silencing (fig. 24).

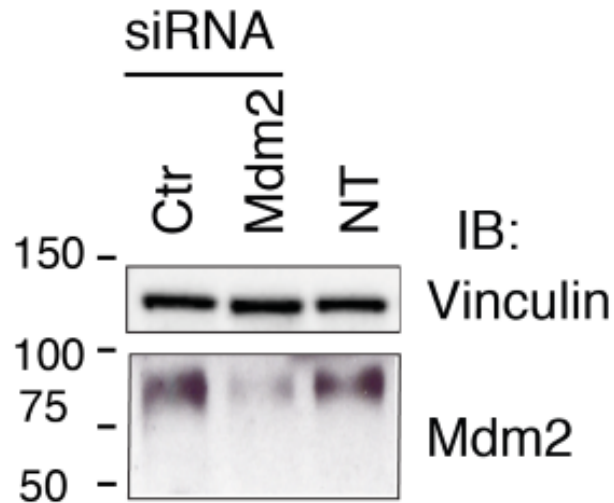


**Fig. 24 Specificity of anti-Mdm2 primary antibody tested by IB**

Lysate of Hek-293 cells transfected with Mdm2 siRNA oligo (10nM), Ctr siRNA or not transfected cells (NT) were analyzed by IB with the antibodies indicated on the right. Vinculin was used as a loading control.

### **5.3 ONLY PTBi-CONTAINING NUMB ISOFORMS ARE ABLE TO REGULATE P53 PROTEIN LEVELS**

Numb is able to protect the tumor suppressor p53 by inhibiting its ubiquitination by Mdm2 and consequently its degradation<sup>63</sup> (see paragraph 2.3.4.7). Considering that we observed that only Numb isoforms 1 and 2 bind strongly to Mdm2, we tested the possibility that only these isoforms might specifically be responsible for p53 regulation. We decided to test the effects of Numb silencing on p53 protein levels in the MCF-10A cell line, by selectively silencing Numb isoforms 1 and 2, isoforms 3 and 4, and all isoforms as a control. We designed siRNA oligos specific for each set of Numb isoforms, exploiting the presence or not of exon 3 (Fig. 25A-B for details). After 72 h from transfection of MCF-10A cells with the siRNA oligos, we assessed p53 protein levels by IB. We observed a marked reduction in p53

levels upon depletion of Numb isoforms 1 and 2, or of total Numb as control, while no effect was observed following depletion of Numb isoforms 3 and 4 (Fig. 25C).

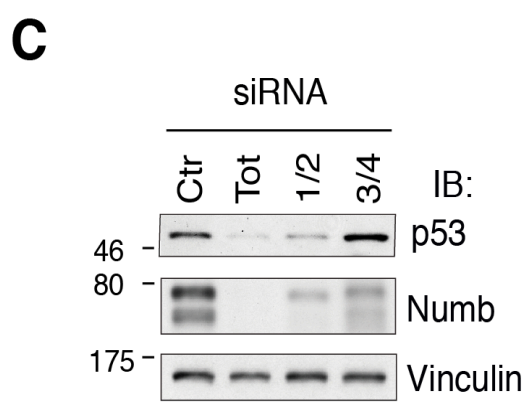
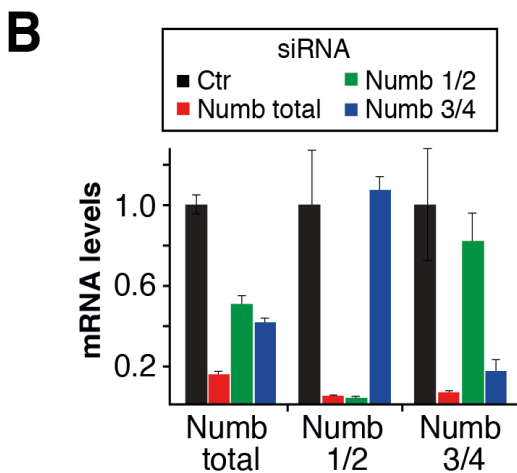
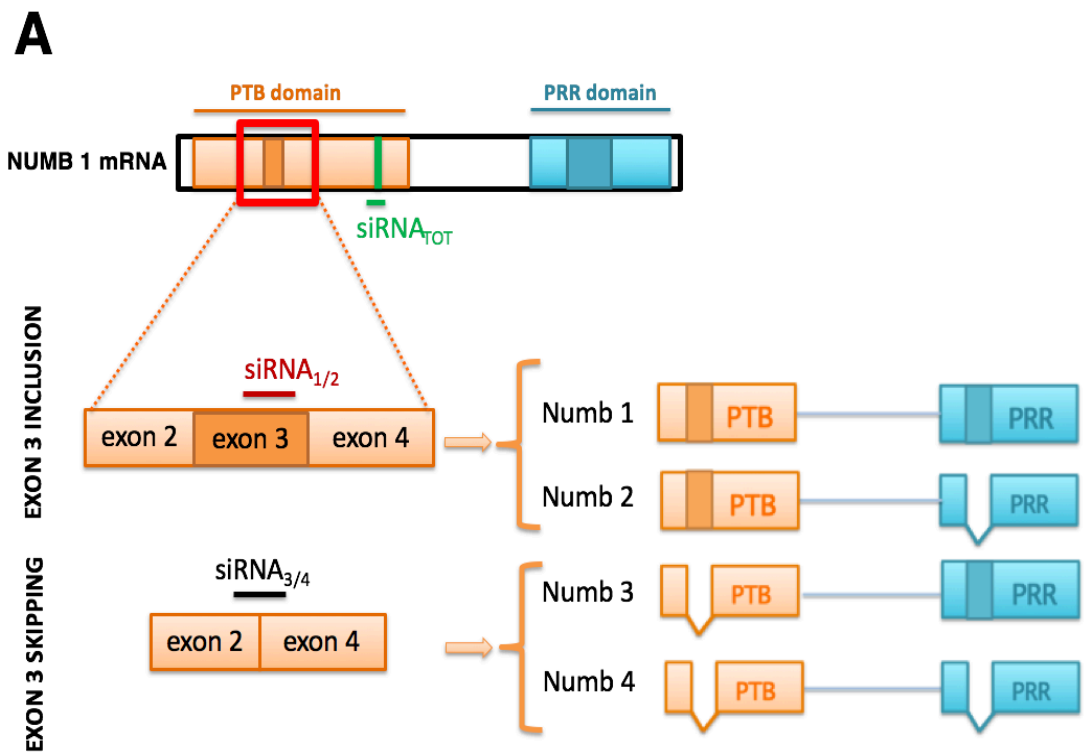


**Fig. 25 Only PTBi-containing Numb isoforms are able to regulate p53 levels**

**A)** Localization of siRNA target sequences at different positions along Numb mRNA. The siRNA oligo to interfere the expression of all Numb isoforms (siRNA TOT, green) was designed in a common region of all the four main Numb isoforms. The siRNA targeting Numb isoforms 1/2 (siRNA 1/2, red) recognizes a region within exon 3, retained specifically in Numb isoforms 1/2, while the siRNA recognizing Numb isoforms 3/4 (siRNA 3/4, black) was

designed in a region spanning the exon 2 and 4 boundary that is created when the exon 3 skipping event occurs. **B)** Efficiency of the interference of Numb isoforms in MCF-10A cells. MCF-10A cells were transfected with siRNA oligos (10 nM) specific for total Numb (Tot), Numb 1/2 or Numb 3/4, as indicated. After 72 h, cells were lysed and analyzed by RT-qPCR to assess the efficiency of Numb isoform silencing. Each target was analyzed in triplicate and the mean + standard deviation (sd) is shown. Results were normalized for each target on Numb mRNA levels of control siRNA (Ctr) transfected cells. **C)** An aliquot of the cells transfected as described in B) were lysed and subjected to IB with the indicated antibodies shown on the right. Control (Ctr) siRNA was used as a reference for basal Numb expression. Vinculin was used as a loading control. Numb protein appears as a doublet (upper band: Numb 1 and 3, 72 and 71 kDa respectively; lower band: Numb 2 and 4, 66 and 65 kDa ,respectively).

Data published in <sup>136</sup>

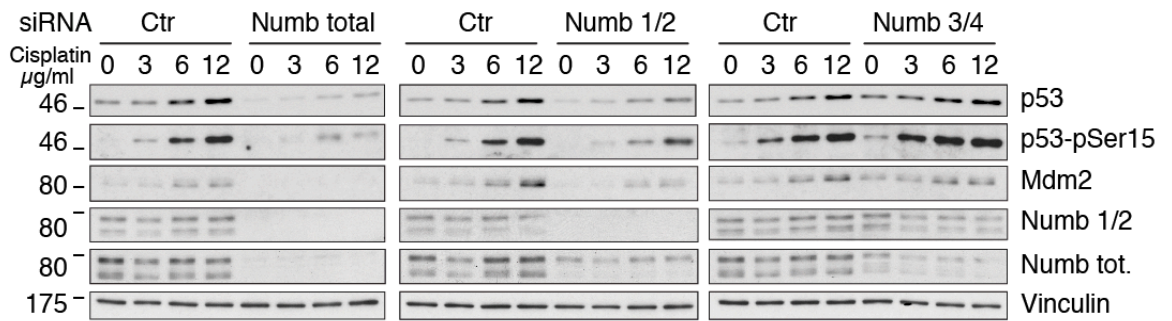
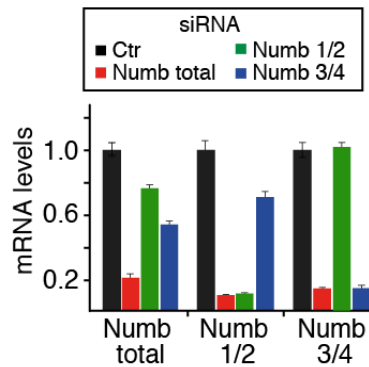
The efficiency of the siRNA silencing was confirmed by RT-qPCR by using Taqman assays designed to detect specifically the PTBi-containing or -lacking isoforms (Fig. 25B).

We concluded that the Numb isoforms have different roles in p53 regulation, with the PTBi-containing isoforms (1 and 2) being specifically required for p53 stabilization, in accordance with their exclusive ability to bind the E3-ligase Mdm2 (Fig. 23 ).

## **5.4 PTBi-CONTAINING NUMB ISOFORMS AFFECT THE P53-DEPENDENT RESPONSE TO GENOTOXIC STRESS**

In MCF-10A cells, loss of Numb results in an impairment of p53 activation in response to genotoxic stress <sup>63</sup>, as a consequence of the exaggerated Mdm2-mediated degradation of p53 itself <sup>44</sup>. To verify whether the regulation of this p53 function is Numb isoform-specific, we repeated the experiment of selective ablation of the Numb isoforms in MCF-10A cells, and, 72 h after transfection, we treated cells with increasing doses of cisplatin for 16 h (Fig. 26A). Cisplatin acts as a genotoxic drug able to trigger p53 activation in response to DNA damage, as assessed by the increasing levels of p53, both as total protein and as the serine 15-phosphorylated activated form (Fig. 26A, Ctr samples). The silencing of total Numb and

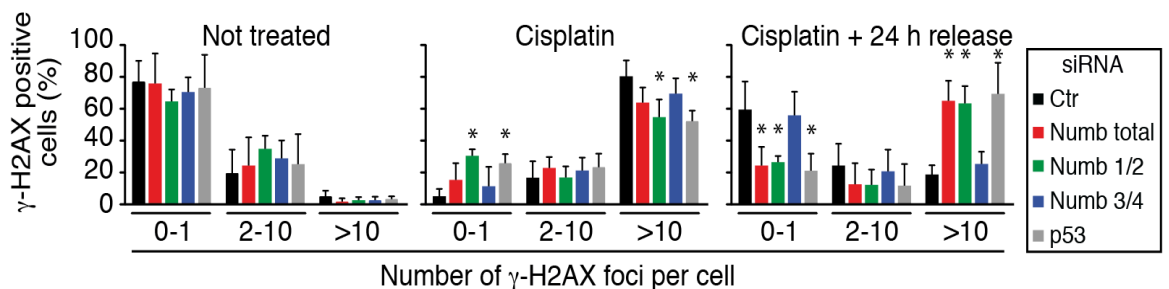
Numb PTBi-containing isoforms 1 and 2 (see Fig. 26B for silencing efficiency), significantly reduced the upregulation of total and activated p53 upon cisplatin treatment, as also confirmed by the reduction of the p53 transcriptional target, Mdm2<sup>170,173</sup>. In contrast, no effect was observed upon silencing the PTBo-containing Numb isoforms 3 and 4 (Fig. 26A). Based on this result, we reasoned that an alteration of Numb isoform 1/2 levels would affect p53-mediated functional responses, such as DNA damage repair. To test this, we focused on the known marker of DNA damage – phosphorylation of serine 139 of histone H2AFX ( $\gamma$ -H2AX) – and the number of foci positive for this marker; the persistence of these foci indicates that DNA damage has not been repaired<sup>174,175</sup>. MCF-10A cells were silenced for total Numb or for specific isoforms (1/2 and 3/4) and then treated for 15 h with cisplatin or vehicle in the untreated control sample. Cisplatin was then washed out and cells cultured in fresh medium for a further 24 hours to allow DNA repair. The untreated samples, and cisplatin-treated samples, before and after washout, were analyzed for the number of  $\gamma$ -H2AX foci by IF (Fig. 27). As expected, after cisplatin treatment, we observed an increase in the percentage of the cells with >10  $\gamma$ -H2AX foci in all samples indicative of DNA damage. Upon washout, this DNA damage was repaired only in Ctr siRNA or Numb 3/4 interfered samples, evidenced by a reduction in the percentage of the cells with >10  $\gamma$ -H2AX foci (Fig. 27A). In contrast, cells silenced for total Numb or Numb isoforms 1/2 did not display DNA repair, with the percentage of the cells with >10  $\gamma$ -H2AX foci remaining equivalent to that observed in p53 silenced cells (Fig. 27A). These data indicate that loss of p53, induced by the p53 siRNA or as consequence of Numb 1/2 silencing, impairs the ability of the cells to repair DNA damage (Fig. 27 A-B), thus confirming the role of Numb isoforms 1/2 in the regulation of p53 levels and activity and, consequently, of p53-mediated responses in the cell.

**A****B**

**Fig. 26 PTBi-containing Numb isoforms are able to regulate the p53 response to genotoxic stress.**

**A)** MCF-10A cells silenced for the indicated Numb isoforms (or with Ctr siRNA) were treated with increasing doses of cisplatin for 16 h. IB was performed using the antibodies indicated on the right. p53-pSer15 represents the activated form of p53 phosphorylated on Ser15. Vinculin was used as a loading control. MW markers are shown on the left. **B)** The efficiency of Numb isoform silencing in the MCF-10A cells described in A was assessed by RT-qPCR analysis. Data represent the mean + sd of technical triplicates, normalized to the Ctr siRNA for each assay.

Data published in <sup>136</sup>.

**A**

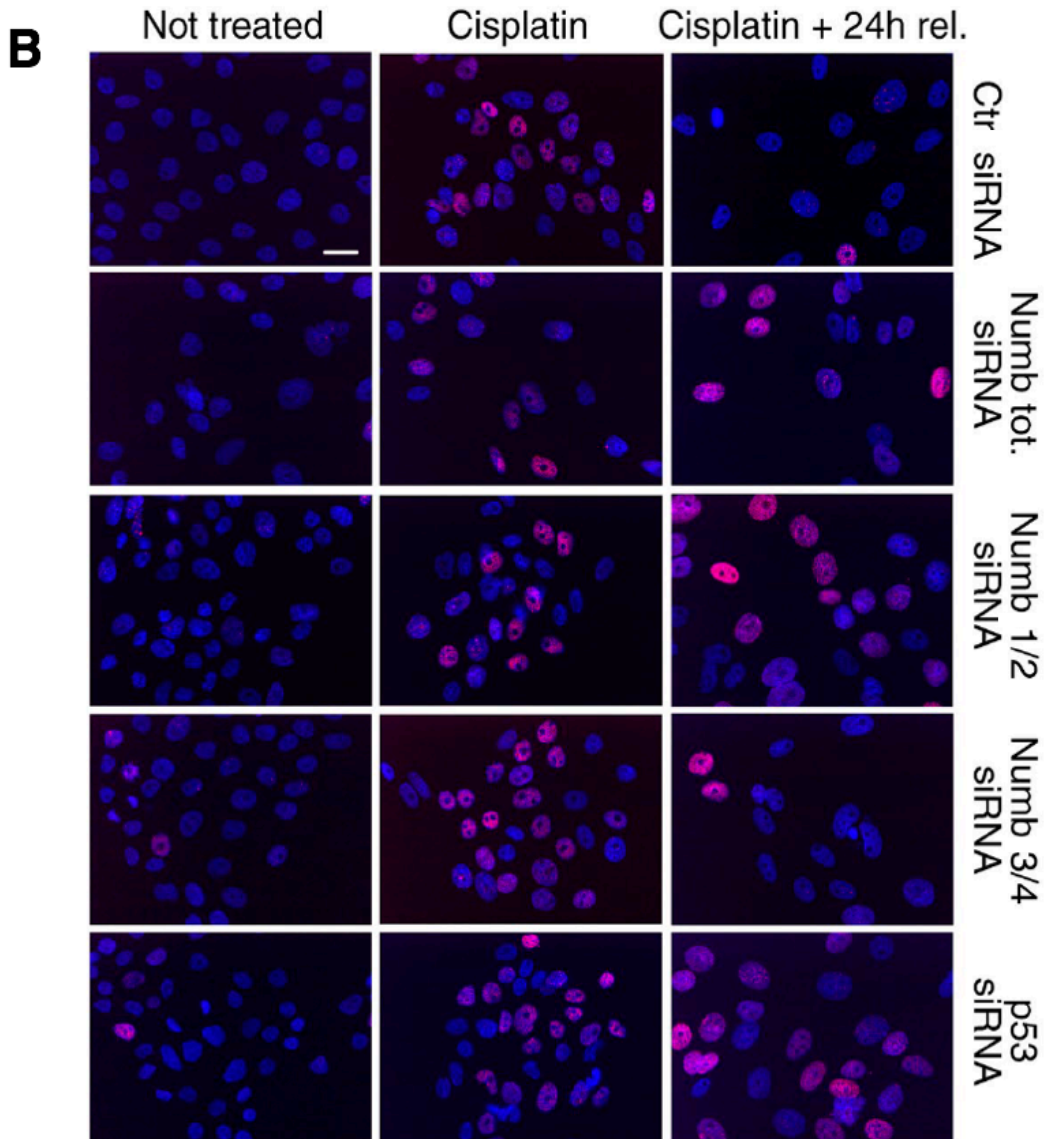


**Fig. 27 Numb PTBi-containing isoforms regulate p53-mediated DNA damage repair upon genotoxic stress.**

**A)** MCF-10A cells were silenced for Numb isoform expression as indicated in the legend on the right. Negative controls were transfected with siRNA (Ctr), while positive controls were transfected with p53 targeting siRNAs. Silenced cells were treated 72 h after transfection with vehicle alone (Not treated), or cisplatin (12  $\mu\text{g}/\text{ml}$ ) for 15 h before washing out drug and culturing in fresh medium for a further 24 h to allow DNA repair. Cells were then analyzed before (Cisplatin) and after (Cisplatin + 24 h release) washout by IF using an anti-phosphorylated  $\gamma\text{-H2AX}$  antibody. For each condition, ten random fields were analyzed (from two independent experiments), counting the number of  $\gamma\text{H2AX}$  foci/cell. In each field, we calculated the percentage of cells displaying 0-1, 2-10, >10  $\gamma\text{H2AX}$  foci/nucleus. The graph reports the mean + sd of these percentages calculated for each condition. \* = P-value  $\leq 0.01$  compared with Ctr-siRNA in each group. **B)** Representative panels showing IF staining with anti-phosphorylated  $\gamma\text{-H2AX}$  (red) and DAPI (blue) on the MCF-10A cells used in A, interfered as indicated on the right. Bar=50  $\mu\text{M}$ .

Data published in <sup>136</sup>.

## **5.5 LOW LEVELS OF PTBi-CONTAINING NUMB ISOFORMS PREDICT RESISTANCE TO GENOTOXIC TREATMENT IN PRIMARY BCs.**

The previous result indicates that the ablation of Numb isoforms 1 and 2 in MCF-10A cells leads to an impaired p53-dependent response to genotoxic stress. We reasoned that also primary BCs deficient in Numb 1/2 expression should display increased resistance to genotoxic stress. To investigate this possibility, we employed 13 primary mammary epithelial cell (MEC) samples derived from breast tumors with a p53-WT sequence. For each sample, we evaluated the relative mRNA levels of total Numb, Numb 1/2 and Numb 3/4 (Fig. 28).

Cells were treated with cisplatin (Fig. 29A) or cisplatin plus Nutlin-3a (Fig. 29B) for 9 h, released for 72 h in fresh medium and then analyzed for their viability (Fig. 29A-B). A significant inverse correlation between the mRNA levels of Numb isoforms 1/2 and cell viability was observed, while no evident correlation could be evidenced with the mRNA levels of Numb isoforms 3/4 and total Numb (Fig. 29C). To understand whether the increased resistance to cisplatin treatment in Numb 1/2-low BCs was due to a lack of p53 response, we treated in parallel the cells with Nutlin-3a, a known inhibitor of the Mdm2-p53 interaction, in order to restore p53 levels independently of Numb levels. The treatment was able to rescue sensitivity to cisplatin in Numb 1/2-low cells (Fig 29D), suggesting that the effect is mediated by p53. To exclude a toxic effect of Nutlin-3a, we also treated in parallel three BCs with only Nutlin-3a, and observed only a slight decrease of the cell viability (Fig. 29B).

In conclusion, we demonstrated that low mRNA levels of PTBi-containing Numb isoforms (1/2) are linked to increased resistance to genotoxic treatments in primary BC cells, likely due to the low levels of p53 in these tumors.

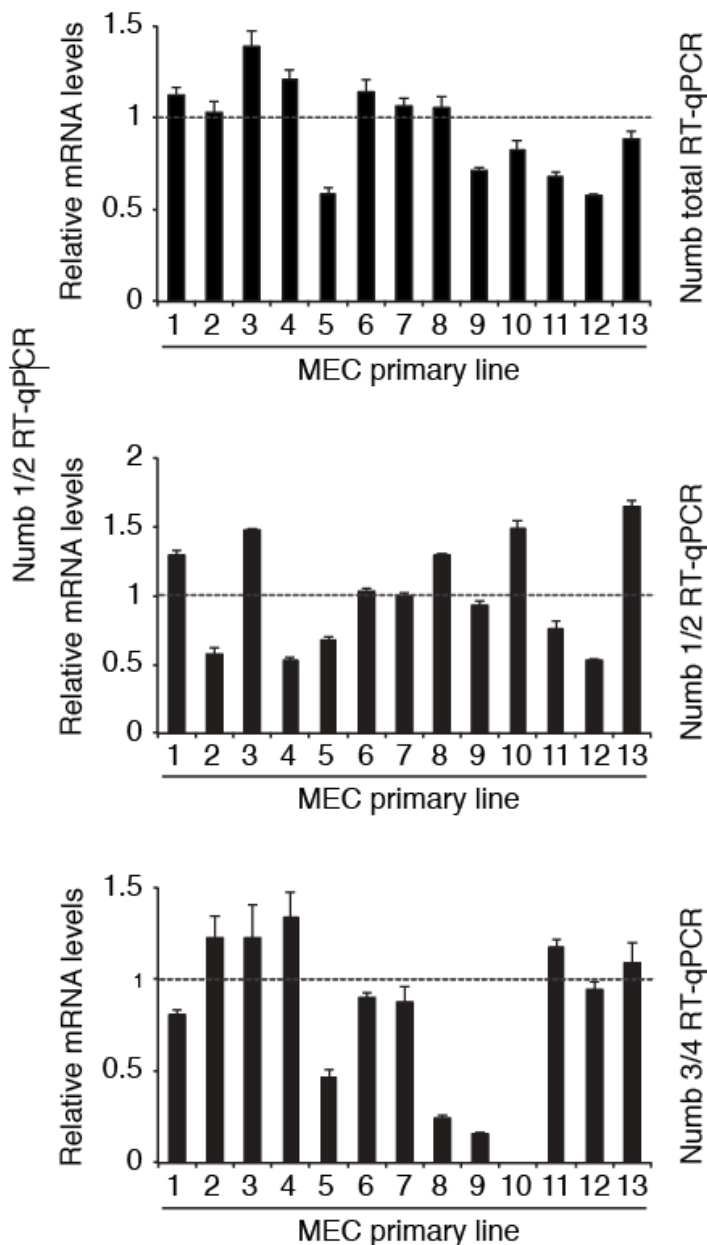


**Fig. 28 RT-qPCR analysis of the mRNA levels of total Numb, Numb 1/2 or Numb 3/4 in 13 primary breast tumors.**

MEC = mammary epithelial cells. Data are expressed as mean + sd of a technical triplicate normalized on mRNA levels MCF-10A cells (= 1; not shown). Data published in <sup>136</sup>.

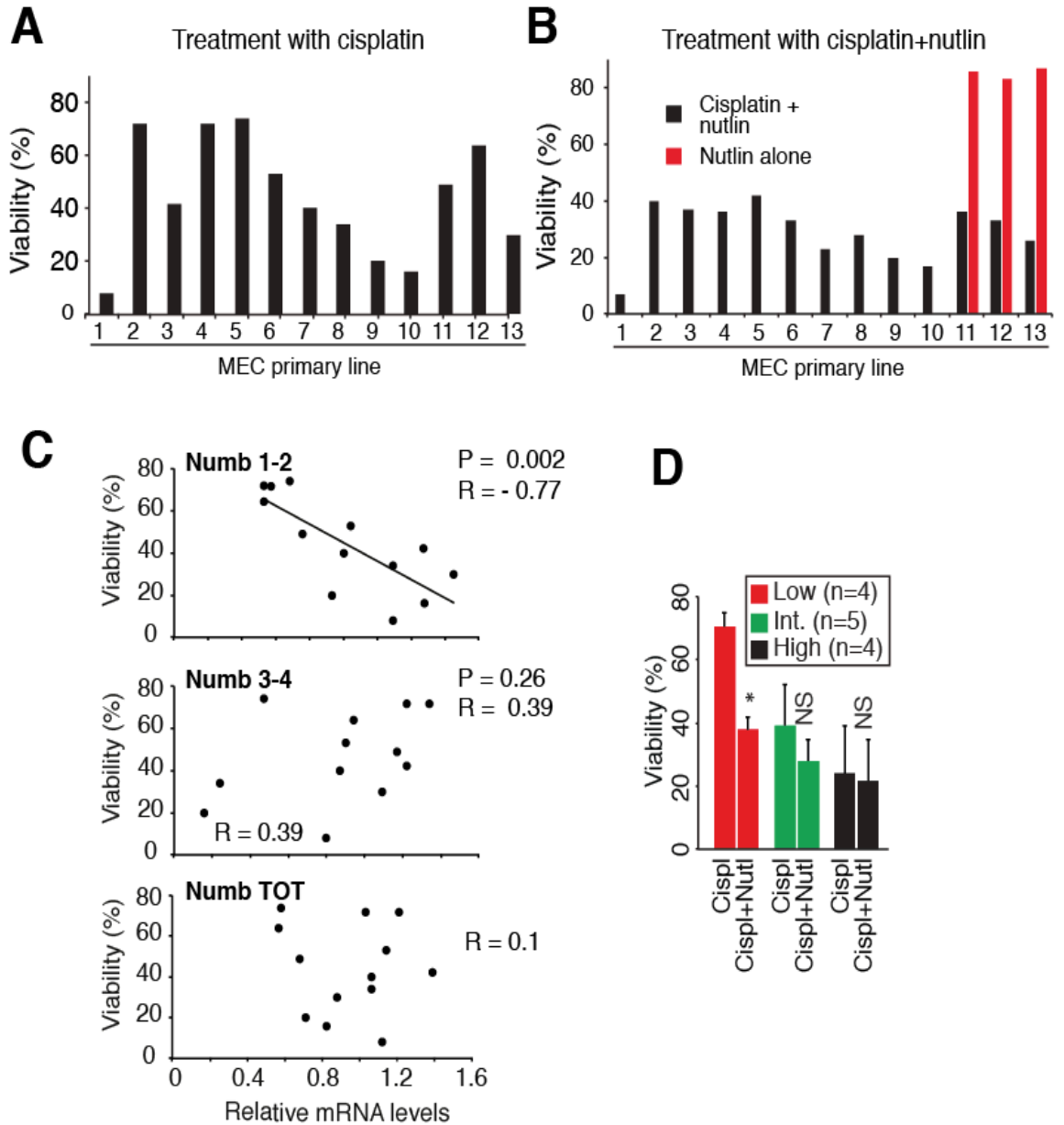


**Fig. 29** The response of primary BC cells to genotoxic treatment correlates with the mRNA levels of Numb 1/2.

**A-B)** Viability of the 13 primary BC samples described in Fig. 28, after 9 h of treatment with 18  $\mu\text{g/ml}$  cisplatin alone (A) or in combination with 10  $\mu\text{M}$  Nutlin-3a (B, black bars), or Nutlin-3 alone (B, red bars), and 72 h of release in fresh medium. Data are from a single experiment. **C)** Correlation between cisplatin sensitivity and Numb isoform expression. The cell viability of the 13 primary BC samples treated with cisplatin alone after release in fresh medium is reported as a function of the mRNA levels of Numb isoforms 1/2 (top), Numb isoforms 3/4 (middle) or total Numb (bottom, Numb-TOT), determined in Fig. 28. R= Pearson correlation coefficient and relative p-value (P) determined using the two tailed Student's t test are shown. **D)** Viability of primary BC cells, as a function of Numb 1/2 mRNA levels, after treatment with cisplatin (Cispl) or cisplatin+Nutlin-3a (Cispl+Nutl). The 13

primary BC cells analyzed in Fig. 28 were grouped according to the level of Numb 1/2 expression (low, intermediate or high) defined as tertiles of expression. The data are shown as the average value within these three groups + sd. P-values were determined using two tailed Student's t test comparing to cisplatin alone in each group. \* =  $P < 0.01$ . NS, not significant. Data published in <sup>136</sup>.

## **5.6 NUMB ISOFORMS PREDICT PROGNOSTIC OUTCOME IN HUMAN BCs**

We reasoned that low mRNA levels of Numb isoforms 1 and 2 in BCs, in addition to conferring resistance to genotoxic agents, might also lead to a more aggressive disease phenotype and potentially drive a worse prognostic outcome. This scenario would be in line with our previous observation that low levels of total Numb protein predict poor prognosis <sup>63</sup>. Therefore, we decided to perform a large-scale screening of a retrospective case-cohort of 890 formalin-fixed paraffin-embedded (FFPE) patients to investigate the correlation between Numb isoform expression and clinical outcome. This case-cohort was selected from a consecutive cohort of 2453 BC FFPE samples collected at the IEO between years 1997-2000; the "IEO cohort" and with at least 10 years of complete follow-up information after surgical resection of primary BC. The clinical endpoint was distant metastasis, defined as the time from removal of primary tumor to the appearance of distant metastasis or death from BC as first event. Details of the case-cohort selection are given in the Materials and Methods paragraph 4.2. The final case-cohort was comprised of 305 patients who experienced distant metastasis and 585 patients that were free of distant metastasis at 10 years of follow up. Clinical-pathological parameters of the "IEO cohort" and the selected case-cohort are shown on Table 1, paragraph 4.2.

To measure Numb isoform expression in the FFPE BC samples of the case-cohort, we used

RT-qPCR. Before performing this analysis, we assessed the specificity of the Taqman assays used for Numb isoform identification and the potential bias introduced by the cDNA pre-amplification step of the RT-qPCR procedure. We used different Taqman assays specific for the detection of PTBi-containing Numb isoforms (1/2), PTBo-containing Numb isoforms (3/4), exon 9-containing Numb isoforms (1/3) and exon 9-lacking Numb isoforms (2/4) (Fig. 30A). RT-qPCR reactions performed using plasmids encoding the single Numb isoforms as templates, verified the specificity of these Taqman assays (Fig. 30B).

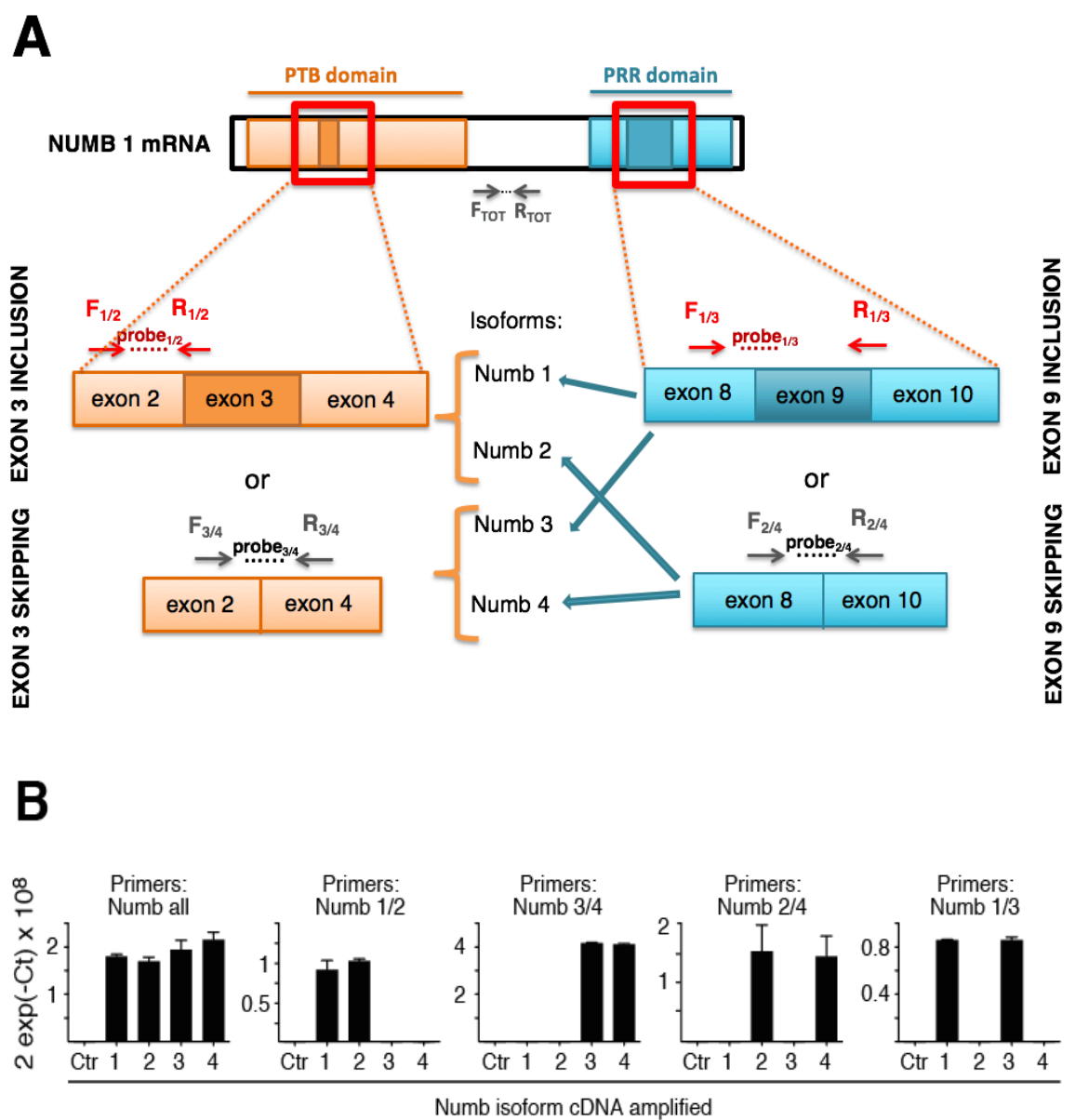


**Fig. 30 Analysis of the specificity of the Taqman assays used for Numb isoform amplification**

**A)** Schematic representation of target sequences recognized by Taqman assays on Numb mRNA. Taqman assays were designed for the specific detection of the different Numb isoforms resulting from the exon 3 (dark orange) and exon 9 (dark blue) alternative splicing events. A zoom of the exon 3 region (left) and the exon 9 region (right) is depicted to show the positions of the Taqman assays for the specific amplification of Numb isoforms 1/2 or 3/4 (left), or Numb isoforms 1/3 or 2/4 (right). Forward primer (F) and reverse primer (R) localization is indicated by the arrows and the position of the probe is identified by dotted lines. Tot= Total Numb, 1/2 = Numb isoforms 1 and 2, 3/4 = Numb isoforms 3 and 4, 1/3 = Numb isoforms 1 and 3, 2/4 = Numb isoforms 2 and 4. **B)** The specificity of the indicated Taqman assays (total: Numb all, Numb 1/2, Numb 3/4, Numb 1/3, Numb 2/4) was tested by RT-qPCR analysis of pcDNA vectors encoding the different Numb isoforms (1, 2, 3, 4). Empty pcDNA (Ctr) was used as a negative control. The analysis was performed in triplicate (values represent the mean + sd) using 0.1 pg of each vector. Data published in <sup>136</sup>.

To evaluate the possible bias introduced by the pre-amplification of the cDNA during the RT-qPCR procedure, we compared this method with digital PCR. This latter approach allowed us to quantify the amplified copies in absence of a pre-amplification step. We extracted RNA from five FFPE samples prepared from breast tumors and retrotranscribed to cDNA. The RT-qPCR analysis (after cDNA pre-amplification) and the digital PCR analysis were performed in parallel. Comparing these two techniques, the trend in the relative expression levels of Numb isoforms was maintained in all samples, albeit with some quantitative differences (Fig. 31). These results confirm that the pre-amplification step does not appear to affect the overall accuracy of the RT-qPCR analysis.

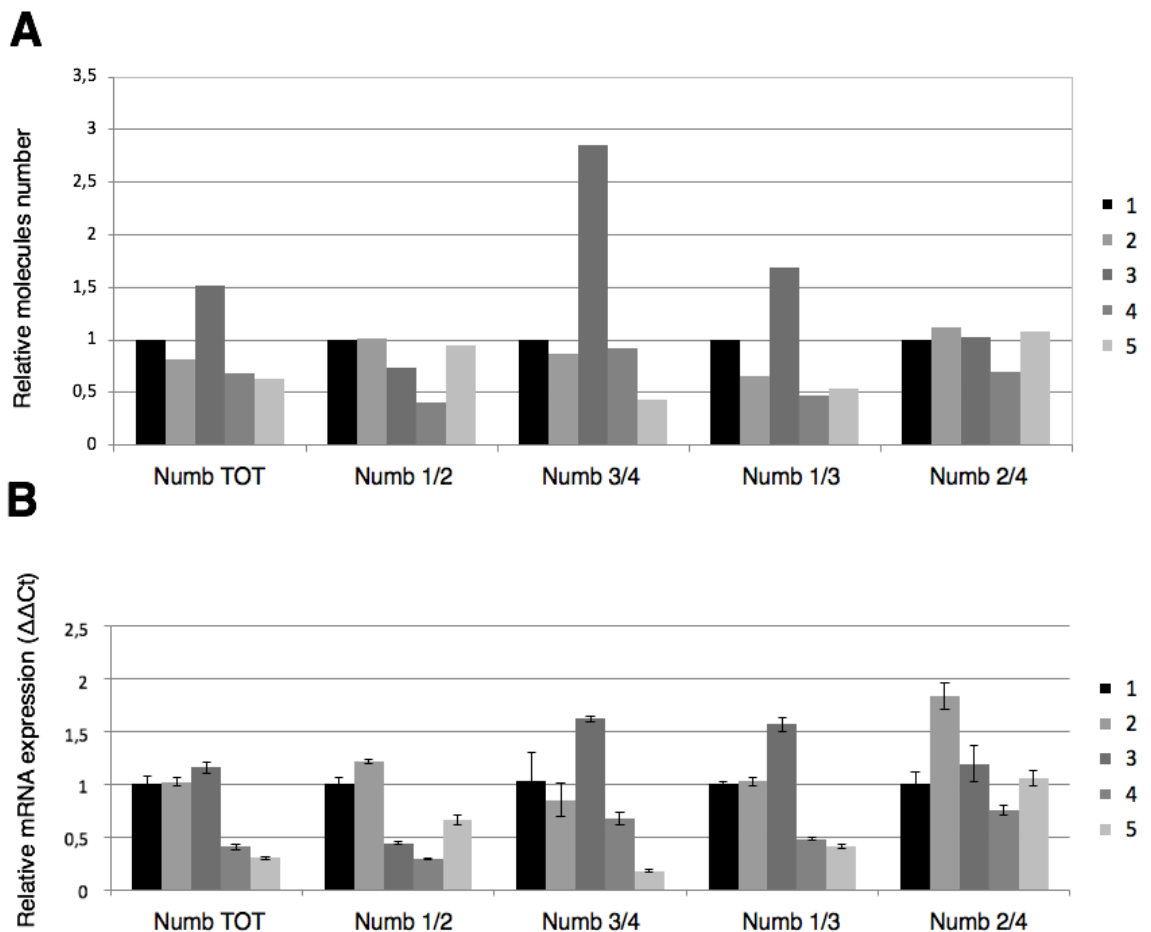


**Fig. 31 Comparison of relative expression levels of Numb isoforms detected by digital PCR and RT-qPCR on mRNA extracted from FFPE samples of BCs.**

**A)** Relative number of molecules of the Numb isoforms, or total Numb (Numb TOT) indicated on x-axis, detected by digital PCR analysis on cDNA retrotranscribed from RNA extracted from 5 FFPE BC samples (1 to 5), relative to sample 1 (assigning value=1 to the molecule numbers of this sample). **B)** The same samples as in A were analyzed by RT-qPCR after pre-amplification of the cDNA. The relative mRNA expression levels, normalized to sample 1, are shown. Data are expressed as the mean  $\pm$  sd of technical triplicate values.

Having verified the technical set-up of the assay, we proceeded with the analysis of the case-cohort of 890 BC patients. RNA extracted from each sample was retrotranscribed, pre-amplified and analyzed for the expression of total Numb, Numb isoforms 1/2 vs. 3/4, and Numb isoforms 1/3 vs. 2/4 (see paragraph 4.4.2 for details). Patients were stratified as “LOW” (the lowest quintile of expression) and “HIGH” (all the rest of the quintiles) for each Numb category (Fig. 32-34).

We next correlated Numb status (LOW vs. HIGH) for each Numb category (Total, Numb 1/2, Numb 3/4, Numb 1/3, Numb 2/4) with the prognosis of BC patients (Fig. 32-34). The prognostic endpoint of the analysis was the cumulative incidence of distant relapse up to 10 year after the surgical removal of the primary tumor.

Concerning the analysis relative to the total Numb category, “LOW” patients displayed a significant higher risk of distant relapse occurrence, compared to the “HIGH” group (Fig. 32): in univariate analysis the HR = 2.22, p-value = < 0.01; in multivariable analysis adjusted for tumor grade, Ki-67, tumor size, number of positive lymph nodes, age at surgery, ERBB2 status and estrogen/progesterone receptor status, the HR = 1.75, p-value = 0.002. This data is in accordance with our previous results indicating that loss of Numb protein, via hyper-degradation, correlates with poor prognosis in BC<sup>63,44</sup>. Our results suggest that loss of Numb mRNA expression is an independent predictor of risk of distant relapse and can be due in some BCs to additional mechanisms acting at the pre-translational level.

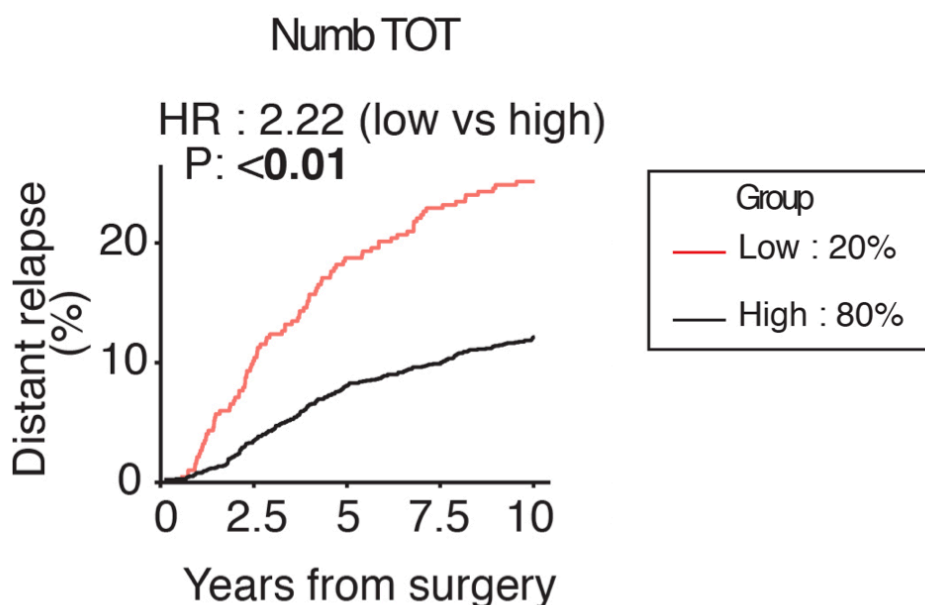


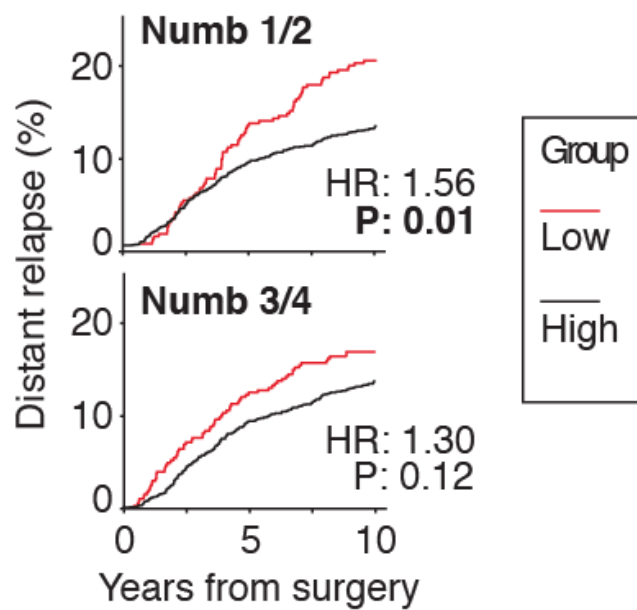
**Fig. 32 Low Total-Numb status correlates with higher risk of distant relapse.**

Cumulative incidence of distant relapse in a case-cohort of 890 BC patients according to their expression level of total Numb mRNA (Numb TOT). Univariate Hazard ratio (HR) was

calculated using univariate Cox proportional hazards regression model. Low, lowest expression quintile: High, remaining four quintiles. HR=hazard ratio; P= p-value. In the entire case-cohort (N=890), multivariable analyses were adjusted for Grade, Ki-67, tumor size, number of positive lymph nodes, age at surgery, ERBB2 status and estrogen/progesterone receptor status.

Regarding the analysis of the mRNA levels of Numb isoforms that differ for the presence of the exon 3 sequence (PTBi-containing Numb 1/2 vs. PTBo-containing Numb 3/4), we found that a “LOW” Numb 1/2 status predicts poor prognosis in a univariate analysis of the entire cohort: HR=1.56 , p=0.01 (Fig. 33A). When BCs were stratified according to their p53 status (WT vs. mutated, see Materials and Methods, paragraph 4.3.3.3 for details), the correlation with Numb 1/2 status in the univariate analysis was maintained only in the p53-WT subgroup of patients (HR=1.72 , p=0.01), while it disappeared in the mutated p53 subgroup (p53 mut) (Fig. 33B). The significance of the correlation, in the entire cohort and in the p53-WT subgroup, was lost in multivariable analysis adjusted for tumor grade, Ki-67, tumor size, number of positive lymph nodes, age at surgery, ERBB2 status and estrogen/progesterone receptor status (Fig. 33B). However, when we considered only the luminal subtype of BCs, which represents almost 70% of all BCs and are enriched in p53-WT tumors<sup>176</sup>, a low Numb 1/2 status emerged as an independent predictor of risk of disease recurrence, in multivariable analysis, both in the entire luminal subcohort (HR=1.54 , p=0.03) and in the p53-WT luminal-subcohort (HR=1.59 , p=0.05). These findings are in accordance with our results indicating an increased resistance to genotoxic treatments in the primary BCs displaying low Numb 1/2 levels (Fig. 29), and argue that also in real cancers the tumor suppressor function of Numb 1/2 is directly linked to its regulation of p53.

In contrast, Numb 3/4 expression levels did not correlate with disease outcome in any case (Fig. 33 A,B).

**A****B**

		Numb 1/2				Numb 3/4			
		Univariate		Multivariable		Univariate		Multivariable	
		HR	P	HR	P	HR	P	HR	P
Entire Cohort (N=890)	ALL	1.56	0.01	1.33	0.11	1.30	0.12	1.19	0.34
	p53-WT	1.72	0.01	1.43	0.12	1.27	0.27	1.09	0.73
	p53-Mut	0.93	0.85	0.85	0.69	1.25	0.47	1.54	0.26
Luminal Cases (N=666)	ALL	1.82	<.01	1.54	0.03	1.28	0.20	1.06	0.77
	p53-WT	1.89	<.01	1.59	0.05	1.28	0.29	1.04	0.89
	p53-Mut	1.08	0.89	1.30	0.68	1.09	0.88	0.72	0.60

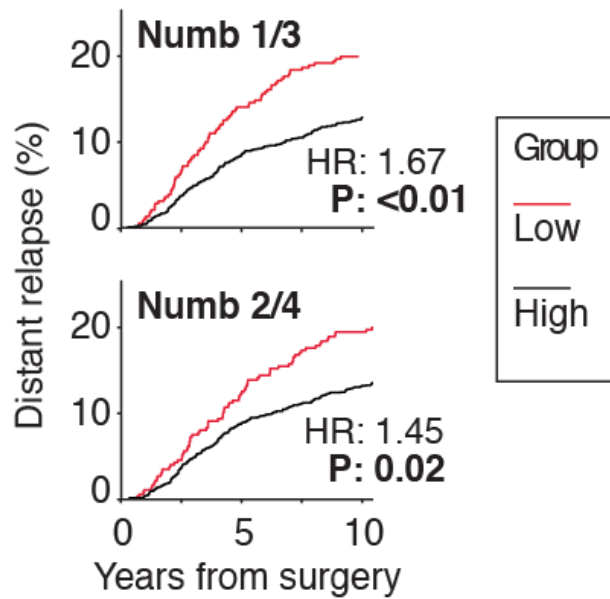
**Fig. 33 Expression of Numb 1/2 is an independent predictor of prognosis in luminal-type BCs with a p53-WT status.**

**A)** Cumulative incidence of distant relapse in a case-cohort of 890 BC patients stratified according to the mRNA expression levels of the indicated Numb isoforms. Group: Low (red, lowest quintile of expression) and High (black, remaining four quintiles). Hazard ratios (HR) and P-values are shown. **B)** Hazard ratio (HR) of distant relapse (with corresponding P-values) of low vs. high Numb 1/2 or Numb 3/4 patients in the entire case-cohort (N=890) or in the luminal subtype of BC (N=666), further stratified for p53 mutational status (WT or mutated). Univariate and multivariable analyses are calculated using the Cox proportional hazards regression model. In the entire case-cohort (N=890), multivariable analyses were adjusted for Grade, Ki-67, tumor size, number of positive lymph nodes, age at surgery, ERBB2 status and estrogen/progesterone receptor status, while in the luminal subtype of BC (N=666) multivariable analyses were adjusted for Grade, Ki-67, tumor size, number of positive lymph

nodes and age at surgery. Data published in <sup>136</sup>

Finally, from the univariate analysis of the mRNA levels of Numb isoforms that differ for the presence of the exon 9 sequence (Numb 1/3 vs. 2/4), we found that a “LOW” status of both Numb 1/3 and Numb 2/4 was associated with a significant increase in the incidence of distant relapse, both in the entire case-cohort and in the p53-WT subgroup (for low Numb 2/4 in p53-WT subgroup there is only a clear tendency but not significant) (Fig. 34). However, in multivariable analysis only the Numb 1/3 results as independent predictor of distant metastasis occurrence (Fig. 34B), both in the entire case-cohort and in the p53-WT subgroup (see discussion).

In conclusion, we found that low mRNA levels of total Numb or Numb 1/2 isoforms, Numb 1/3 and 2/4 are indicative of poor prognosis in BCs, whereas no correlation came from Numb 3/4 status. The result was further evidenced in the p53-WT patients, indicating an effect mediated principally by the downregulation of the p53 pathway by Numb 1/2 isoforms.

**A****B**

		Numb 1/3				Numb 2/4			
		Univariate		Multivariable		Univariate		Multivariable	
		HR	P	HR	P	HR	P	HR	P
Entire Cohort (N=890)	ALL	1.67	<.01	1.56	0.01	1.45	0.02	0.95	0.80
	p53-WT	1.82	<.01	1.70	0.03	1.45	0.07	0.84	0.47
	p53-Mut	1.41	0.27	1.70	0.17	1.12	0.72	0.96	0.93

**Fig. 34** Low levels of Numb isoforms 1/3 and of Numb isoforms 2/4 correlate with adverse prognosis.

**A)** Cumulative incidence of distant metastasis in a case-cohort of 890 BC patients clustered in two groups according to the mRNA expression levels of the indicated Numb isoforms. Group: Low (red, lowest quintile of expression) and High (black, remaining four quintiles). Hazard ratios and P-values are shown.

**B)** Hazard ratios (HR) of risk of distant metastasis (with corresponding P-values) in low vs. high Numb 1/3 or Numb 2/4 patients in the entire case-cohort (N=890), further stratified for p53 mutational status (WT or Mut). Univariate and multivariable analyses are calculated using the Cox proportional hazards regression model. Multivariable analyses were adjusted as described in fig. 32.

## 6 DISCUSSION

### 6.1 THE ROLE OF NUMB ISOFORMS IN THE REGULATION OF THE p53 PATHWAY.

An organized picture of cancer hallmarks was proposed in 2000 by Hanahan and Warburg in their widely cited review <sup>177</sup>. The overwhelming complexity of cancer biology was systematically simplified in a few major cancer properties. They include sustaining proliferative signaling, resisting cell death, evading growth suppressors, enabling replicative immortality, inducing angiogenesis, and activating invasion and metastasis <sup>178</sup>. In addition to these established hallmarks, coordinated, aberrant alternative splicing is emerging as a common driver of carcinogenesis and tumor progression, thus, justifying its consideration as one of the cancer hallmarks <sup>179</sup>. The vast majority of human genes, perhaps over 94%, are alternatively spliced. Cancer-associated genes can be expressed as splice variants that either favor or counteract cancer cell development. Thus, deregulation of alternative splicing could drive the switch towards the inappropriate expression of multiple oncogenic splice isoforms <sup>147,179</sup>.

Numb is among the genes that encode for different isoform variants, deriving from alternative splicing events occurring at the level of exon 3 and exon 9 during Numb pre-mRNA maturation. To date little is known about the specific roles of these isoforms (see paragraph 2.3.6). The interest of our lab in Numb started from the discovery of its tumor suppressor role in breast cancer <sup>44</sup>, where loss of Numb was detected in around 30% of cases, correlating with poor prognostic outcome <sup>44,63</sup>. More recently, we demonstrated

how the role of Numb in the regulation of the Mdm2-p53 circuitry contributes to its tumor suppressor function<sup>63</sup>, leading to p53 downregulation upon loss of Numb. In particular, a detailed structural and biochemical characterization of the Numb-Mdm2 binding interface, highlighted a critical role of a short region of Numb, including the exon 3-coded sequence, in the inhibition of the Mdm2 ubiquitin-ligase activity on p53<sup>136</sup>. As result of alternative splicing events, the Numb exon 3 region is included in two out of four Numb isoforms (Numb 1/2) suggesting a Numb isoform-specific role in Mdm2-p53 circuitry regulation.

In this thesis, we demonstrated that only Numb isoforms 1/2 are indeed able to efficiently bind to Mdm2, thereby stabilizing p53 protein levels, as indicated by the reduction of the p53 levels observed upon Numb 1/2 silencing in human mammary epithelial cells.

p53 tumor suppressor function guarantees the ability of the cell to respond to genotoxic damage by activating p53-dependent DNA repair or apoptosis of damaged cells. Loss of Numb isoforms 1/2 is able to functionally mimic p53 dysregulation, resulting in increased resistance of cells to DNA damage stimuli and persistence of unrepaired DNA lesions, while no effect was induced by loss of Numb isoforms 3/4, highlighting the importance of exon 3 in the p53-dependent DNA damage response.

We reasoned that levels of the Numb isoforms could therefore have an impact on breast cancer sensitivity to genotoxic treatment. In this regard, analyzing different p53-WT primary breast tumors, we found that low Numb 1/2 expression was associated with an increased resistance to genotoxic agents. Moreover, Numb 1/2-low BCs can be re-sensitized to treatment by rescuing p53 levels with Nutlin-3a (an inhibitor of Mdm2). Of note, Nutlin-3a is also able to revert CSC expansion associated with Numb-deficient breast cancer

<sup>162</sup>. These observations not only confirm the role of Numb 1/2 in p53 regulation, but open the way to a possible therapeutic strategy for overcoming resistance to chemotherapy and preventing CSC-driven tumor relapse of Numb 1/2-low BCs. The extensive mapping study of the Numb-Mdm2 interaction <sup>136</sup> could be exploited for the design of molecules that, by mimicking the Numb exon 3-encoded surface on Mdm2 could rescue p53 function in Numb-deficient tumors.

## **6.2 PROGNOSTIC VALUE AND RELEVANCE OF THE NUMB ISOFORM EXPRESSION IN BREAST TUMORIGENESIS.**

Low Numb 1/2 expression levels, which confers resistance of BC cells to chemotherapeutic treatment, is linked to a more aggressive disease and poor prognosis, as emerged from our screening on a case-cohort of 890 BC patients. Interestingly, by stratifying patients according to p53 mutational status, we were able to unmask the prognostic role of low Numb 1/2 specifically in p53-WT BCs. These results further support the idea that the relevance of Numb 1/2 isoform expression in BC is mainly attributable to the regulation of p53. It is plausible that in tumors where p53 is already deregulated or not functional (due to mutations of the gene for instance), the downmodulation of Numb 1/2 levels would not provide an additional growth advantage or contribute significantly to the adverse prognostic outcome. These results are particularly interesting since BCs, compared to other tumors, display a relatively lower p53 mutation rate <sup>172</sup>, in particular, among luminal subtype cases, which are described to be largely p53-WT <sup>176</sup>.

In luminal BCs, or more widely in p53-WT BCs, p53 dysfunction might depend on indirect mechanisms that lead to p53 inactivation. Among these mechanisms, loss of ARF (Mdm2 inhibitor) <sup>180</sup> and *MDM2* gene amplification <sup>181</sup> result in decreased p53 activity. However,

these alterations are infrequent in BC, being detected in 20% and 10% of tumor cases, respectively<sup>182,183</sup>. In this thesis, we propose that the altered alternative splicing of Numb exon 3, might be an additional mechanism impacting on p53 stability in p53-WT BCs. Indeed, a low Numb 1/2 expression has an even stronger prognostic value in luminal BCs and emerges as an independent predictor of poor prognosis in these tumors.

A more complex scenario emerged from the analysis of the mRNA levels of the Numb isoforms in the BC case cohort. In particular, in tumors displaying low levels of all the Numb isoforms (Numb total low), we observed a worse prognosis, with an effect even stronger than we found in Numb 1/2 low BCs.

Until now, the best characterized mechanism underlying the alteration of Numb expression in Numb-deficient BCs has been represented by post-translational events causing enhanced ubiquitination, and ensuing proteasomal degradation, of the Numb protein<sup>44</sup>. However, our results demonstrate that also pre-translational deregulation of Numb might be an additional mechanism responsible for loss of Numb in some BCs. In order to better stratify the BC patients according the mechanism responsible of Numb deficiency we are planning to characterize the case-cohort by IHC for the expression of Numb protein. The combined analysis of Numb mRNA and protein levels will provide a more complete scenario about the alteration present in the Numb deficient patients, thus accordingly directing a more precise targeted therapeutic approach.

To complete the picture, we also observed a worse prognosis in BC patients displaying low expression levels of Numb 1/3 and Numb 2/4 (with or without the region coded by exon 9, respectively), while no significant effect was found for low levels of Numb 3/4 (the

isoforms without the exon 3 coded region). It is likely that the prognostic-predictive effect for Numb 1/3 and 2/4 is driven by loss of Numb 1 or 2 respectively, having demonstrated their relevance in p53 regulation.

Low Numb 1/3 emerges in particular as an independent predictor of prognosis in the analysis of the entire case-cohort and specifically in the p53-WT subgroup of patients. This result is prompting us to further investigate the role of the single Numb isoforms in BC. It is clear that the impact on the tumorigenesis (and consequently on the prognosis) of the Numb isoforms might derive from a combination of the multiple pathways regulated by Numb and for a fully comprehension of the prognostic values of the Numb isoforms will be necessary to better elucidate the precise contribution of each individual Numb isoform to cellular processes. For instance some studies have highlighted a differential role of Numb 1/3 vs. Numb 2/4 in Notch signaling regulation, in particular in the neuronal lineage<sup>20</sup> and further investigations are necessary to uncover possible isoform-specific functions in other Numb-regulated pathways, such as Hedgehog signaling. The impact on tumorigenesis and prognosis could be ascribable to the balance of the different pro- e anti-tumorigenic pathways controlled by the single Numb isoforms. In this regard, it is interesting to remark how the loss of all the Numb isoforms (observed with the total Numb mRNA levels) showed the strongest predictive value of poor prognosis in BCs.

In the near future, we are planning to further characterize the function of Numb isoforms 1 to 4, individually, having demonstrated that they are the main Numb isoforms present in breast cells. To this purpose, we have set up an 'artificial' Numb-deficient cellular model system, MCF-10A cells stably silenced for Numb, in which we plan to re-express each single isoform to study their specific contribution to signaling pathways epistatically controlled by

Numb (e.g., Notch, Hedgehog, p53) and phenotypes involved in tumor progression, such as proliferation, response to genotoxic stress, stem cell homeostasis and migration.

Moreover, it will be interesting to understand how and whether the different subcellular localizations of the Numb isoforms, that has been observed in some cellular systems<sup>19,156</sup>, might be linked to their role in controlling different pathways and whether also the endocytosis participates in the regulation of p53, considering that Numb has been described as an endocytic protein<sup>21,2</sup>.

## **6.3 THE MULTIPLE WAYS LEADING TO NUMB DYSFUNCTION IN TUMORS AND THE POSSIBLE THERAPEUTIC INTERVENTIONS.**

The scenario that is emerging to explain Numb deficiency in BC seems to be complex and to involve multiple layers of deregulation. The deregulation of Numb stability by post-translational ubiquitination and degradation is only one of the possible mechanisms responsible for Numb deficiency. In this context, an obvious possibility is that the genetic lesion responsible for the excessive Numb degradation leads to the enhanced activity of an E3 ligase, reduced activity of a deubiquitinating enzyme (DUB), or to the deregulation of signaling molecules regulating the ubiquitination machinery, e.g., kinases, phosphatases, and neddylation enzymes. Consistent with this hypothesis, different E3-ligases, such as LNX<sup>184</sup>, Siah-1<sup>185</sup>, Mdm2<sup>186</sup> and NAK serine/threonine kinase<sup>187</sup> have been associated with the modulation of Numb levels. Whatever the case, the therapeutic restoration of Numb function might in principle be achieved by pharmacologically inhibiting the enzyme(s) responsible for its degradation.

The current study defines new layers in the regulation of Numb functions. We demonstrated that also upstream mechanisms related to pre-translational deregulation could be associated with loss of all or some specific Numb isoforms in BCs, thus, affecting BC aggressiveness. Low Numb total mRNA levels could be dictated by different mechanisms ranging from deregulation of the transcription machinery to the oncogenic activity of some miRNA, such as, miR-146a and miR-34, which have been described to target Numb and suppress its expression<sup>188,189</sup>. The relevance of Numb transcriptional deregulation has emerged also recently in the prostate cancer context, where Numb mRNA downregulation is negatively associated with prostate cancer progression<sup>159</sup>.

The elucidation of the transcription factors or miRNAs involved in the pre-translational regulation of Numb might pave the way to the identification of new therapeutic targets for restoring Numb levels in Numb-deficient tumors. In particular, we plan to evaluate whether miR-146a, miR-34 and other miRNA candidates predicted to target Numb mRNA, display a differential expression in a panel of breast tumors expressing low or high mRNA levels of total Numb.

Concerning the alterations in Numb alternative splicing, our findings are consistent with the aforementioned role of the aberrant functionality of the splicing machinery in oncogenesis and are prompting us to investigate the biological mechanisms regulating the balance of Numb isoforms. Although some splicing factors, such as RBM 4/5/6/10 have been implicated in regulation of Numb exon 9 AS<sup>151,153</sup>, the investigation remains open, in particular, for the discovery of regulators that dictate the Numb exon 3 AS, with the consequent impact on the p53 regulation.

Together the results of this thesis depict a more complex scenario to explain the loss of Numb function in BCs, where probably multiple mechanisms, ranging from proteasomal hyperdegradation to deregulated Numb mRNA transcription and alternative splicing, might be responsible for the altered Numb-regulated pathways observed in these BCs, such as p53 and Notch signaling. The identification of all the molecular players involved will be important to find new possible therapeutic strategies for the treatment of the Numb-deficient BCs.

## 7 ACKNOWLEDGEMENTS

I would like to thank all the people I encountered during my PhD who have made a precious contribution to my thesis work and to my daily life in the lab. I am grateful to Prof. Pier Paolo di Fiore for the opportunity to join his lab, for giving me guidance in my project and for putting me in front of big challenges. I would like to thank also Prof. Salvatore Pece for his enthusiasm in discussing science and for his scientific supervision.

A special thanks goes to Ivan Colaluca for his constant supervision, for being an example of scientific honesty, for his help in troubleshooting experiments, for his scrupulous guidance and for being as serious as supervisor as he is funny as a person. Thanks to Prof. Andrea Basile, for his insightful and experienced advice. I would like to thank Ivan and Prof. Basile for their friendship and for the nice lab time we shared.

I would like to thank Rosalind Gunby for his detailed and critical revision of this thesis work as well as Mariagrazia Malabarba for her suggestions. I want to thank Emanuela Orlando for being helpful, professional and always kind. Thanks to Davide di Salvatore for his help with the statistical analysis of the breast cancer case-cohort and to Manuela Vecchi and her team, Micol Tillhon, Stefania Pirroni, and Francesca De Santis, for their valuable help with the case-cohort analysis.

Thanks to all my lunch family, present and past, for all the laughs and for the good times together that made me feel at home.

I would like to express thanks to the Lab A and Lab B people of IFOM, as well as all the PPDF and MolMed team for welcoming me, during the different periods of my PhD experience and for the ones that became more friends than colleagues.

For the time they dedicated to me in discussing my project, I would like to thank my Internal Advisor, Prof. Marina Mapelli, and my External Advisor, Prof. Andrea Brancale.

Thanks to all the facilities both at IFOM and IEO (sequencing, RT-qPCR facility, kitchen, imaging, FACS-sorting) for their precious help as well to the warehouse and canteen people for being always nice.

## 8 BIBLIOGRAPHY

1. Uemura, T., Shepherd, S., Ackerman, L., Jan, L. Y. & Jan, Y. N. numb, a gene required in determination of cell fate during sensory organ formation in *Drosophila* embryos. *Cell* (1989). doi:10.1016/0092-8674(89)90849-0
2. Pece, S., Confalonieri, S., R. Romano, P. & Di Fiore, P. P. NUMB-ing down cancer by more than just a NOTCH. *Biochimica et Biophysica Acta - Reviews on Cancer* (2011). doi:10.1016/j.bbcan.2010.10.001
3. Gönczy, P. Mechanisms of asymmetric cell division: Flies and worms pave the way. *Nature Reviews Molecular Cell Biology* (2008). doi:10.1038/nrm2388
4. Rhyu, M. S., Jan, L. Y. & Jan, Y. N. Asymmetric distribution of numb protein during division of the sensory organ precursor cell confers distinct fates to daughter cells. *Cell* (1994). doi:10.1016/0092-8674(94)90112-0
5. Spana, E. P. & Doe, C. Q. Numb antagonizes Notch signaling to specify sibling neuron cell fates. *Neuron* (1996). doi:10.1016/S0896-6273(00)80277-9
6. Spana, E. P., Koczcynski, C., Goodman, C. S. & Doe, C. Q. Asymmetric localization of numb autonomously determines sibling neuron identity in the *Drosophila* CNS. *Development* (1995).
7. Zhong, W. *et al.* Asymmetric localization of a mammalian numb homolog during mouse cortical neurogenesis. *Neuron* (1996). doi:10.1016/S0896-6273(00)80279-2
8. Lee, C. Y. *et al.* *Drosophila* Aurora-A kinase inhibits neuroblast self-renewal by regulating aPKC/Numb cortical polarity and spindle orientation. *Genes Dev.* (2006). doi:10.1101/gad.1489406
9. Wirtz-Peitz, F., Nishimura, T. & Knoblich, J. A. Linking Cell Cycle to Asymmetric Division: Aurora-A Phosphorylates the Par Complex to Regulate Numb Localization. *Cell* (2008). doi:10.1016/j.cell.2008.07.049
10. Smith, C. A. *et al.* aPKC-mediated phosphorylation regulates asymmetric membrane localization of the cell fate determinant Numb. *EMBO J.* (2007). doi:10.1038/sj.emboj.7601495
11. Lu, B., Rothenberg, M., Jan, L. Y. & Jan, Y. N. Partner of Numb colocalizes with numb during mitosis and directs numb asymmetric localization in *Drosophila* neural and muscle progenitors. *Cell* (1998). doi:10.1016/S0092-8674(00)81753-5
12. Neumüller, R. A. & Knoblich, J. A. Dividing cellular asymmetry: Asymmetric cell division and its implications for stem cells and cancer. *Genes and Development* (2009). doi:10.1101/gad.1850809
13. Cayouette, M. & Raff, M. Asymmetric segregation of Numb: A mechanism for neural specification from *Drosophila* to mammals. *Nature Neuroscience* (2002). doi:10.1038/nn1202-1265
14. Knoblich, J. A., Jan, L. Y. & Jan, Y. N. Asymmetric segregation of numb and prospero during cell division. *Nature* (1995). doi:10.1038/377624a0
15. Yan, B. Numb - From flies to humans. *Brain and Development* (2010). doi:10.1016/j.braindev.2009.03.008
16. Gulino, A., Di Marcotullio, L. & Screpanti, I. The multiple functions of Numb.

- Experimental Cell Research* (2010). doi:10.1016/j.yexcr.2009.11.017
17. Zhong, W., Jiang, M. M., Weinmaster, G. & Jan, Y. N. Differential expression of mammalian Numb, Numbl-like and Notch1 suggests distinct roles during mouse cortical neurogenesis. *Development* (1997). doi:10.1242/dev.01619
  18. Zwahlen, C., Li, S. C., Kay, L. E., Pawson, T. & Forman-Kay, J. D. Multiple modes of peptide recognition by the PTB domain of the cell fate determinant Numb. *EMBO J.* (2000). doi:10.1093/emboj/19.7.1505
  19. Dho, S. E., French, M. B., Woods, S. A. & McGlade, C. J. Characterization of four mammalian numb protein isoforms. Identification of cytoplasmic and membrane-associated variants of the phosphotyrosine binding domain. *J. Biol. Chem.* (1999). doi:10.1074/jbc.274.46.33097
  20. Verdi, J. M. *et al.* Distinct human NUMB isoforms regulate differentiation vs. proliferation in the neuronal lineage. *Proc. Natl. Acad. Sci. U. S. A.* (1999). doi:10.1073/pnas.96.18.10472
  21. Santolini, E. *et al.* Numb is an endocytic protein. *J. Cell Biol.* (2000). doi:10.1083/jcb.151.6.1345
  22. Carbone, R. *et al.* eps15 and eps15R are essential components of the endocytic pathway. *Cancer Res.* (1997).
  23. Coda, L. *et al.* Eps15R is a tyrosine kinase substrate with characteristics of a docking protein possibly involved in coated pits-mediated internalization. *J. Biol. Chem.* (1998). doi:10.1074/jbc.273.5.3003
  24. Smith, C. A. The Cell Fate Determinant Numb Interacts with EHD/Rme-1 Family Proteins and Has a Role in Endocytic Recycling. *Mol. Biol. Cell* (2004). doi:10.1091/mbc.E04-01-0026
  25. Zobel, M. *et al.* A NUMB-EFA6B-ARF6 recycling route controls apically restricted cell protrusions and mesenchymal motility. *J. Cell Biol.* (2018). doi:10.1083/jcb.201802023
  26. Sorensen, E. B. & Conner, S. D. AAK1 regulates Numb function at an early step in clathrin-mediated endocytosis. *Traffic* (2008). doi:10.1111/j.1600-0854.2008.00790.x
  27. Nishimura, T. *et al.* CRMP-2 regulates polarized Numb-mediated endocytosis for axon growth. *Nat. Cell Biol.* (2003). doi:10.1038/ncb1039
  28. Nishimura, T. & Kaibuchi, K. Numb Controls Integrin Endocytosis for Directional Cell Migration with aPKC and PAR-3. *Dev. Cell* (2007). doi:10.1016/j.devcel.2007.05.003
  29. Hutterer, A. & Knoblich, J. A. Numb and  $\alpha$ -Adaptin regulate Sanpodo endocytosis to specify cell fate in *Drosophila* external sensory organs. *EMBO Rep.* (2005). doi:10.1038/sj.embor.7400500
  30. Roegiers, F. Regulation of Membrane Localization of Sanpodo by lethal giant larvae and neuralized in Asymmetrically Dividing Cells of *Drosophila* Sensory Organs. *Mol. Biol. Cell* (2005). doi:10.1091/mbc.E05-03-0177
  31. Berdnik, D., Török, T., González-Gaitán, M. & Knoblich, J. A. The endocytic protein  $\alpha$ -adaptin is required for numb-mediated asymmetric cell division in *Drosophila*. *Dev. Cell* (2002). doi:10.1016/S1534-5807(02)00215-0
  32. Knoblich, J. A. Mechanisms of Asymmetric Stem Cell Division. *Cell* (2008). doi:10.1016/j.cell.2008.02.007
  33. Shao, X. *et al.* Mammalian numb protein antagonizes notch by controlling postendocytic trafficking of the notch ligand delta-like 4. *J. Biol. Chem.* (2017). doi:10.1074/jbc.M117.800946

34. McGill, M. A., Dho, S. E., Weinmaster, G. & McGlade, C. J. Numb regulates post-endocytic trafficking and degradation of notch1. *J. Biol. Chem.* (2009). doi:10.1074/jbc.M109.014845
35. Artavanis-Tsakonas, S. Notch Signaling: Cell Fate Control and Signal Integration in Development. *Science (80-. )*. (1999). doi:10.1126/science.284.5415.770
36. Hori, K., Sen, A. & Artavanis-Tsakonas, S. Notch signaling at a glance. *J. Cell Sci.* (2013). doi:10.1242/jcs.127308
37. Guo, M., Jan, L. Y. & Jan, Y. N. Control of daughter cell fates during asymmetric division: Interaction of Numb and Notch. *Neuron* (1996). doi:10.1016/S0896-6273(00)80278-0
38. O'Connor-Giles, K. M. & Skeath, J. B. Numb inhibits membrane localization of sanpodo, a four-pass transmembrane protein, to promote asymmetric divisions in *Drosophila*. *Dev. Cell* (2003). doi:10.1016/S1534-5807(03)00226-0
39. Schweisguth, F. Regulation of Notch Signaling Activity. *Current Biology* (2004). doi:10.1016/S0960-9822(04)00038-7
40. Fortini, M. E. & Bilder, D. Endocytic regulation of Notch signaling. *Current Opinion in Genetics and Development* (2009). doi:10.1016/j.gde.2009.04.005
41. McGill, M. A. & McGlade, C. J. Mammalian Numb proteins promote Notch1 receptor ubiquitination and degradation of the Notch1 intracellular domain. *J. Biol. Chem.* (2003). doi:10.1074/jbc.M302827200
42. Nowell, C. S. & Radtke, F. Notch as a tumour suppressor. *Nature Reviews Cancer* (2017). doi:10.1038/nrc.2016.145
43. Bolós, V., Grego-Bessa, J. & De La Pompa, J. L. Notch signaling in development and cancer. *Endocrine Reviews* (2007). doi:10.1210/er.2006-0046
44. Pece, S. *et al.* Loss of negative regulation by Numb over Notch is relevant to human breast carcinogenesis. *J. Cell Biol.* (2004). doi:10.1083/jcb.200406140
45. Leong, K. G. & Karsan, A. Recent insights into the role of Notch signaling in tumorigenesis. *Blood* (2006). doi:10.1182/blood-2005-08-3329
46. Flores, A. N., McDermott, N., Meunier, A. & Maignol, L. NUMB inhibition of NOTCH signalling as a therapeutic target in prostate cancer. *Nature Reviews Urology* (2014). doi:10.1038/nrurol.2014.195
47. Ingham, P. W., Nakano, Y. & Seger, C. Mechanisms and functions of Hedgehog signalling across the metazoa. *Nature Reviews Genetics* (2011). doi:10.1038/nrg2984
48. Ruiz I Altaba, A. Gli proteins and Hedgehog signaling: Development and cancer. *Trends in Genetics* (1999). doi:10.1016/S0168-9525(99)01840-5
49. Stecca, B. & Ruiz I Altaba, A. The therapeutic potential of modulators of the Hedgehog-Gli signaling pathway. *Journal of Biology* (2002). doi:10.1186/1475-4924-1-9
50. Evangelista, M., Tian, H. & De Sauvage, F. J. The Hedgehog signaling pathway in cancer. *Clinical Cancer Research* (2006). doi:10.1158/1078-0432.CCR-06-1736
51. Varjosalo, M. & Taipale, J. Hedgehog: Functions and mechanisms. *Genes and Development* (2008). doi:10.1101/gad.1693608
52. Bürglin, T. R. The Hedgehog protein family. *Genome Biol.* (2008). doi:10.1186/gb-2008-9-11-241
53. Nybakken, K. & Perrimon, N. Hedgehog signal transduction: Recent findings. *Current Opinion in Genetics and Development* (2002). doi:10.1016/S0959-437X(02)00333-7
54. Di Marcotullio, L. *et al.* Numb is a suppressor of Hedgehog signalling and targets Gli1 for Itch-dependent ubiquitination. *Nat. Cell Biol.* (2006). doi:10.1038/ncb1510

55. Di Marcotullio, L. *et al.* Numb activates the E3 ligase Itch to control Gli1 function through a novel degradation signal. *Oncogene* (2011). doi:10.1038/onc.2010.394
56. Sanchez, P. *et al.* Inhibition of prostate cancer proliferation by interference with SONIC HEDGEHOG-GLI1 signaling. *Proc. Natl. Acad. Sci. U. S. A.* (2004). doi:10.1073/pnas.0404956101
57. Goodrich, L. V., Milenković, L., Higgins, K. M. & Scott, M. P. Altered neural cell fates and medulloblastoma in mouse patched mutants. *Science* (80-. ). (1997). doi:10.1126/science.277.5329.1109
58. Kappler, R. & von Schweinitz, D. A better way forward: targeting hedgehog signaling in liver cancer. *Front. Biosci. (Schol. Ed.)*. (2012).
59. Eichenmüller, M. *et al.* Blocking the hedgehog pathway inhibits hepatoblastoma growth. *Hepatology* (2009). doi:10.1002/hep.22649
60. Hamed, S. *et al.* Accelerated Induction of Bladder Cancer in Patched Heterozygous Mutant Mice. *Cancer Res.* (2004). doi:10.1158/0008-5472.CAN-03-2031
61. Kappler, R. *et al.* Profiling the molecular difference between Patched- and p53-dependent rhabdomyosarcoma. *Oncogene* (2004). doi:10.1038/sj.onc.1208133
62. Rubin, L. L. & de Sauvage, F. J. Targeting the Hedgehog pathway in cancer. *Nature Reviews Drug Discovery* (2006). doi:10.1038/nrd2086
63. Colaluca, I. N. *et al.* NUMB controls p53 tumour suppressor activity. *Nature* (2008). doi:10.1038/nature06412
64. Levine, A. J. p53, the cellular gatekeeper for growth and division. *Cell* (1997). doi:10.1016/S0092-8674(00)81871-1
65. Lane, D. P. Cancer. p53, guardian of the genome. *Nature* (1992). doi:10.1038/358015a0
66. Kruse, J. P. & Gu, W. Modes of p53 Regulation. *Cell* (2009). doi:10.1016/j.cell.2009.04.050
67. Biegging, K. T., Mello, S. S. & Attardi, L. D. Unravelling mechanisms of p53-mediated tumour suppression. *Nature Reviews Cancer* (2014). doi:10.1038/nrc3711
68. Vousden, K. H. & Prives, C. Blinded by the Light: The Growing Complexity of p53. *Cell* (2009). doi:10.1016/j.cell.2009.04.037
69. Kruiswijk, F., Labuschagne, C. F. & Vousden, K. H. P53 in survival, death and metabolic health: A lifeguard with a licence to kill. *Nature Reviews Molecular Cell Biology* (2015). doi:10.1038/nrm4007
70. Cicalese, A. *et al.* The Tumor Suppressor p53 Regulates Polarity of Self-Renewing Divisions in Mammary Stem Cells. *Cell* (2009). doi:10.1016/j.cell.2009.06.048
71. Spike, B. T. & Wahl, G. M. P53, stem cells, and reprogramming: Tumor suppression beyond guarding the genome. *Genes and Cancer* (2011). doi:10.1177/1947601911410224
72. Vogelstein, B., Lane, D. & Levine, A. J. Surfing the p53 network. *Nature* (2000). doi:10.1038/35042675
73. Stavridi, E. S., Huyen, Y., Sheston, E. A. & Halazonetis, T. D. The three-dimensional structure of p53. in *The p53 Tumor Suppressor Pathway and Cancer* (2005). doi:10.1007/0-387-30127-5\_2
74. Joerger, A. C. & Fersht, A. R. The tumor suppressor p53: from structures to drug discovery. *Cold Spring Harbor perspectives in biology* (2010). doi:10.1101/cshperspect.a000919
75. Kamada, R., Toguchi, Y., Nomura, T., Imagawa, T. & Sakaguchi, K. Tetramer formation of tumor suppressor protein p53: Structure, function, and applications. *Biopolymers*

- (2016). doi:10.1002/bip.22772
76. Haupt, Y., Maya, R., Kazaz, A. & Oren, M. Mdm2 promotes the rapid degradation of p53. *Nature* (1997). doi:10.1038/387296a0
  77. Kubbutat, M. H. G., Jones, S. N. & Vousden, K. H. Regulation of p53 stability by Mdm2. *Nature* (1997). doi:10.1038/387299a0
  78. Freeman, J. A. & Espinosa, J. M. The impact of post-transcriptional regulation in the p53 network. *Brief. Funct. Genomics* (2013). doi:10.1093/bfgp/els058
  79. Biderman, L., Manley, J. L. & Prives, C. Mdm2 and MdmX as Regulators of Gene Expression. *Genes and Cancer* (2012). doi:10.1177/1947601912455331
  80. Murray-Zmijewski, F., Slee, E. A. & Lu, X. A complex barcode underlies the heterogeneous response of p53 to stress. *Nature Reviews Molecular Cell Biology* (2008). doi:10.1038/nrm2451
  81. Nag, S., Qin, J., Srivenugopal, K. S., Wang, M. & Zhang, R. The MDM2-p53 pathway revisited. *J. Biomed. Res.* **27**, 254–271 (2013).
  82. Chène, P. Inhibiting the p53-MDM2 interaction: An important target for cancer therapy. *Nature Reviews Cancer* (2003). doi:10.1038/nrc991
  83. Ganguli, G. & Wasylyk, B. p53-independent functions of MDM2. *Mol. Cancer Res.* (2003).
  84. Karni-Schmidt, O., Lokshin, M. & Prives, C. The Roles of MDM2 and MDMX in Cancer. *Annu. Rev. Pathol. Mech. Dis.* (2016). doi:10.1146/annurev-pathol-012414-040349
  85. Dolezelova, P., Cetkovska, K., Vousden, K. H. & Uldrijan, S. Mutational analysis reveals a dual role of Mdm2 acidic domain in the regulation of p53 stability. *FEBS Lett.* (2012). doi:10.1016/j.febslet.2012.05.034
  86. Arena, G. *et al.* Mitochondrial MDM2 Regulates Respiratory Complex I Activity Independently of p53. *Mol. Cell* (2018). doi:10.1016/j.molcel.2018.01.023
  87. Barak, Y., Gottlieb, E., Juven-Gershon, T. & Oren, M. Regulation of mdm2 expression by p53: Alternative promoters produce transcripts with nonidentical translation potential. *Genes Dev.* (1994). doi:10.1101/gad.8.15.1739
  88. Maya, R. *et al.* ATM-dependent phosphorylation of Mdm2 on serine 395: Role in p53 activation by DNA damage. *Genes Dev.* (2001). doi:10.1101/gad.886901
  89. Mayo, L. D. & Donner, D. B. A phosphatidylinositol 3-kinase/Akt pathway promotes translocation of Mdm2 from the cytoplasm to the nucleus. *Proc. Natl. Acad. Sci.* (2001). doi:10.1073/pnas.181181198
  90. Momand, J., Jung, D., Wilczynski, S. & Niland, J. The MDM2 gene amplification database. *Nucleic Acids Research* (1998). doi:10.1093/nar/26.15.3453
  91. Zietz, C. *et al.* MDM-2 oncoprotein overexpression, p53 gene mutation, and VEGF up-regulation in angiosarcomas. *Am. J. Pathol.* (1998). doi:10.1016/S0002-9440(10)65729-X
  92. Stefanou, D. G. *et al.* p53/MDM-2 immunohistochemical expression correlated with proliferative activity in different subtypes of human sarcomas: A ten-year follow-up study. *Anticancer Res.* (1998).
  93. Rayburn, E., Zhang, R., He, J. & Wang, H. MDM2 and human malignancies: expression, clinical pathology, prognostic markers, and implications for chemotherapy. *Curr. Cancer Drug Targets* (2005). doi:10.2174/1568009053332636
  94. Wallace, M., Worrall, E., Pettersson, S., Hupp, T. R. & Ball, K. L. Dual-Site Regulation of MDM2 E3-Ubiquitin Ligase Activity. *Mol. Cell* (2006). doi:10.1016/j.molcel.2006.05.029
  95. Ma, J. *et al.* A second p53 binding site in the central domain of Mdm2 is essential for

- p53 ubiquitination. *Biochemistry* (2006). doi:10.1021/bi060661u
96. Meek, D. W. Regulation of the p53 response and its relationship to cancer. *Biochem. J.* (2015). doi:10.1042/BJ20150517
  97. Wang, X. & Jiang, X. Mdm2 and MdmX partner to regulate p53. *FEBS Letters* (2012). doi:10.1016/j.febslet.2012.02.049
  98. Huang, L. *et al.* The p53 inhibitors MDM2/MDMX complex is required for control of p53 activity in vivo. *Proc. Natl. Acad. Sci.* (2011). doi:10.1073/pnas.1102309108
  99. Honda, R. & Yasuda, H. Association of p19(ARF) with Mdm2 inhibits ubiquitin ligase activity of Mdm2 for tumor suppressor p53. *EMBO J.* (1999). doi:10.1093/emboj/18.1.22
  100. Louria-Hayon, I. *et al.* The promyelocytic leukemia protein protects p53 from Mdm2-mediated inhibition and degradation. *J. Biol. Chem.* (2003). doi:10.1074/jbc.M301264200
  101. Korgaonkar, C. *et al.* Nucleophosmin (B23) Targets ARF to Nucleoli and Inhibits Its Function. *Mol. Cell. Biol.* (2005). doi:10.1128/MCB.25.4.1258-1271.2005
  102. Yang, H.-Y., Wen, Y.-Y., Chen, C.-H., Lozano, G. & Lee, M.-H. 14-3-3 Positively Regulates p53 and Suppresses Tumor Growth. *Mol. Cell. Biol.* (2003). doi:10.1128/MCB.23.20.7096-7107.2003
  103. Chen, D. *et al.* RYBP stabilizes p53 by modulating MDM2. *EMBO Rep.* (2009). doi:10.1038/embor.2008.231
  104. Olivier, M., Hollstein, M. & Hainaut, P. TP53 mutations in human cancers: origins, consequences, and clinical use. *Cold Spring Harbor perspectives in biology* (2010). doi:10.1101/cshperspect.a001008
  105. Petitjean, A., Achatz, M. I. W., Borresen-Dale, A. L., Hainaut, P. & Olivier, M. TP53 mutations in human cancers: functional selection and impact on cancer prognosis and outcomes. *Oncogene* (2007). doi:10.1038/sj.onc.1210302
  106. Hong, B., van den Heuvel, a P. J., Prabhu, V. V, Zhang, S. & El-Deiry, W. S. Targeting Tumor Suppressor p53 for Cancer Therapy: Strategies, Challenges and Opportunities. *Curr. Drug Targets* (2014). doi:10.2174/1389450114666140106101412
  107. Clayman, G. L. *et al.* In vivo molecular therapy with p53 adenovirus for microscopic residual head and neck squamous carcinoma. *Cancer Res.* (1995).
  108. Zhang, W. W. *et al.* High-efficiency gene transfer and high-level expression of wild-type p53 in human lung cancer cells mediated by recombinant adenovirus. *Cancer Gene Ther.* (1994).
  109. Yang, C., Passaniti, A., Cirielli, C., Capogrossi, M. C. & Cirielli, C. Adenovirus-mediated Wild-Type p53 Expression Induces Apoptosis and Suppresses Tumorigenesis of Prostatic Tumor Cells. *Cancer Res.* (1995).
  110. Kock, H. *et al.* Adenovirus-mediated p53 gene transfer suppresses growth of human glioblastoma cells in vitro and in vivo. *Int J Cancer* (1996). doi:10.1002/(SICI)1097-0215(19960917)67:6<808::AID-IJC9>3.0.CO;2-V
  111. Zhu, J. xin *et al.* [Treatment of recurrent malignant gliomas by surgery combined with recombinant adenovirus-p53 injection]. *Zhonghua Zhong Liu Za Zhi* (2010).
  112. Nemunaitis, J. *et al.* Biomarkers Predict p53 Gene Therapy Efficacy in Recurrent Squamous Cell Carcinoma of the Head and Neck. *Clin. Cancer Res.* (2009). doi:10.1158/1078-0432.CCR-09-1044
  113. Yang, Z. *et al.* Clinical study of recombinant adenovirus-p53 combined with fractionated stereotactic radiotherapy for hepatocellular carcinoma. *J. Cancer Res.*

- Clin. Oncol.* (2010). doi:10.1007/s00432-009-0701-6
114. Klein, C. & Vassilev, L. T. Targeting the p53-MDM2 interaction to treat cancer. *British Journal of Cancer* (2004). doi:10.1038/sj.bjc.6602164
  115. ElSawy, K. M. *et al.* On the interaction mechanisms of a p53 peptide and nutlin with the MDM2 and MDMX proteins: A Brownian dynamics study. *Cell Cycle* (2013). doi:10.4161/cc.23511
  116. Bykov, V. J. N. *et al.* Restoration of the tumor suppressor function to mutant p53 by a low-molecular-weight compound. *Nat. Med.* (2002). doi:10.1038/nm0302-282
  117. Thor, a D. *et al.* Accumulation of p53 tumor suppressor gene protein: an independent marker of prognosis in breast cancers. *J. Natl. Cancer Inst.* (1992).
  118. Alsner, J. *et al.* A comparison between p53 accumulation determined by immunohistochemistry and TP53 mutations as prognostic variables in tumours from breast cancer patients. *Acta Oncol. (Madr).* (2008). doi:10.1080/02841860802047411
  119. Lukashchuk, N. & Vousden, K. H. Ubiquitination and degradation of mutant p53. *Mol. Cell. Biol.* (2007). doi:10.1128/MCB.00050-07
  120. Muller, P. A. J. & Vousden, K. H. Mutant p53 in cancer: New functions and therapeutic opportunities. *Cancer Cell* (2014). doi:10.1016/j.ccr.2014.01.021
  121. Duffy, M. J., Synnott, N. C. & Crown, J. Mutant p53 as a target for cancer treatment. *European Journal of Cancer* (2017). doi:10.1016/j.ejca.2017.06.023
  122. Chada, S., Mhashilkar, A., Roth, J. A. & Gabrilovich, D. Development of vaccines against self-antigens: the p53 paradigm. *Curr Opin Drug Discov Devel* (2003).
  123. Yemelyanova, A. *et al.* Immunohistochemical staining patterns of p53 can serve as a surrogate marker for TP53 mutations in ovarian carcinoma: An immunohistochemical and nucleotide sequencing analysis. *Mod. Pathol.* (2011). doi:10.1038/modpathol.2011.85
  124. Bartley, A. N. & Ross, D. W. Validation of p53 immunohistochemistry as a prognostic factor in breast cancer in clinical practice. *Arch. Pathol. Lab. Med.* (2002). doi:10.1043/0003-9985(2002)126<0456:VOPIAA>2.0.CO;2
  125. Xue, W. *et al.* Senescence and tumour clearance is triggered by p53 restoration in murine liver carcinomas. *Nature* (2007). doi:10.1038/nature05529
  126. Martins, C. P., Brown-Swigart, L. & Evan, G. I. Modeling the Therapeutic Efficacy of p53 Restoration in Tumors. *Cell* (2006). doi:10.1016/j.cell.2006.12.007
  127. Ventura, A. *et al.* Restoration of p53 function leads to tumour regression in vivo. *Nature* (2007). doi:10.1038/nature05541
  128. Zhang, Z. *et al.* Radiosensitization by Antisense Anti-MDM2 Mixed-Backbone Oligonucleotide in in Vitro and in Vivo Human Cancer Models. *Clin. Cancer Res.* (2004). doi:10.1158/1078-0432.CCR-0245-03
  129. Kenjo, E. *et al.* Systemic delivery of small interfering RNA by use of targeted polycation liposomes for cancer therapy. *Biol. Pharm. Bull.* (2013). doi:10.1248/bpb.b12-00817
  130. Yu, H. *et al.* Induction of apoptosis in non-small cell lung cancer by downregulation of MDM2 using pH-responsive PMPC-b-PDPA/siRNA complex nanoparticles. *Biomaterials* (2013). doi:10.1016/j.biomaterials.2012.12.042
  131. Tovar, C. *et al.* Small-molecule MDM2 antagonists reveal aberrant p53 signaling in cancer: implications for therapy. *Proc. Natl. Acad. Sci. U. S. A.* (2006). doi:10.1073/pnas.0507493103
  132. Lakoma, A. *et al.* The MDM2 small-molecule inhibitor RG7388 leads to potent tumor

- inhibition in p53 wild-type neuroblastoma. *Cell Death Discov.* (2015). doi:10.1038/cddiscovery.2015.26
133. Ding, Q. *et al.* Discovery of RG7388, a potent and selective p53-MDM2 inhibitor in clinical development. *J. Med. Chem.* (2013). doi:10.1021/jm400487c
  134. Yang, Y. *et al.* Small molecule inhibitors of HDM2 ubiquitin ligase activity stabilize and activate p53 in cells. *Cancer Cell* (2005). doi:10.1016/j.ccr.2005.04.029
  135. Zhang, Q., Zeng, S. X. & Lu, H. Targeting p53-MDM2-MDMX loop for cancer therapy. *Subcell. Biochem.* (2014). doi:10.1007/978-94-017-9211-0\_16
  136. Colaluca, I. N. *et al.* A Numb-Mdm2 fuzzy complex reveals an isoform-specific involvement of Numb in breast cancer. *J. Cell Biol.* (2018). doi:10.1083/jcb.201709092
  137. Rašin, M. R. *et al.* Numb and Numbl are required for maintenance of cadherin-based adhesion and polarity of neural progenitors. *Nat. Neurosci.* (2007). doi:10.1038/nn1924
  138. Harris, T. J. C. & Tepass, U. Adherens junctions: From molecules to morphogenesis. *Nature Reviews Molecular Cell Biology* (2010). doi:10.1038/nrm2927
  139. Hartsock, A. & Nelson, W. J. Adherens and tight junctions: Structure, function and connections to the actin cytoskeleton. *Biochimica et Biophysica Acta - Biomembranes* (2008). doi:10.1016/j.bbamem.2007.07.012
  140. Wang, Z., Sandiford, S., Wu, C. & Li, S. S. C. Numb regulates cell-cell adhesion and polarity in response to tyrosine kinase signalling. *EMBO J.* (2009). doi:10.1038/emboj.2009.190
  141. Steed, E., Balda, M. S. & Matter, K. Dynamics and functions of tight junctions. *Trends in Cell Biology* (2010). doi:10.1016/j.tcb.2009.12.002
  142. Wang, Z., Li, Y., Kong, D. & H. Sarkar, F. The Role of Notch Signaling Pathway in Epithelial-Mesenchymal Transition (EMT) During Development and Tumor Aggressiveness. *Curr. Drug Targets* (2010). doi:10.2174/138945010791170860
  143. Qi, S. *et al.* Aberrant expression of Notch1/numb/snail signaling, an epithelial mesenchymal transition related pathway, in adenomyosis. *Reprod. Biol. Endocrinol.* (2015). doi:10.1186/s12958-015-0084-2
  144. Bani-Yaghoob, M. *et al.* A switch in numb isoforms is a critical step in cortical development. *Dev. Dyn.* (2007). doi:10.1002/dvdy.21072
  145. Rajendran, D., Zhang, Y., Berry, D. M. & McGlade, C. J. Regulation of Numb isoform expression by activated ERK signaling. *Oncogene* (2016). doi:10.1038/onc.2016.69
  146. Liu, S. & Cheng, C. Alternative RNA splicing and cancer. *Wiley Interdisciplinary Reviews: RNA* (2013). doi:10.1002/wrna.1178
  147. Sveen, A., Kilpinen, S., Ruusulehto, A., Lothe, R. A. & Skotheim, R. I. Aberrant RNA splicing in cancer; Expression changes and driver mutations of splicing factor genes. *Oncogene* (2016). doi:10.1038/onc.2015.318
  148. Lu, Y. *et al.* Alternative splicing of the cell fate determinant Numb in hepatocellular carcinoma. *Hepatology* (2015). doi:10.1002/hep.27923
  149. Misquitta-Ali, C. M. *et al.* Global Profiling and Molecular Characterization of Alternative Splicing Events Misregulated in Lung Cancer. *Mol. Cell. Biol.* (2011). doi:10.1128/MCB.00709-10
  150. Zhao, Y. J. *et al.* Alternative splicing of VEGFA, APP and NUMB genes in colorectal cancer. *World J. Gastroenterol.* (2015). doi:10.3748/wjg.v21.i21.6550
  151. Bechara, E. G., Sebestyén, E., Bernardis, I., Eyras, E. & Valcárcel, J. RBM5, 6, and 10 differentially regulate NUMB alternative splicing to control cancer cell proliferation.

- Mol. Cell* (2013). doi:10.1016/j.molcel.2013.11.010
152. Kim, K. K., Nam, J., Mukoyama, Y. S. & Kawamoto, S. Rbfox3-regulated alternative splicing of Numb promotes neuronal differentiation during development. *J. Cell Biol.* (2013). doi:10.1083/jcb.201206146
  153. Tarn, W.-Y. *et al.* RBM4 promotes neuronal differentiation and neurite outgrowth by modulating Numb isoform expression. *Mol. Biol. Cell* (2016). doi:10.1091/mbc.E15-11-0798
  154. Ntelios, D., Berninger, B. & Tzimagiorgis, G. Numb and Alzheimers disease: The current picture. *Frontiers in Neuroscience* (2012). doi:10.3389/fnins.2012.00145
  155. Kyriazis, G. A. *et al.* Numb endocytic adapter proteins regulate the transport and processing of the amyloid precursor protein in an isoform-dependent manner: Implications for Alzheimer disease pathogenesis. *J. Biol. Chem.* (2008). doi:10.1074/jbc.M802072200
  156. Dho, S. E. Dynamic Regulation of Mammalian Numb by G Protein-coupled Receptors and Protein Kinase C Activation: Structural Determinants of Numb Association with the Cortical Membrane. *Mol. Biol. Cell* (2006). doi:10.1091/mbc.E06-02-0097
  157. Sato, K. *et al.* Numb controls E-cadherin endocytosis through p120 catenin with aPKC. *Mol. Biol. Cell* (2011). doi:10.1091/mbc.E11-03-0274
  158. Westhoff, B. *et al.* Alterations of the Notch pathway in lung cancer. *Proc. Natl. Acad. Sci.* (2009). doi:10.1073/pnas.0907781106
  159. Guo, Y. *et al.* Numb<sup>-low</sup> enriches a castration-resistant prostate cancer cell subpopulation associated with enhanced Notch and Hedgehog signaling. *Clin. Cancer Res.* (2017). doi:10.1158/1078-0432.CCR-17-0913
  160. Siddique, H. R. *et al.* NUMB phosphorylation destabilizes p53 and promotes self-renewal of tumor-initiating cells by a NANOG-dependent mechanism in liver cancer. *Hepatology* (2015). doi:10.1002/hep.27987
  161. Tosoni, D. *et al.* The Numb/p53 circuitry couples replicative self-renewal and tumor suppression in mammary epithelial cells. *J. Cell Biol.* (2015). doi:10.1083/jcb.201505037
  162. Tosoni, D. *et al.* Pre-clinical validation of a selective anti-cancer stem cell therapy for Numb-deficient human breast cancers. *EMBO Mol. Med.* (2017). doi:10.15252/emmm.201606940
  163. Knoblich, J. A. Asymmetric cell division: Recent developments and their implications for tumour biology. *Nature Reviews Molecular Cell Biology* (2010). doi:10.1038/nrm3010
  164. Morrison, S. J. & Kimble, J. Asymmetric and symmetric stem-cell divisions in development and cancer. *Nature* (2006). doi:10.1038/nature04956
  165. Faraldo, M. M. & Glukhova, M. A. Regulating the regulator: Numb acts upstream of p53 to control mammary stem and progenitor cell. *Journal of Cell Biology* (2015). doi:10.1083/jcb.201510104
  166. Goldhirsch, A. *et al.* Progress and promise: highlights of the international expert consensus on the primary therapy of early breast cancer 2007. *Ann. Oncol.* (2007). doi:10.1093/annonc/mdm271
  167. Bric, A. *et al.* Functional Identification of Tumor-Suppressor Genes through an In Vivo RNA Interference Screen in a Mouse Lymphoma Model. *Cancer Cell* (2009). doi:10.1016/j.ccr.2009.08.015
  168. Robles, A. I. & Harris, C. C. Clinical Outcomes and Correlates of TP53 Mutations and Cancer. *Cold Spring Harb. Perspect. Biol.* (2009). doi:10.1101/cshperspect.a001016

169. Wu, X., Bayle, J. H., Olson, D. & Levine, A. J. The p53-mdm-2 autoregulatory feedback loop. *Genes Dev.* (1993). doi:10.1101/gad.7.7a.1126
170. Barak, Y., Juven, T., Haffner, R. & Oren, M. Mdm2 Expression Is Induced By Wild Type P53 Activity. *EMBO J.* (1993).
171. Petitjean, A. *et al.* Impact of mutant p53 functional properties on TP53 mutation patterns and tumor phenotype: Lessons from recent developments in the IARC TP53 database. *Hum. Mutat.* (2007). doi:10.1002/humu.20495
172. Pharoah, P. D., Day, N. E. & Caldas, C. Somatic mutations in the p53 gene and prognosis in breast cancer: a meta-analysis. *Br. J. Cancer* (1999). doi:10.1038/sj.bjc.6690628
173. Wu, L. & Levine, A. J. Differential regulation of the p21/WAF-1 and mdm2 genes after high-dose UV irradiation: p53-dependent and p53-independent regulation of the mdm2 gene. *Mol. Med.* (1997).
174. Rogakou, E. P., Pilch, D. R., Orr, A. H., Ivanova, V. S. & Bonner, W. M. DNA double-stranded breaks induce histone H2AX phosphorylation on serine 139. *J. Biol. Chem.* (1998). doi:10.1074/jbc.273.10.5858
175. Paull, T. T. *et al.* A critical role for histone H2AX in recruitment of repair factors to nuclear foci after DNA damage. *Curr. Biol.* (2000). doi:10.1016/S0960-9822(00)00610-2
176. Dumay, A. *et al.* Distinct tumor protein p53 mutants in breast cancer subgroups. *Int. J. Cancer* (2013). doi:10.1002/ijc.27767
177. Hanahan, D. & Weinberg, R. A. The hallmarks of cancer. *Cell* (2000). doi:10.1007/s00262-010-0968-0
178. Hanahan, D. & Weinberg, R. A. Hallmarks of cancer: The next generation. *Cell* (2011). doi:10.1016/j.cell.2011.02.013
179. Ladomery, M. Aberrant alternative splicing is another hallmark of cancer. *International Journal of Cell Biology* (2013). doi:10.1155/2013/463786
180. Sherr, C. J. Tumor surveillance via the ARF-p53 pathway. *Genes and Development* (1998). doi:10.1101/gad.12.19.2984
181. Oliner, J. D., Kinzler, K. W., Meltzer, P. S., George, D. L. & Vogelstein, B. Amplification of a gene encoding a p53-associated protein in human sarcomas. *Nature* (1992). doi:10.1038/358080a0
182. McCann, A. H. *et al.* Amplification of the MDM2 gene in human breast cancer and its association with MDM2 and p53 protein status. *Br. J. Cancer* (1995). doi:10.1038/bjc.1995.189
183. Vestey, S. B. *et al.* p14ARF expression in invasive breast cancers and ductal carcinoma in situ--relationships to p53 and Hdm2. *Breast Cancer Res.* (2004). doi:10.1186/bcr912
184. Nie, J. *et al.* LNX functions as a RING type E3 ubiquitin ligase that targets the cell fate determinant Numb for ubiquitin-dependent degradation. *EMBO J.* (2002). doi:10.1093/emboj/21.1.93
185. Susini, L. *et al.* Siah-1 binds and regulates the function of Numb. *Proc. Natl. Acad. Sci. U. S. A.* (2001). doi:10.1073/pnas.261571998
186. Juven-Gershon, T. *et al.* The Mdm2 oncoprotein interacts with the cell fate regulator Numb. *Mol. Cell. Biol.* (1998). doi:10.1128/MCB.18.7.3974
187. Chien, C. T., Wang, S., Rothenberg, M., Jan, L. Y. & Jan, Y. N. Numb-associated kinase interacts with the phosphotyrosine binding domain of Numb and antagonizes the function of Numb in vivo. *Mol. Cell. Biol.* (1998). doi:10.1128/MCB.18.1.598

188. Hung, P. S. *et al.* miR-146a enhances the oncogenicity of oral carcinoma by concomitant targeting of the IRAK1, TRAF6 and NUMB genes. *PLoS One* (2013). doi:10.1371/journal.pone.0079926
189. Bu, P. *et al.* A miR-34a-Numb Feedforward Loop Triggered by Inflammation Regulates Asymmetric Stem Cell Division in Intestine and Colon Cancer. *Cell Stem Cell* (2016). doi:10.1016/j.stem.2016.01.006